ION CHANNELS OF CULTURED HUMAN RETINAL PIGMENT EPITHELIAL CELLS

Claire H. Mitchell
Institute of Ophthalmology
University of London
1994

Thesis presented to the University of London for the degree of
Doctor of Philosophy

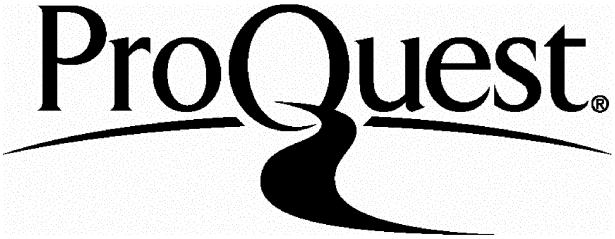

Abstract

In this thesis, the patch clamp technique has been used to examine single channels of cultured human retinal epithelial (RPE) cells. Three main channel types were detected in the cell-attached recording mode. They had mean conductances of 24 pS, 59 pS and 96 pS with physiological solutions present. All three channel types were primarily permeable to potassium. Under physiological conditions the activity of all three channel types was voltage dependant, and increased as the patches were depolarized. However, all channel types had low levels of activity at the membrane potential. The activity of the 96 pS channel type was time dependent; the channel inactivated in response to depolarizing steps. This channel type was also sensitive to the concentration of calcium; when the cells were bathed in low calcium solution the channel open probability fell towards zero. The 96 pS channel is thus similar to the maxi-K channels in other epithelia. The presence of microvilli on the top surface of these cells supports a comparison to the apical membrane. Single channel recordings on fresh bovine RPE were also attempted, but most of the channel openings were obscured by a large, noisy conductance. The voltage-sensitivity of channel activity found in cultured cells suggests that these channels may provide a mechanism for integrating dynamic transport across the RPE.

Table of Contents

Table of Contents - Details

Figures

Tables

Appendices

Appendix I.

Appendix II.

Appendix III.

Appendix IV.

Acknowledgements

I would like to thank my supervisor, Professor G.B. Arden for his assistance throughout this thesis. Thanks to Shatish Kundaiker, for his help in building the experimental system and to Dr. M. Boulton for providing the cultured cells used in this work. A special thanks to Dr. T.J.C. Jacob for his useful advice, discussions, and most of all for giving me the confidence to finish this work.

Dedication

This thesis is dedicated to Pat, Graham and Tony.
Their support, faith and love has made it all possible.

Chapter I. Introduction

I.A. General Overview

The complex system which produces the integrated transport of ions across the retinal pigment epithelium (RPE) is not static; it is responsive to local changes in ion concentration induced by light. Increasing evidence is accumulating which shows that hormones and neurotransmitters can also modify the transport system and may increase the flexibility of its interactions with light. Because the RPE is complex and affected by many variables, the ways in which it may malfunction are equally various and may result in a number of diseases. It is of considerable practical importance in ophthalmology to understand the biophysics of the RPE. It is thus critical to develop a dynamic model of ionic transport across the RPE that explains the interactions which occur in vivo.

This thesis is concerned with the properties of some of the channels which transport ions across the retinal pigment epithelium. Understanding these properties is of basic interest but is also important because they play an important role in the relationship between the RPE and light, or fluid transport. The introduction and historical sections of this thesis therefore include matter related to the ionic events associated with these functions, as well as an account of the analysis of transport across the RPE, and the membrane mechanisms which underlie the passage of ions and the maintenance of ionic gradients across the cell membrane.

I.B. Anatomy

I.B.1. Basic Structure of the Retinal Pigment Epithelium

The RPE and the retina are both derived from the neuroectoderm (Nilsson, 1964). In the adult eye this close physical relationship is maintained as the RPE extends across the whole of the retina, from the edge of the optic nerve head posteriorly to the ora serrata anteriorly. The apical surface of the RPE cells, which are closest to the retina, are covered with microvilli which

extend towards the outer retina and interdigitate with the photoreceptors (Steinberg and Wood, 1974) . The posterior side of the RPE is separated from the choroidal blood supply by Bruch's membrane. The RPE cell is tightly joined to its neighbours by junctional complexes on the lateral membrane; the sheet of cells thus forms a continuous blood-retinal barrier. The basic structure of the RPE, and its anatomical relationship to the photoreceptors and the choroid is shown in Figure I.1.

The size of RPE cells varies with their location. In the central macular region of humans, cells are approximately 12-18 μm tall and 10 μm wide, but become wider and flatter towards the periphery (Gao and Hollyfield, 1992; Warwick, 1976). The cell interior contains several structures in addition to the standard cellular organelles. Numerous melanin granules, which give the tissue its pigmented appearance, phagosomes and lysosomes are clearly visible in electron micrographs as membrane-bound vesicles (Clark, 1986). There is a decline in the number of RPE cells with age (Dorey et al.. 1989); some cells die, and others may migrate to the inner part of the retina. The remaining cells become larger and flatter, and junctional complexes reform between remaining cells.

I.B.2. Anatomy of the RPE Membranes

To be of functional significance, information on the ionic transport across the RPE must relate to the external environment of the membranes in vivo. This section will describe the anatomical characteristics of these membranes and their surrounding milieu.

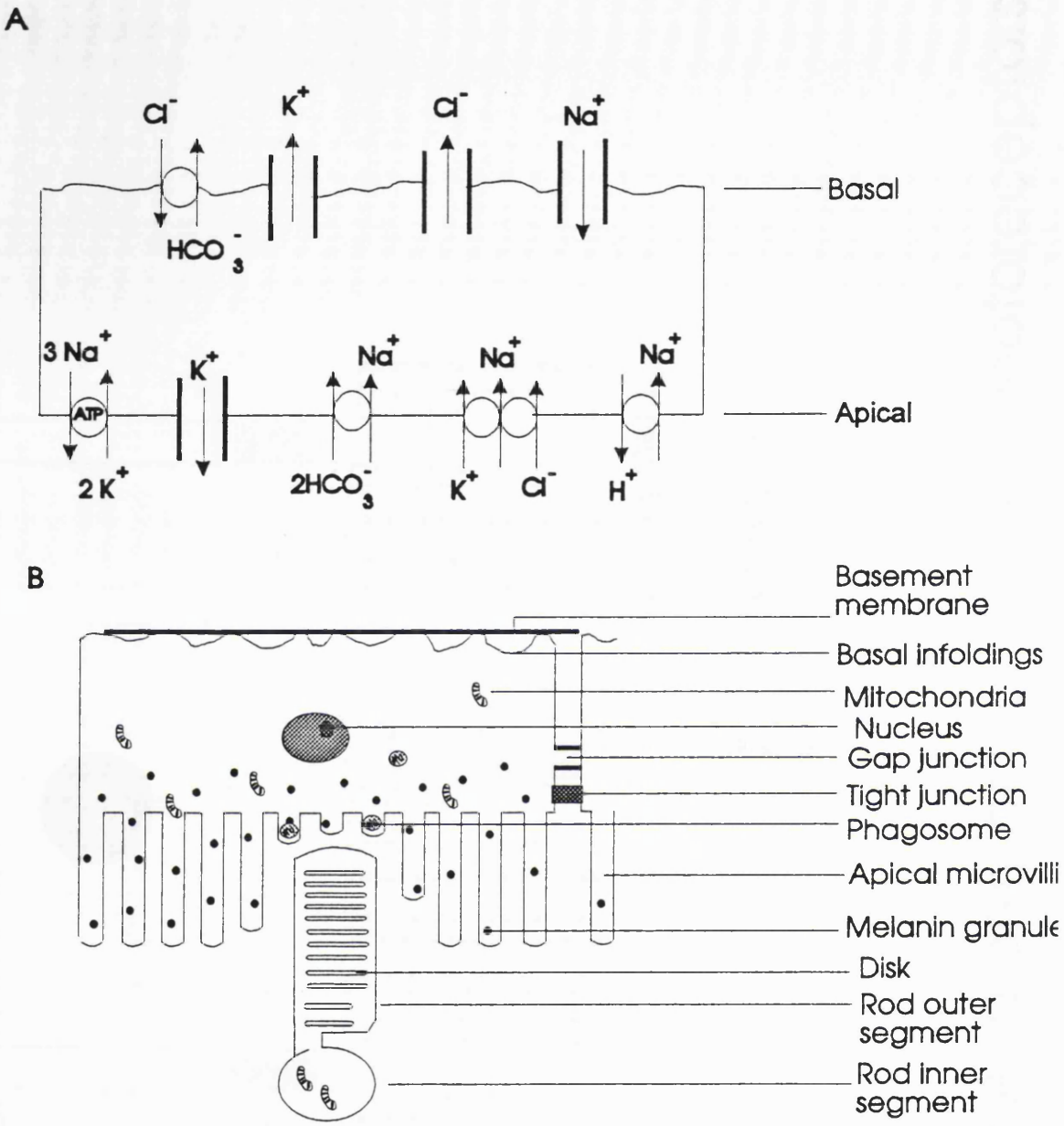

Figure I.1. Basic anatomy and transport physiology of the RPE. A) The main active and passive ion transport mechanisms of the apical and basal membranes. The mechanisms have been found in a range of species; see text for details. B) The basic physical arrangement between the the photoreceptor outer segment and the RPE is shown. Major sub-cellular details of the RPE are also shown.

I.B.2.a. Apical Membrane of the RPE

The surface of the mammalian apical membrane contains several types of cytoplasmic extensions which are made clearly visible by electron microscopy. Short processes 3-4 μm long were shown to ensheath the tips of human rods (Spitznas and Hogan,1970). Steinberg and Wood (1974) found the cones of cats were surrounded by concentric layers of laminae which extend 30-40 μm along the entire length of the cone outer segment. Microvilli of intermediate length (5-7 μm) project in between the outer segments.

Although the apical extensions associate closely with the photoreceptors there is no evidence of junctional connections between the outer segments and the RPE microvilli, even within the extensive cone complex, where the two cells are separated by only 10-20 nm (Steinberg and Wood, 1974). Instead, the subretinal space which separates them (often referred to as the interphotoreceptor matrix or IPM) is composed of a mixture of proteoglycans, glycoproteins, fluid, ions and metabolites. The structure of the molecules varies with their location; the region between the apical membrane and the photoreceptor tips consists predominantly of sialic acid derivatives while the sides of the outer segments are surrounded by chondroitin sulfates (Porello and LaVail, 1986). Fluorescence microscopy shows that the cones are surrounded by a glycosaminoglycan cone-matrix sheath which binds to peanut agglutinin (Hageman and Johnson, 1987) while the rods are engulfed in a more soluble type of glycosaminoglycan which binds to wheat germ agglutinin. It is currently unknown if the differential location of these molecules leads to anatomical differences in the movement of ions through subretinal space.

I.B.2.b. Basal Membrane of the RPE

The basal membrane of the RPE is highly convoluted with numerous infoldings which increase the surface area available for absorption. This plasma membrane is separated from an underlying basement membrane by an

average distance of 1000 Å (Hogan, Alvarado and Weddel, 1971) and the two are joined by hemidesmosome connections which are thought responsible for the strong adhesion of the RPE to the basement membrane (Miki, Bellhorn and Henkind, 1975). The basement membrane forms the inner portion of Bruch's membrane; a multilayered structure approximately 3.5 μm thick consisting of collagen fibrils and elastic fibres. The outer basement membrane of Bruch's is present only over areas where capillaries are present.

I.B.2.c. Lateral Membranes of the RPE

The lateral membranes of RPE cells are relatively smooth and contain tight junction complexes. The zonulae occludentes are found near the apical cell surface, and fuse adjacent cells. They produce a continuous barrier between the choroid and the retina. For this reason it is usual to refer to the two faces of the RPE (as is done in the rest of this thesis) as the apical and basolateral membranes. Two other types of junction are found, the zona adherens and the gap junctions. The role of the former is not well established. The latter are thought to provide a low resistance pathway between adjacent RPE cells, and thus turn the sheet of cells into a synctium.

I.B.3. Photoreceptor Structure

The photoreceptors lie between the RPE and the secondary neurones of the neural retina. They are long cells, with a complex structure. The outer limbs are adjacent to the RPE. Their exact form varies depending upon the type of photoreceptor and the species. The outer limb contains the visual pigment in specialised organelles. It is connected to the inner limb by a short modified cilium. The inner limb, also elongate, contains numerous mitochondria. The main glia of the retina the Müller cells, form condensates around the inner limb at the junction with the layer of photoreceptor cell bodies. These form the outer limiting membrane, which impedes the passage of molecules larger than its

pores; 3.0 - 3.5 nm. (Bunt-Milam et al., 1985). Between the inner limb and the termination of the photoreceptor layer are found the more "neural" portions of the photoreceptors, the connecting process, the nucleus, and the synaptic terminals. There are two main types of photoreceptor: cones and rods. In most animals, rods are by far more numerous. Cones, associated with photopic vision, are so called because of the tapering outer limbs seen in the retinal periphery. They are more concentrated in the macular region while the rods occur more frequently in the periphery. In humans, macular cone outer limbs are slender cylinders approximately 30 μm long. The peripheral cone outer limbs are half this length or less, and taper (Warwick, 1976). In mammals, rods are cylinders of approximately 20 μm in length and 1.2 μm in diameter (Sigelman and Ozanics, 1986) There is great variation in size between species, with amphibian photoreceptors generally larger than mammalian ones.

The inner limb is joined to the cell body region by a connecting process which in foveal cones can be very long. A synaptic pedicle is attached to the anterior end of the cell body region of cones by another connecting process. In foveal cones, the inner limb is separated from the cell body by a greatly elongated process the fibres of Henle. Electron microscopy showed the primate pedicle contains several synaptic ribbons in an area invaginated by numerous bipolar and horizontal cell processes (Dowling and Boycott, 1966; Kolb, 1970). Rod spherules contain only one ribbon, and fewer invaginations. In addition, extensions of the synaptic pedicle can be seen to form gap junctions with adjacent photoreceptors (Gold and Dowling, 1979). Rod-rod junctions are most common, but cone-cone and rod-cone junctions have been reported and all are electrically coupled (Detwiler and Hodgkin, 1979; Attwell et al., 1984).

The most prominent feature of the outer segments is the disks. Each photoreceptor contains between 600 and 2000 disks (Warwick, 1976; Dowling, 1987). In the rod, each disk is an autonomous membrane sack isolated from the external solution except at the base of the outer segment where new disks

are formed by invaginations of the cell membrane. Cones differ in that the membrane infoldings do not close to form true discs. The stack of deeply folded invaginated membrane is partially covered by the surface membrane. The disks contain the photosensitive pigments. Rhodopsin molecules are approximately 20 nm apart, but the disk membrane is relatively fluid and there is considerable lateral movement of the molecule (Poo and Cone, 1974).

Müller cells are retinal glial cells that extend radially throughout the retina, from its vitreal surface, where their end feet form the inner limiting membrane, to the inner segments of the photoreceptors, where they form the outer limiting membrane. In lower animals, extensions of the outer limiting membranes interdigitate with the microvilli of the RPE. The trans-retinal structure of the Müller cells allows them to transport potassium ions away from the photoreceptors and toward the vitreous humour (Newman, 1985).

The retina is supplied blood from two sources. The anterior retinal capillaries supply the ganglion cells, amacrine cells horizontal cells and the bipolar cells, while the choroidocapilliaries provide for the photoreceptors (Sigelman and Ozanics, 1986). The tight-junctional complexes of the RPE mean that any exchange of substances between the choroidocapilliaries and the photoreceptors is mediated by RPE transport.

I.C. Non-Transport Functions of the RPE

The RPE is responsible for a variety of functions which are not necessarily related to ionic transport. They are briefly mentioned here because of their importance to the visual process, and because disruption of these functions can lead to disease. All of these functions depend upon a close physical relationship between the RPE and the photoreceptors, and transport of ions and fluid by the RPE helps maintain the retina in this position (Negi and Marmor, 1986).

1.C.1. Phagocytosis of Photoreceptor Discs

Photoreceptor discs are periodically renewed, and old disks are phagocytosed by the apical membrane of the RPE. Young and Bok (1969) showed that radioactively labelled amino acids from the discs disappeared from the rods and reappeared inside the RPE. A stack of 20-40 discs is detached from the outer segment and subsequently phagocytosed by the RPE apical membrane (Bok, 1985). The discs then are digested with hydrolytic enzymes and the reusable portions are returned to the rods and are incorporated into newly synthesised disks (Young and Bok, 1969). Most of the undigested remains are thought to be exocytosed through the basal membrane. The occurrence of disk shedding is thought to maintain a diurnal rhythm in rats (LaVail, 1981) although the persistence of this rhythm during periods of prolonged darkness suggests that hormonal factors may be important. There is some evidence that a similar renewal process occurs in cones (Hogan et al., 1974), although the absence of distinct discs complicates the interpretation of the findings.

The importance of phagocytosis can be seen with the mutant RCS rats, whose RPE cells have lost the ability to phagocytose discs because the correct signal is not given to the cellular contractile filaments (Chaitin and Hall, 1983). The lack of phagocytotic action leads to an accumulation of disc membrane fragments in the IPM. Eventually, macrophages enter to remove the blockage but simultaneously degrade photoreceptors. This leads to retinal degeneration and loss of sight LaVail, 1979.

I.C.2. The Visual Cycle

The light-sensitive molecule rhodopsin is composed of the protein opsin and the chromophore retinal. Higher animals are incapable of synthesising retinal and it must be obtained from the diet in the form of vitamin-A: retinol. This precursor is stored in the liver and transported through the blood by the

carrier, retinol binding protein (RBP). The basal membrane of the RPE contains receptors for RBP which facilitate the transfer of all-trans retinol from the plasma into the RPE. Once inside the RPE, all-trans retinol is bound to a cellular retinol binding protein (CRBP). An ester synthetase forms retinol esters, which are either stored, or isomerised into 11-cis retinol. 11-cis retinol is then oxidised to 11-cis retinal. 11-cis retinal is transported to the photoreceptors using the carrier protein interstitial retinal binding protein (IRBP) and incorporated into newly synthesised disks at the base of the outer segment (Bok, 1985).

When photons strike rhodopsin, the photoisomerization converts 11-cis retinal to all-trans retinal. The photoreceptors are unable to regenerate the photopigment. A dehydrogenase converts all-trans retinal into all-trans retinol. (Pugh and Cobbs, 1986), The photoreceptors lack the enzymes necessary to complete the regeneration of 11-cis retinal, and all- trans retinol is transported by IRBP back to the RPE, where the series of enzymatic actions outlined above convert the molecule into 11-cis retinal. It is then transferred to the photoreceptors and recycled into new disks (Bok, 1985).

I.C.3. Transport of Metabolites.

Taurine is present in high concentrations in outer nuclear layer of the retina, and is necessary for normal vision (Lake et al.., 1977). For reasons not yet fully understood, it is released into subretinal. space following the onset of light (Scharschmidt et al., 1988). Taurine is then removed from subretinal space by an active sodium-linked uptake mechanism on the apical membrane of the RPE which alters the balance of ions across the membrane and initiates a series of electrical changes in the RPE (Miller and Steinberg, 1976). The ultimate triggering of this response by light has implications for the wider range of light-induced RPE- photoreceptor interactions (See section I.D.2.).

Transport of glucose across the blood-retinal barrier of the rat is

mediated by a stereospecific carrier, for D-glucose entered the vitreous at a rate six times that of L-glucose (DiMattio and Zadunaisky, 1981). In bullfrog, glucose uptake was found to be facilitated, for metabolic inhibitors such as DNP did not effect the rate of uptake (DiMattio and Streitman, 1986)

In isolated bovine RPE clamped in an Ussing-type chamber, a retina to choroid flux of glutamic and aspartic acid was shown (Paulter and Tengerdy, 1986). As glutamate is probably a neurotransmitter used by rods (Slaughter and Miller, 1983), this uptake may influence the transmission of the visual signal.

I.D. Transport Across the RPE

I.D.1. Basic Concepts of Transport

The fundamental requirements of membrane transport have been recognised for many years, although the mechanisms have only recently been understood on a molecular level (Hille, 1992). A brief historical outline of the development of the relevant concepts in ion transport has been included to place the recent knowledge in perspective.

While examining the rate of fluid movement through bladder membranes in 1843, Brücke proposed there were fluid-filled pathways in the membrane only a few water molecules wide that allowed the passage of fluid. In 1899, Overton showed that replacing the hydrogen of a non-electrolyte molecule with a methyl group increased its ability to cross the cell membrane and enter a cell. This implied that the membrane was composed of lipids and molecules not soluble in lipids crossed with difficulty. This experiment underlines one of the basic principles of ion transport; the cell membrane is predominantly hydrophobic, and hydrated ions can only pass through hydrophilic areas in the membrane.

The basis of membrane transport still centres around aqueous pores which pass ions in a selective manner. For some time, the pores were thought

of as a molecular sieve, permeable only by hydrated ions of a certain maximal size. Boyle and Conway (1941) found that anions and cations of similar size passed through the membrane of frog muscle with approximately the same ease and interpreted this finding to mean that the channels selected by size and not charge of the ion. In 1959, Mullins suggested that to enter a narrow pore, the water molecules forming the shell of the ion were shed and replaced by groups bonding from inside the pore. If the ions did not fit properly into the pore, the surrogate water could not bind and the ion would not pass through the channel.

The forces which control the movement of ions through pores are not necessarily dependent upon the pores themselves, or even membranes, but rather upon the energy present in a system with an uneven electrical and chemical distribution of ions across the membrane. The Nernst-Planck equation states that the current across the membrane depends on the potential and concentration difference, and the laws of thermodynamics (Hille, 1992). It predicts that at a precise electrical and chemical distribution, the forces are balanced. No net current will flow across the membrane at this state of equilibrium. For example, if a membrane is permeable to potassium ions, and the concentration of these ions on the two sides of the membrane are unequal, potassium will tend to move down the concentration gradient. The movement of the charged ion sets up a potential difference across the membrane, which discourages the passage of ions: eventually an equilibrium is set up, at which a given concentration difference of potassium will produce no net flow is given by

$$E_K = (RT/zF) \ln \frac{[K^+]_o}{[K^+]_i}$$

where E_K is the potassium equilibrium potential, $[K^+]_o$ and $[K^+]_i$ the different potassium concentrations, R is the gas constant, T the absolute temperature, F is the Faraday constant and z the ionic valence.

In 1902, Bernstein showed that there was an uneven distribution of ions

across the cell membrane, and predicted that the Nernst-Planck relationship for potassium underlay the potential across the cell membrane. However, potassium was not the only permeable ion which contributed to the membrane potential. Goldman (1943) extended the result to all ions. The Goldman-Hodgkin-Katz (GHK) constant field equation predicted that the membrane potential was an equilibrium determined by the distribution of all internal and external ions and the ratios of their permeability across the membrane;

$$E_m = (RT/F) \ln \frac{P_K[K]_o + P_{Na}[Na]_o + P_{Cl}[Cl]_i}{P_K[K]_i + P_{Na}[Na]_i + P_{Cl}[Cl]_o}$$

These equations assume that the electric field either side of the membrane is constant, and that the movement of each ion is independent of that of other ions. They also predict that the current carried across the membrane by an ion was determined by the potential, the concentration difference and the permeability of the membrane to the ion. This predicted that the current-voltage relationship changed as the concentration of ions was increased; the function rectified with increasing ion concentration (Kuffler et al., 1984). In other words, the conductance was not Ohmic. However, the degree of rectification induced by this mechanism is comparatively small.

The importance of the permeability factors in the constant field equation was apparent when the concepts were applied to "excitable" membranes. It was shown that the permeability could be changed in response to particular stimuli, in this case potential (Hodgkin and Huxley, 1952). A description of this work is outside the scope of this thesis. However, certain concepts are relevant to the work presented here, for most membranes contain channels which do not act like passive pores; instead, the activation of these channels is controlled or gated. The potential across the membrane frequently influences channel permeability. The electric field has been shown to control channel opening by causing the movement of an equivalent gating charge across the membrane

(Armstrong and Bezanilla, 1974). This gating charge presumable induces allosteric changes in the channel protein which effect the conducting state.

The GHK equation applies to both the entire cell membrane and an individual channel; the physical laws that determine the relationship are the same. Ions must move through channels in a direction that brings their electochemical gradients to rest. However, the establishment of an electrical gradient requires pumps: mechanisms which do work to move charged ions against the concentration gradient. This is referred to as active transport. An external energy force is required, usually in the form of ATP. Once an ionic disequilibrium has been established, ions can be transported against their gradient if the movement is coupled with that of a different type of ion moving with its gradient. The energy released by the later must be greater than the energy required to move the former: i.e. the coupled process must be energetically favourable. Pumps can be electrogenic and transfer charge across the membrane or they can be electrically neutral. The particular combination of pumps and their distribution are determined by functional requirements of the cell.

I.D.2. RPE Transport

Ions are transported across a layer of tissue if it has asymmetries between its apical and basal membranes and a high paracellular resistance. The apical and basal membranes of the RPE contain different transport proteins and are separated by tight junctions; transport thus occurs across the RPE. The differential location of electrogenic pumps and transporters, and the effectiveness of the paracellular resistance means that the potential difference across the apical membrane to be greater than that across the basolateral membrane in all species tested (Frambach and Mistfelt, 1983; Joseph and Miller, 1991; Miller and Steinberg, 1977b; Tsuboi et al., 1986; Steinberg et al.., 1978). This difference in the membrane potential of apical and basolateral

membranes gives rise to a transepithelial potential (TEP) across the tissue which is apical-side positive. The TEP effects the movement of ions from the subretinal space to the choroid and vice versa in the way a transmembrane potential effects the transport of ions into and out of a single cell.

I.D.2.a. Active Transport Across the RPE

The central features of ionic transport across the RPE have been elucidated during the past fifteen years. Much of this work has involved the Ussing chamber; a system which maintains a sheet of RPE cells with the tight junctions intact and thus allows independent manipulation of the solutions bathing the apical and basolateral faces of the cell membrane. The transport proteins on both sides are expected to respond in a way comparable to that in vivo because the separation of the apical and basolateral membranes is maintained. The potential across the apical membrane is greater than that across the basal membrane; this creates a current which flow internally from the basal to the apical membrane. There is thus a net movement of positive ions towards the apical side. The TEP will fall to zero when a current is passed of equal magnitude but in the opposite direction to that caused by the net ionic flow. This is called the short circuit current (SCC). A drop in the SCC could be caused by a decrease in the net flow of cations towards the apical membrane or an increase in the net flow of anions towards the basal membrane. Thus changes in the SCC indicate changes in ion movement. It follows that the sum of all net ionic fluxes equals the SCC.

Ionic fluxes through hydrophilic pores can be greatly reduced by short circuiting the tissue to remove any electrical gradient while bathing the apical and basal membranes in an identical solution to also remove the chemical gradient across the epithelial layer. This unmasks the pumps and the summed electrical activity of all actively transported ions can be measured. If radioisotopes are used some conclusions can be drawn about the movement of

one ion type through all relevant pumps. Measuring the change in SCC or the membrane potential, as indicated by intracellular recording, induced by specific pump blockers or the removal of an individual ion type on one side of the Ussing chamber can also indicate the presence of a particular mechanism.

I.D.2.a.i. Na^+/K^+-ATPase

The current model of ionic transport across the RPE membranes has been developed over the past twenty five years. Much of the early work concentrated on characterising the Na^+/K^+-ATPase. This pump initially establishes the gradients which power all other forms of ion transport across the RPE. In frog RPE there was a net basal- to- apical flux of Na^+ which accounted for 30-40% of the SCC (Steinberg and Miller, 1973; Miller and Steinberg, 1977a). Most of this flux was inhibited by apical application of 10^{-4} M ouabain, a drug known to block the Na^+/K^+-ATPase in other epithelial cells. Basolateral application of the drug had no effect, suggesting that the Na^+/K^+-ATPase was located on the apical membrane.

Subsequent reports have reinforced the polarised distribution of the Na^+/K^+-ATPase. Autoradiographic studies with tritiated ouabain confirmed the apical location of the pump in frog (Bok, 1980), and the activity of the pump was isolated to the apical membrane (Ostwald and Steinberg, 1980). With the exception of the choroid plexus, which shares the same embryological origin as the RPE, the Na^+/K^+-ATPase is found on the basal membrane of all other epithelial cells which contain it. The Na^+/K^+-ATPase has been shown to be apically located in cat (Steinberg et al. 1980), dog (Tsuboi et al., 1986) chick (Frambach and Misfeldt, 1983) bovine (Miller and Edelman, 1990), cultured human (Kennedy, 1990), toad (Griff, 1990) and foetal human (Quinn and Miller, 1992) RPE cells. The report on toad clarified some confusion surrounding the species, as one of the earliest studies on RPE transport that stated ouabain had no effect on the SCC of toad tissue (Lasansky and DeFrish,

1966).

Additional studies have outlined some of the parameters which influence this pump. In common with the Na^+/K^+-ATPase found in other cells, this pump is electrogenic, pumping three Na^+ ions out of the cell for every two K^+ ions pumped in (Miller et al, 1980, Miller and Steinberg, 1982). The pump thus hyperpolarizes the apical membrane and establishes the sodium gradient. The light-induced changes in subretinal K^+ levels (see section I.D.) led early investigators to examine the influence of the apical K^+ concentration, $[K^+]_a$, on the pump. A decrease in $[K^+]_a$ or an increase in the internal K^+ level, $[K^+]_i$, caused a reduction in the SCC (Oakley, Miller and Steinberg, 1978). It was then shown that the pump rate increased as the $[K^+]_a$ was raised from 0.5 mM to 5 mM (Miller and Steinberg, 1982) i.e. the range over which the concentration varies due to action of light. In addition, this change in $[K^+]_a$ was shown to alter the transepithelial flux of K^+. It was calculated that the reaccumulation of potassium in the subretinal space after prolonged illumination could be achieved in part through the decreased activity of this pump.

The dependence of the Na^+/K^+-ATPase on the $[K^+]_i$ and $[K^+]_o$ indicates that the pump can be indirectly affected by stimuli, such as light, which alter the concentration of these ions. Indirect stimulation may also occur by other methods. The Na^+/K^+-ATPase is activated by cAMP (Hughes et al., 1988). Apical application of cAMP induced a three phase change in the potential across the apical and basolateral membranes; the second phase, a hyperpolarization of the apical membrane, was inhibited by addition of apical ouabain and thus thought to represent an increase in the pump activity. The third phase is a repolarization of the membranes. The proposed mechanism involves (in phase one) an increase in the basolateral membrane anion conductance and basal depolarisation. This has recently been supported by whole cell recordings discussed in section I.D.2.b.i. (Hughes and Segawa, 1993).The resulting increase in TEP increases the driving force for Na^+-coupled

anion transport across the apical membrane, which would increase $[Na^+]_i$ (phase 2). Elevations in $[Na^+]_i$ have been associated with an increase in the activity of the Na^+/K^+-ATPase in other tissues (Beauge, 1984); if the RPE pump is similarly sensitive, this would explain the observed increase in pump activity.

Stimulation of the Na^+/K^+-ATPase by increased $[Na^+]_i$ would also explain the increase in pump activity after apical administration of taurine, as taurine is thought to enter the RPE through an apically-located Na^+-uptake mechanism (Scharschmidt et al., 1988). The complex interactions which can potentially alter the Na^+/K^+-ATPase represent the interrelated nature affecting other mechanisms of RPE ionic transport.

I.D.2a.ii. Regulation of Internal pH

The difficulty in separating out the actual mechanisms responsible for ion transport is evident when studies into the regulation of internal pH (pH_i) are examined. Contradiction exists repeatedly in the literature; even the direction of net HCO_3^- active transport has been reported as both from apical to basal (Miller and Steinberg, 1977b; DiMattio et al., 1983) and from basal to apical (Tsuboi et al., 1986). Species differences, diurnal and seasonal variation and differences in protocol may all contribute to the contradictions. An additional source of confusion arises because the many of the blockers used to determine the specific transport mechanism are not specific themselves. The situation is ultimately complicated because it is not possible to isolate a mechanism free of the indirect influences of other cells.

One of the earliest applications of an Ussing chamber to the study of transport across the RPE was reported by Lasansky and DeFrish (1966). They measured transport across toad RPE by using radioisotopes in conjunction with measurements of the SCC. The active flux of $^{36}Cl^-$ towards the choriod accounted for 66% of the SCC. Apical administration of the carbonic-anhydrase inhibitor acetazolamide did not affect the transport of $^{36}Cl^-$, but did reduce the

SCC by 20%. This suggested that acetazolamide was inhibiting a mechanism which pumped anions towards the choroid, possibly HCO_3^-. They concluded that HCO_3^- is actively transported towards the choroid.

In frog RPE however, the apical to basal Cl^- flux was reduced by apically applied acetazolamide (10^{-3} M) and a 90% reduction in apical [HCO_3^-] (Miller and Steinberg, 1977b). This suggested that the active transport of HCO_3^- was linked with that of Cl^- . This report also found that the net apical to basal flux of Cl^- was seasonally dependent, peaking in the spring and declining in the summer. Although DiMattio et al. (1983) found no evidence of such variation in the same species, the possibility of some seasonal influences remains, in amphibians at least, because of the seasonal nature of their life cycles. This paper contradicted the findings of Steinberg and Miller in other ways; ouabain reportedly inhibited Cl^- flux while the removal of HCO_3^- did not. Bathing the tissue in a Na^+-free solution in the presence of ouabain reduced the SCC to zero. This suggested that all active transport involved Na^+ through a Na^+/Cl^- and a Na^+/HCO_3^- transporter, but the two mechanisms function independently. A study on dog further complicated the model for it suggested both a HCO_3^-/Cl^- exchanger and a Na^+/Cl^- transporter, as Cl^- transport was partially inhibited by ouabain (Tsuboi et al., 1986).

Recent studies on frog have been more consistent. An electrogenic transporter was reported on the apical membrane of frogs which moved one Na^+ and two HCO_3^-, and thus one negative charge, out of the cell with each rotation (Hughes et al., 1989). Removing Cl^- had no effect on this transporter, while the anion transport and conductance blocker, DIDS, (10^{-3} M) depolarized the cell. This would be expected if the drug was blocking the hyperpolarizing action of the transporter. When the potential across the apical membrane is increased, the pump can reverse and transport both HCO_3^- and Na^+ into subretinal space. The electrogenic properties of the Na^+/HCO_3^- transporter imply that any conditions changing the potential across the apical membrane

can alter pH_i.

Using ion selective electrodes, a similar transporter was identified on frog RPE by LaCour (1989). Removal of either Na^+ or HCO_3^- from the solution bathing the apical medium led to a decrease in the internal level of the other ion and depolarised the membrane. The same paper reported that passing a basal to apical current of 30 $\mu A/cm^2$ caused an increase in pH_i and $[Na^+]_i$. These changes were blocked by SITS, which has been reported to block the Na^+/HCO^-_3 - transporter in other cells.

The evidence above appears to strongly support the existence of an electrogenic Na^+/HCO_3^- transporter. However, the two drugs used to block the transported, DIDS and SITS, are not particularly selective. For example DIDS (5×10^{-4} M) reduced the open probability of single Cl^- channels in excised patches, where there can be no possibility of an indirect effect (Light et al., 1990). Because the experiments above rely upon an indirect measurement of activity, it is important to ensure the blockers are not just blocking channels. The electrochemical gradient predicts that Cl^- will passively flow out of the cell and thus blocking these channels should hyperpolarize the cell, not depolarize it (Hughes et al., 1989). In addition, the depolarizing effect of DIDS was absent when either Na^+ or HCO_3^- was removed from the apical bath. These experiments suggest that, in this case, DIDS is producing its effect by blocking the Na^+/HCO_3^- transporter. However, the results from experiments based upon the blocking action of these drugs should be interpreted with caution.

The existence of a $Na^+/-HCO_3^-$ and a Na^+/H^+ transporter has been supported with the fluorescent pH sensitive dye, BCECF, (Lin and Miller, 1991*a*). A NH_4Cl prepulse was used to increase intracellular pH_i ; the recovery from this alkanization could occur if the apical bath contained either HCO_3^-or HCO_3^- -free solution. If HCO_3^- was present, the recovery was blocked by DIDS and Cl^- removal had no effect upon this block; this suggesting a $Na^+/-HCO_3^-$ transporter controlled pH_i. If HCO_3^- was absent, amiloride blocked the

recovery. When $[K^+]_a$ was raised from 2mM to 5mM, the pH_i increased. The apical membrane depolarisation caused by the increase in $[K^+]_a$ was thought to increase the driving force on the Na^+-HCO_3^- transporter. However, this depolarization would also increase the driving force for H^+ exit.

These mechanisms are also present in mammalian cells. When HCO_3^- was removed, at constant pH, from the apical side of bovine RPE, the apical membrane depolarised (Joseph and Miller, 1986). In human cells, fluorescent work with BCECF has shown that removal of Na^+ acidifies the cells (Lin et al., 1992.) The recovery from acid load in these cells required Na^+ and was blocked by 1 mM apical amiloride. This drug inhibits the Na^+/H^+ exchanger in other epithelial cells at this concentration, but it has also been shown to reduce the open probability of single Na^+ channels in other ocular epithelia at a concentration of 5×10^{-5} M (Jacob et al., 1985). A reduction of K^+ from 5 to 2 mM caused a decrease in pH_i ; this acidification did not occur in the absence of HCO_3^-. These results suggest that human RPE cells possess a Na^+/H^+ exchanger and Na^+/HCO_3^- transporter, and that the later may effect the intracellular pH in response light-induced changes in K^+. They do not rule out some role for Na^+ channels, although it is difficult to speculate on what that role might be.

The presence of both a Na^+/H^+ and a Na^+/HCO_3^-exchanger on the top surface of cultured bovine RPE cells was suggested by Keller et al. (1988), although questions surrounding the polarity of cultured cells make the assignment of this mechanism to the either side of the membrane difficult. An increase in pH_i was caused by removing sodium acetate from the solution bathing these cells, while a decrease in pH_i was caused by the removal of NH_4Cl. The recovery from acid load required Na^+ and was blocked by 10^{-3} M amiloride. Again, it is possible that this involves a Na^+ channel, although it is difficult to propose a role. The recovery from increased pH required Cl^- in the bath and was inhibited by DIDS. Furthermore, DIDS did not inhibit the apical

uptake of $^{22}Na^+$, which suggests that a Na^+/HCO_3^- transporter was not present on these cells. The action of DIDS may have been to block Cl^- channels; this suggests a possible role for a HCO_3^-/Cl^- exchanger, although this inference cannot be drawn from these inconclusive studies.

The presence of a HCO_3^-/Cl^- exchanger on the basolateral membrane has tentatively been suggested in frog RPE. $[Cl^-]_i$, as measured with an ion selective electrode, increased when HCO_3^- was removed from the basal membrane (Fong et al., 1988). The apical to basal movement of Cl^- in frog was also was inhibited by basal application of DIDS (Edelman et al., 1988). The HCO_3^-/Cl^- exchanger found in cultured bovine cells may be present on the basolateral membrane in vivo, as polarity is not always preserved in cultured cells.

I.D.2.a.iii. Na^+-K^+-Cl^- Cotransporter

The evidence in section I.D.2.a.ii. above suggests that a mechanism for actively transporting Cl^- across the apical membrane exists, although it is distinct from the Na^+/HCO_3^- transporter. An early model of frog RPE indirectly suggested the coupled Na^+/Cl^- transport through a mechanism inhibited by furosemide, bumetanide and SITS (DiMattio et al., 1983). In embryonic chick RPE, evidence was presented for an apical $Na^+/K^+/Cl^-$ cotransporter (Frambach and Misfeldt, 1983); the removal of either $[Cl-]_o$ or $[Na^+]_o$, or the presentation of furosemide caused TEP to fall, but the effect was not cumulative suggesting all these conditions inhibited a $Na^+/K^+/Cl^-$ mechanism. Similar results suggested a $Na^+/K^+/Cl^-$ transporter on cultured bovine RPE (Frambach et al.,1989). Direct evidence for the involvement of K^+ came from studies on cultured human RPE (Kennedy, 1990) The fraction of ^{86}Rb flux not inhibited by ouabain was dependent upon the presence of both Na^+ and Cl^- and was inhibited by bumetanide. In bovine RPE, bumetanide reduced the ^{86}Rb and the ^{36}Cl apical to basal flux (Miller and Edelman, 1990). Bumetanide

induces similar electrical change in foetal human RPE cells (Quinn and Miller, 1992). In bullfrog RPE, the $Na^+/K^+/Cl^-$ cotransporter is responsible for reswelling the cell after the presentation of a hyperosmotic pulse (Adorante and Miller, 1990). Most significantly, the reswelling required that $[K^+]_o$ was raised from 2mM to 5mM, suggesting the transporter is extremely sensitive to changes in $[K^+]_o$ within this range.

I.D.2.b. Passive Transport Across the RPE

The passive transport of ions through channels in the RPE has not been researched as thoroughly as the mechanisms for active transport, but the basic principals are known. Ussing chamber work has helped isolate the conductances to either membrane but cannot distinguish between different types of channels passing the same type of ion. The single channel and whole-cell variants of the patch clamp technique can be used to separate these individual currents and the channels that produce them.

Miller and Steinberg (1977*b*) changed the concentration of ions in the solution bathing either side of frog RPE mounted in an Ussing chamber and monitored the resultant changes in the membrane potential of a single cell with a microelectrode. Raising the apical concentration of potassium from 2 mM to 55 mM depolarized the apical membrane by 25 mV, while an equivalent increase in the basal potassium depolarized the basal membrane by 30 mV (Miller and Steinberg, 1977*b*). A ten fold increase in the concentration of Na^+, or Cl^- changed the membrane potential by less than 3 mV. This was taken to mean that both membranes were primarily permeable to potassium. More recently, the basolateral membrane has been shown has a Cl^- permeability which is inhibited by DIDS (Edelman et al., 1988). However, the unspecific blocking action of DIDS means further evidence is required to support this interpretation. This has recently been provided for toad RPE using Cl^- - selective electrodes (Fujii et al., 1992). They showed that the intracellular

concentration was above its equilibrium, indicating it was actively transported. By changing the level of Cl^- outside the basal membrane and monitoring changes in intracellular potential and $[Cl^-]_i$, they concluded that 45% of the basal membrane conductance was carried by Cl^-. In addition, passing a transepithelial current which depolarized the basal membrane led to an increase in $[Cl^-]_i$, while hyperpolarization led to a decrease in $[Cl^-]_i$; these changes followed Nernstian predictions.

In bovine RPE, increasing apical K^+ four-fold depolarized the apical membrane by 25 mV (Joseph and Miller, 1991). This response was nearly Nernstian, and indicated that 90% of apical conductance was carried by potassium. Raising basolateral $[K^+]$ by from 5 to 50 mM depolarized the basal membrane by 2 mV. However, decreasing basolateral Cl^- from 130 to 12 mM depolarized the basal membrane by 9 mV. The voltage responses to changes in the concentration of Na^+ and HCO_3^- were negligible. Thus the basolateral membrane of bovine RPE possesses considerable Cl^- conductance.

Information has begun to accumulate about human RPE cells (Quinn and Miller, 1992). With foetal cells, raising apical potassium from 5 to 20 mM depolarized the apical membrane by 16 mV. Ba^{++} reduced this response by 80%. Raising basolateral potassium depolarized the basolateral membrane by 6 mV. The apical membrane of adult human RPE was depolarized by 13 mV after a corresponding increase in apical potassium. The relative basolateral conductance to Cl^- was not tested.

Recordings using the whole cell variant of the patch clamp technique support the predominance of potassium permeability in frog (Hughes and Steinberg, 1990), turtle (Fox and Steinberg, 1992), monkey and human RPE (Wen et al., 1993). Single channel data also shows a preponderance of potassium channels (Fox et al., 1988). These reports are closely related to the findings of this thesis and are discussed in more detail in Chapter VI. A brief description is presented here to provide a more complete view of passive

transport across the RPE. The references above apply to the entire section; individual work can be identified by the species being discussed. The patch clamp technique is discussed in detail in later chapters, but an outline of the technique follows.

In whole cell recording, the entire cell is voltage clamped, and the currents recorded represent an average of all the channels in the cells. The current evoked by a series of hyperpolarizing and depolarizing voltage steps from a holding potential indicates the properties of channels in the cell membrane, for example whether the channels rectify, or whether the state of activation changes with time. The particular type of ion responsible for the current can be determined by examining the potential at which the tail current reverses: the channels are briefly open after an activating pulse and no current will flow through them at the Nernst equilibrium potential of the permeant ion. In single channel recording, current flowing through individual channels is measured. The change in current in response to different potentials will indicate the channel characteristics

Voltage-dependence of channel activation has been shown by all of the whole cell studies. For example, inwardly rectifying currents have been shown in frog, monkey and human cells. Tail currents reversed close to the Nernst potential for potassium, indicating potassium selectivity. In foetal human and cultured human cells, these currents showed a time-dependent inactivation which disappeared when the cells were bathed in Na^+-free solution.

Outwardly rectifying currents were recorded in all species. In turtle, this current activated when the cell was depolarized to potentials more positive than -42 mV. The current inactivated, and the time constant of inactivation shortened as the test potential became more positive. A similar current was recorded in frog. The current was activated by depolarizing voltage pulses more positive than -30 mV, and although it did inactivate, the rate of inactivation was not effected by potential. In fresh monkey, adult human and

some cultured human cells, a current was activated by depolarizations more positive than -20 mV, but this current did not inactivate. However, some cultured human and all foetal human cells, a transient outward current was recorded. This current was activated by depolarizing voltage pulses more positive than -30 mV and inactivated rapidly, but the rate of inactivation was not effected by potential. Tail current analysis showed the outward currents described above for all species were carried by potassium. In addition , the currents were reduced by potassium channel blockers: 4-AP blocked the current in frog (1 mM), foetal human (5 mM) and turtle (10 mM) cells. 20 mM TEA blocked the current in frog and adult human cells and 25mM TEA blocked turtle RPE cells. These are large concentrations of TEA, and in frog and human preparations, the amount of NaCl was correspondingly reduced to keep the osmolarity constant. Interestingly, 20mM TEA did not effect the current seen in foetal human cells.

Additional currents were described in some of the reports. For example, a non-inactivating outward current was sometimes observed in frog RPE when the cells were depolarized to potentials more positive than +10 mV. This current reversed close to the Cl^- equilibrium potential. In turtle, depolarization to potentials more positive than +40 mV induced slowly activating outward currents which did not inactivate. The tail current reversed at -40 mV when the cells were bathed in dilute bath solution, indicating the current is cation selective. Hyperpolarizing pulses in turtle cells activated a non-inactivating inward current. The reversal potential of the tail current shifted when the solution bathing the cells was changed from NaCl to NaGluconate, which indicates some anion permeability. However, the current was increased by reducing external Na^+; it is possible that Na^+ and Cl^- are transported together in this current. This current was recorded with TEA, 4-AP, quinidine, EGTA and DIDS in the bath, but was reduced by 100 μM $LaCl_3$.

Recently, cAMP has been shown to activate a current in frog RPE

(Hughes and Segawa, 1993). This current does not rectify very much, nor does it inactivate. This current was not affected by Ba^{++}, or by changing the concentration of K^+, Na^+ or HCO_3^-, but it was reduced by the Cl^- channel blockers DIDS, DNDS and niflumic acid. In addition, the tail currents reversed at the Cl^- reversal potentials over a variety of Cl^- concentrations. It was concluded that cAMP activates a Cl^- selective channel .

Single channel recording of cultured human RPE cells has shown three different types of potassium selective channel with mean conductances of 27pS, 45 pS and 99 pS (Fox et al., 1988). A 300 pS channel was also described, although it did not appear to discriminate between anions and cations very strongly. None of the channels showed any voltage dependence of activity; the probability of the channel being in the conducting state was not effected by the potential across the membrane. The relationship between these channels and the currents observed in the whole cell studies is unclear, for all of the whole cell reports described voltage dependent currents. This inconsistency forms the basis for the work in this thesis

I.E. The Influence of Light

The transport of ions across the RPE is indirectly altered by light. The relationship is reciprocal, and the transport of ions across the RPE can alter the photoreceptor's response to light. These issues are discussed in section I.E.2. Since the influence of light is important to the RPE, this raises the question of the mechanisms of phototransduction. First, it is necessary to examine the ionic basis of the photoreceptor light response.

I.E.1. Effect of Light on the Photoreceptors

In the dark, a constant current flows into the outer limb from the more vitreal portion of the rod (Hagins et al., 1970). This causes the outer segment to be more negative than the inner. Most of this current is produced by Na^+

flowing in through "light sensitive" channels on the outer segment and K^+ leaking out of channels in the inner segment. The light-sensitive channels are unselective and, in the presence of 1mM Ca^{2+}, allow Li^+, Na^+, K^+, Rb^+ and Cs^+ to pass through with the relative permeabilities of 1.14:1.0:0.72:0.49:0.24 (Hodgkin et al., 1985). However, in physiological saline, the electrochemical gradients dictate that the current is carried predominantly by sodium, with Ca^{2+} contributing approximately 10% (Nakatani and Yau, 1988). Calcium passes through the channel more slowly than sodium, and thus reduces the net current through the channel (Menini et al., 1988).

The light-sensitive pigment rhodopsin is bound to the disk membrane, and therefore an intermediate must cross the cytoplasm and modify the state of the light-sensitive channel on the plasma membrane. For some time it was unclear whether changes in the concentration of Ca^{2+} or cGMP conveyed this message. The identity of the messenger was eventually confirmed by Fesenko et al. (1985), who used the inside out variant of the patch clamp technique to show that cGMP and not Ca^{2+} opened the channel when applied to the intracellular face of the rod membrane. The light sensitive conductance is the only pore in the outer limb: and the slope of the relation of [cGMP] to conductance shows that three cGMP molecules need to bind in order to open the channel (Zimmerman and Baylor, 1986). In the dark, less than 5% of these channels are usually open (Yau and Baylor, 1989). This increases the sensitivity of the system because the requirement for three cGMP molecules means that small increases in [cGMP]i produce the greatest change in membrane current when the nucleotide is at low concentrations, and thus few channels are open.

An electrogenic $Na^+(Ca^{2+}\text{-}K^+)$ exchanger located on the outer segment contributes 5% to the dark current (Hodgkin and Nunn, 1987). This brings four Na^+ into the rod and extrudes one Ca^{2+} and one K^+ with each rotation (Cervetto et al., 1989). The exchanger is powered by K^+ gradients (Schnetkamp et al.,

1989) and helps remove Ca^{2+} which entered through the light-sensitive channel. The leak of K^+ through inner segment channels carries the majority of the dark current out of the photoreceptor. K^+ and Na^+ gradients are maintained by the inner segment Na^+/K^+-ATPase which pumps three Na^+ out and two K^+ into the rod (Steinberg and Wood, 1975).

When light strikes the retina, the absorption of photon energy by rhodopsin causes the isomerization of the retinol portion of the molecule from 11-cis to all-trans and leads, via several intermediary stages, to the formation of metarhodopsin II. This initiates the enzyme cascade known as phototransduction. This activated form of rhodopsin, Rh* moves laterally along the disk membrane until it interacts with the G-protein transducin. Rh* initiates the release of GDP from transducin (Fung and Stryer, 1980) and this vacated binding site is then filled by GTP. The α-subunit separates and carries the signal by binding to phosphodiesterase (PDE) and removing two of its gamma subunits. This active form of PDE leaves the disk membrane and moves into the cytoplasm, where it catalysis the hydrolysis of cGMP to GDP (McNaughton, 1990). As mentioned above, cGMP directly opens cation channels on the outer segment plasma membrane (Fesenko et al., 1985); when light initiates the hydrolysis of cGMP to cGDP, the channels close, and the resulting hyperpolarization of the rods reduces the amount of transmitter released from the synaptic vesicles. The gain on the system is substantial; each Rh* can activate 500 G-proteins (Fung et al., 1981), and while the α-GTP activates only one PDE, each PDE can hydrolyse 100 cGMP molecules. Thus one isomorization can cleave 105 cGMP, which causes 0.05% of the light-sensitive channels to close (McNaughton, 1990).

The internal levels of Ca^{2+} must be precisely regulated because and increase in $[Ca^{2+}]_i$causes the light-sensitive channels to close and can alter the shape of the light-induced current measured in the rods by suction electrodes (Hodgkin et al., 1985). If $[Ca^{2+}]_i$ is kept constant by introducing calcium buffers

to the rod, the response to a flash of light was not dependent upon the state of light adaptation, suggesting Ca^{++} contributed to the smaller current response usually seen in the light adapted rod (Torre et al., 1986). This is thought to occur because physiological levels of calcium inhibit the cyclase which produces cGMP (Lolley and Racz, 1982). The drop in $[Ca^{2+}]_i$ resulting from the closure of light-sensitive channels increases cyclase activity and thus the number of open channels. Unregulated changes in $[Ca^{2+}]_i$ can therefore alter the dark, and light, currents.

I.E.2. Effect of Light on the RPE

In addition to its effect on the neural retina, light initiates three major electrical changes in the RPE which can be recorded with a corneal electrode. The earliest of these can be detected in the c-wave of the electroretinogram (ERG) and occurs within a few seconds of the light flash in all species tested, including cats (Steinberg et al., 1970) and humans (Nilsson and Skoog, 1975). The fast oscillation trough (FOT) and the light peak occur approximately 20 seconds and 5 minutes respectively after the light stimuli. These last two responses are not present in frog but are found in reptiles, birds, mammals and toads (Griff, 1990). The electroretinogram is illustrated in Figure I.2.

The lack of any physical connection between the photoreceptors and the RPE implies that an indirect method must be responsible for these three light induced electrical responses measured in the RPE. In 1976, Oakley and Green found that $[K^+]_o$ dropped from 5mM to 2mM in the subretinal space of frogs and that this decrease closely paralleled the time course of the c-wave of the ERG. This decrease occurs because the light-induced closure of the outer-segment channels very quickly hyperpolarizes the photoreceptor and stops the passive leak of potassium from the inner segment. The Na^+/K^+-ATPase on photoreceptor inner segments continues pumping K^+ into the cell for some time, causing a decrease in subretinal K^+ which reaches its lowest point at the

inner segment level (Oakley et al., 1979). If the light stimulus is maintained, the concentration of potassium in the subretinal space recovers towards its original level and subsequently overshoots the baseline when the light is removed (Steinberg et al., 1980). Both responses were eliminated by ouabain, indicating that the recovery was caused by a reduction in the rate that the photoreceptor Na^+/K^+-ATPase as $[Na^+]_i$ drops (Shimazaki and Oakley, 1984).

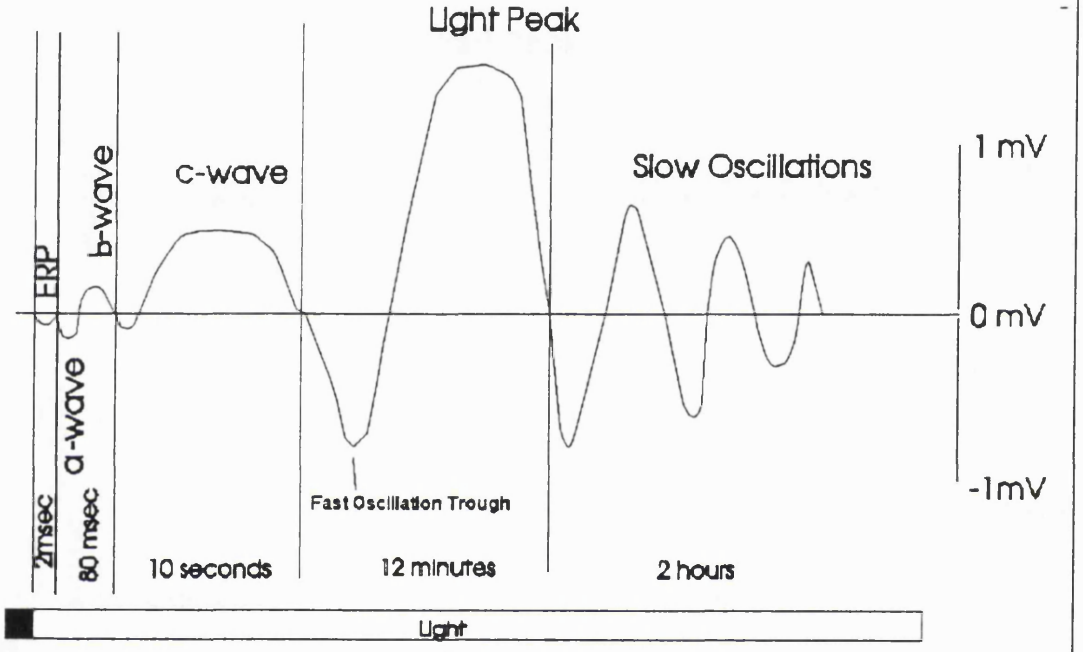

Figure I.2 Diagram of the DC electroretinogram. Response as would be recorded on human cornea. Note changing time scale. Adapted from Marmor and Lurie, 1979.

The drop in $[K^+]_o$ hyperpolarizes the apical membrane of the RPE, increasing the TEP across the tissue (Oakley, 1977), which leads to the RPE contribution to the c-wave. However, both the light peak and the FOT have been associated with conductance changes in the basal membrane. The FOT is a delayed basal hyperpolarization (DBH) associated with a decrease in the basal membrane conductance, G_b (Griff and Steinberg, 1984). In bovine tissue,

it has recently been shown that the DBH, averaging 7.2 mV, coincides with a drop in intracellular Cl^-, as measured with fluorescent dyes (Joseph and Miller, 1991). The DBH in bovine tissue is blocked by basal application of DIDS and by apical application bumetanide, which is thought to inhibit the $Na^+/K^+/Cl^-$ cotransporter. While the DBH is mediated by the apical membrane, the light peak is associated with a depolarization of the basolateral membrane and is blocked by basolateral DIDS (Gallenmore and Steinberg, 1989); this implies that the light peak results from an increase flow of Cl^- out of the basolateral membrane. It is still uncertain what causes the change from decreased basal chloride conductance in the FOT to the increase of the light peak; Fujii et al. (1991) showed that voltage-gated channels are not responsible for the changes in chick RPE. However, work on bovine tissue suggests this switch could be triggered by a potential light-induced release of epinephrine, as the drug increases basal chloride conductance, and indirect evidence suggests this occurs via an increase in internal Ca^{2+} (Joseph and Miller, 1992).

The interactions between various mechanisms suggest alternative methods by which light may alter RPE transport. A pH-sensitive mechanism could contribute to the conductance changes in some as yet unknown way, as raising $[K^+]a$ from 2mM to 5mM raised internal pH of frog RPE if HCO_3^-- was present in the bath (Lin and Miller, 1991*b*). This shift in pH_i probably occurs because the rise in $[K^+]_a$ depolarises the apical membrane and the Na^+/HCO_3^- transporter is activated by depolarization (Hughes et al., 1989). The $Na^+/K^+/Cl^-$ cotransporter can also contribute to the light- evoked responses. As mentioned in section I.D.2.a.iii., this transporter seems to work at 5mM $[K^+]_a$, but not at 2mM $[K^+]_a$ (Adorante and Miller, 1990). This may explain the observation that raising $[K^+]_a$ from 2 - 5 mM changes the direction of energy driven Cl^- transport from absorption to secretion (Fong et al., 1988); less Cl- can enter the cell when the potassium driving force is removed because their movement is coupled. This still does not explain how basal conductance is increased in the

light peak, but the action of the $Na^+/K^+/Cl^-$ cotransporter, at least, may contribute to the FOT.

The ionic system which co-ordinates the three light responses seen in the RPE can also modify the ionic environment surrounding the photoreceptors. This is important because the transmission of the photoreceptor signal, like that of all neurones, depends upon the ratio of internal and external ionic concentrations. In photoreceptors, this need is accentuated because Ca^{2+} inhibits guanylate cyclase and thus modifies the light response. Calcium levels are controlled by maintaining an equilibrium between the inflow of Ca^{2+} through the light sensitive channels and its extrusion through the Na^+-(K^+-Ca^{2+}) transporter. The activity of the Na^+-(K^+-Ca^{2+}) transporter, however, is influenced by the concentration of K^+ in subretinal space. Raising $[K^+]_o$ from 2.5 mM to 10 mM reduced the inward current through light-sensitive channels by 34%, and the time needed for the current levels to return to baseline after a flash was dependent upon $[K^+]_o$ in the range 0 mM - 10 mM (Hodgkin et al., 1985). Increasing $[K^+]_o$ dropped the driving force on K^+ exit through the transporter, and as this is coupled to the Ca^{2+} extrusion, $[Ca^{2+}]_i$ rose and guanylate cyclase was inhibited. As this is the within the range of $[K^+]_o$ present in both light and dark, mechanisms which influence potassium levels can modify the photoreceptor response.

The RPE contributes in several ways to maintaining a constant level of K^+ in subretinal space. The decrease in $[K^+]_a$ induced by light is capable of slowing the Na^+/K^+-ATPase pump on the RPE apical membrane of frog (Miller et al., 1980) and toad (Griff, 1990), which indicates the pump removes less K^+ from subretinal space when levels are already low. The K^+ channels on the RPE apical membrane are thought to contribute more significantly to keeping $[K^+]_a$ constant, and several different mechanisms have been proposed. Both are based upon the observation that the apical to basal flow of K^+ is adjusted when changes in $[K^+]_a$ occur. The first maintains that the

depolarisation of the apical membrane caused by increasing $[K^+]_a$ at the onset of dark is sufficient to increase the outward drive of K^+ ions across the basal membrane of frog RPE (Immel and Steinberg, 1986). When the apical membrane was depolarised by blocking K^+ channels with Ba^+, the Na^+-K^+ATPase with ouabain or both, $[K^+]i$ was assumed not to change. This led to the conclusion that the reduction of the inward electrical gradient across the basal membrane was itself sufficient to increase K^+ efflux across the basal membrane. The second theory was based upon the proposed effect of the electrochemical gradient upon the permeabilities of both apical and basal membrane (LaCour et al., 1986). The results suggested that the conductance of both membranes changed when $[K^+]_a$ was altered; G_a increased at low $[K^+]_a$ allowing more K^+ to return to subretinal space and at high $[K^+]_a$, g_a fell and forced more K^+ to exit via the basal membrane. Possible mechanisms underlying the conductance change were not presented.

Both models explained how the membrane mechanisms of the RPE could contribute to the homeostasis of subretinal K^+ levels, but both were limited by their assumption that the K^+ channels were not gated by voltage or any second messenger. However, Hughes and Steinberg (1990) have reported the existence of voltage-sensitive K^+ currents in frog RPE. It has yet to be determined whether the light-induced changes in $[K^+]_a$ are sufficient to activate these currents. Miller and Farber (1984) have shown that forskolin elevates internal levels of cAMP in frog RPE, and that this increase caused a rise in the active apical to basolateral flux of K^+. It was later shown this was caused by the stimulation of the Na^+-K^+ pump (Hughes et al., 1988). If light led to a reduction in subretinal space of substances that produced a similar effect on cAMP levels, this would contribute to the regulation of potassium levels. Recent experiments on bovine RPE suggest that after a short delay, epinephrine decreases the apical K^+ conductance and increases basal Cl^- conductance (Joseph and Miller, 1992). Catecholamines are released in the retina by the

onset of light (Deary and Burnside, 1989); if epinephrine can diffuse into subretinal space it may provide an additional way to modify $[K^+]_a$. An epinephrine-induced decrease in apical K^+ conductance at light on-set is not consistent with the conductance increases observed in changing $[K^+]_a$ (LaCour et al., 1986). Further work must be done to clarify the timing of any epinephrine signal and determine the messenger systems involved, for both Ca^{++} and cAMP have been suggested. Nevertheless, the hormonal modification of the RPE's response to light is very possible, and must be considered in any dynamic model.

Recently, concrete evidence has been presented which shows potassium channels on the apical membrane can largely explain spatial buffering of subretinal potassium (Segawa and Hughes, 1993). Whole cell recordings demonstrated that, at the normal resting membrane potential, current through the inward rectifier increased as the external concentration of potassium was decreased from 5 mM to 2 mM. At the potential, the current will flow out of the cell. As the inward rectifier channels are expected to be on the apical membrane, this means that more potassium flows out through these channels and into subretinal space when external potassium levels are low. As these experiments were performed in voltage clamp, it was clear that this effect was based solely upon the level of potassium, and not indirectly via a change in the membrane potential.

In addition to these major physiological classifications, some information is known about the effect of light upon other transport mechanisms. For example, it has been suggested that calcium enters the RPE through a Na^+/Ca^+ exchanger, for the uptake of ^{45}Ca into frog RPE cells required extracellular sodium and was not blocked by the Ca^{2+} channel blocker verapamil (Salceda, 1989). The uptake of $^{45}Ca^{2+}$ was greatest in the light, suggesting a role for K^+ transport and the Na^+/K^+-ATPase pump.

I.F. Ionic Control of Fluid Movement Across the RPE

I.F.1. Clinical Relevance

Fluid moves across membranes with ions. In the RPE this movement is particularly important because the active transport of fluid towards the choroid contributes to retinal adhesion (Negi and Marmor, 1986). In diseases such as Central Serous Chorioretinopathy (CSC) a loss of vision occurs because defective transport mechanisms on the RPE membrane cause an accumulation of fluid in the subretinal space, between the photoreceptors and the retinal pigment epithelium (Marmor, 1989). The causes of senile macular degeneration, the most common cause of blindness in the western world, and rhegmatogenous retinal detachment are not initially in RPE transport mechanisms, but it is the long-term accumulation of fluid in subretinal space which leads to a loss of sight (Steinberg, 1986). Effective treatment of these conditions depends upon an clear understanding of the basic physiology behind fluid movement.

I.F.2. Basic Mechanisms

Fluid absorption has been linked with the active transport of HCO_3^- and Cl^-. Removal of HCO_3^- reduced both fluid transport and the SCC by 70% in frog, suggesting the movement of fluid results from the active transport of HCO_3^- (Hughes et al., 1984). In dog, however, HCO_3^- removal had no effect in the rate of fluid transport, while furosemide and a Cl^--free solution nearly abolished fluid movement (Tsuboi, 1987). It has not yet been established if these conflicting reports actually represent species differences, or if other factors are responsible. In either case, the mechanisms already identified are sufficient to explain how both ions, and thus fluid, cross the RPE. It likely that Cl^- enters the cell through the $Na^+/K^+/Cl^-$ cotransporter and leaves through basal channels. HCO_3^- crosses the apical membrane with the electrogenic Na^+/HCO_3^- transporter and is moved out of the cell by the basal HCO_3^-/Cl^-

exchanger, or is converted into CO_2 by the enzyme carbonic anhydrase and diffuses out of the cell.

I.F.3. Modification of Fluid Transport

Conditions which modify the Na^+/HCO_3^- and $Na^+/K^+/Cl^-$ transporters may alter the rate of fluid movement. Depolarising the apical membrane activates the electrogenic Na^+/HCO_3^- transporter (Hughes et al., 1989), while decreasing $[K^+]_a$ slows the $Na^+/K^+/Cl^-$ cotransporter (Adorante and Miller, 1990). Light would reduce the fluid transport through both of these, as the light-induced reduction in $[K^+]_a$ hyperpolarizes the apical membrane and the Na^+/HCO_3^- transporter is slowed by hyperpolarization. The observation that ouabain reduces the rate of fluid transport by 83% (Tsuboi, 1987) suggests that the decrease in Na^+/K^+-ATPase activity caused by the light-induced drop in $[K^+]_a$ may also lead to a reduction in fluid flow after the onset of light.

The reduced contribution of these transporters to fluid absorption in light may be compensated for by epinephrine. When applied to the apical side of the tissue, 100 nM epinephrine tripled the rate of fluid transport in bovine RPE (Edelman and Miller, 1991). Apical bumetanide blocked this effect, implicating the involvement of the $Na^+/K^+/Cl^-$ cotransporter. Further studies showed epinephrine increased the depolarisation of the basolateral membrane seen when $[Cl^-]_b$ was reduced, and that basolateral application of DIDS blocked the depolarizations normally observer with epinephrine (Joseph and Miller, 1992). These results strongly imply that epinephrine increases fluid absorption by increasing Cl^- transport across the RPE. Epinephrine increases internal levels of Ca^{2+} (Lin and Miller, 1991) and pharmacological evidence supports Ca^{2+} as the internal messenger. It is not known, however, how calcium might change the chloride conductance.

In addition to Ca^{2+}, cAMP may also be involved as a second messenger in the epinephrine response. Epinephrine has been shown to triple the

concentration of intracellular cAMP in bovine RPE (Edelman and Miller, 1991). When elevations in [cAMP]i were caused by the phosphodiesterase inhibitor IBMX, the observed depolarization of the basolateral membrane was similar to that seen after application of epinephrine (Hughes et al., 1987, Joseph and Miller, 1992). However, elevation of intracellular cAMP reduced the fluid transport across frog RPE by 84% (Hughes at al, 1984), so it is unclear what contribution cAMP might make to the epinephrine response.

Epinephrine is present in the retina (Hadjiconstantinou et al., 1983) and may be released after light like another catacholamine, dopamine (Deary and Burnside, 1989) and diffuse into the subretinal space. At present, this cannot be substantiated. The delay involved in this possible diffusion, however, may correlate with the timing of the light peak, which is thought to involve an increase in basolateral Cl^- conductance.

I.G. Justification of Thesis

It is apparent from the proceeding review that the numerous interactions between membrane mechanisms of the RPE have made it difficult to identify or distinguish between primary and secondary effects of stimuli such as light. It is also evident that a knowledge of the individual mechanisms present on the membrane allows a logical sequence of events to be proposed which can explain diverse experimental observations. The majority of this research has concentrated upon the pumps and transporters, and there is a paucity of information of the mechanisms which control passive transport across the RPE.

In this thesis, the basic characteristics of individual channels in the RPE membrane have been studied with the use of a patch clamp amplifier. This allows the parameters which influence a particular mechanism to be separated and described. As with the mechanisms responsible for active transport, an understanding of the passive characteristics on a microscopic level can isolate the contribution of the channels to the entire RPE transport system. This will

eventually allow some of the responses observed in fluid transport and the light-RPE interactions to be precisely attributed to specific membrane mechanisms, and will clarify the dynamic model of RPE transport.

Chapter II. Methods

II.A. Introduction

The description of ionic transport across the RPE in Chapter I emphasised the difficulty in attributing the electrical responses recorded from a tissue in the Ussing chamber configuration to an individual membrane mechanism. This is particularly true for channels as the current which flows through them is large when compared with active transport mechanisms, and the change in intercellular potential which results makes it difficult to characterise the voltage-dependent attributes of channel action. It is also difficult to distinguish between different channel types passing the same type of ion when using macroscopic techniques, such as the measurement of membrane potential, and many such channel types have been reported in other epithelial cells. To determine what channels were present in the RPE, therefore, the membrane has to be voltage clamped and individual channel types separated.

The patch clamp technique (Hamill et al., 1981) allows small patches of membrane approximately 1 μm in diameter to be voltage clamped and the current flowing through individual ion channels can be measured. In most cases, different channel types can be distinguished from each other and the characteristics of each type determined. The basic procedure involves placing a fire- polished electrode up to a cell membrane uncontaminated by extracellular debris. The pressure inside the electrode is reduced by applying gentle suction through a side tube, and the membrane is drawn up into the electrode; a high resistance "gigaseal" (1 GΩ) is then formed between the glass electrode and the membrane. The resolution of a current signal is limited by the Johnson, or thermal noise of the source, which is inversely related to the resistance. The formation of a high resistance therefore makes it possible to resolve the minute currents that flow through a single channel.

Ionic channels are usually either closed, when they do not pass current,

or open, when ions flow through at a constant rate. When a patch clamped channel opens, the electrode-membrane seal forces the current into the recording pipette and to the amplifier. The channel alternates between the open and closed state, and as the transition itself occurs within 0.1-1 msec (Hille, 1992) the current trace recorded by the amplifier is characterised by a series of rectangular pulses. Two types of information are thus available from the patch clamp record; the amount of current passing through a channel and the timing and nature of the changes in current.

In this thesis, the current passing through single channels of the RPE has been recorded using the cell-attached variant of the patch clamp technique. In this configuration, the electrode filling solution bathes the outside of the patch and its composition is known. The other side of the channel faces the cytoplasm, and the precise ionic composition of this intracellular solution is not known. However, the cellular machinery is intact, and second messengers capable of modifying channel activity in response to certain signals are present. Therefore, the information obtained from cell-attached records can provide potential information about the function of these channels in vivo.

This chapter is divided into two parts. The patch clamping system was initially assembled for this work, and the first part of the chapter describes the basic components and necessary accessories of the system. Particular problems in the development of the system, and their eventual resolution, are also mentioned. The second section deals with the basic theory behind the analysis of single channel data and the practical approaches used in this work.

It must be noted that this chapter concerns the methods which underlie the main body of this thesis. The protocols specifically associated with tissue culture are described in Chapter IV. Deviations from the main analysis routines were utilised for the bovine records and are described in Chapter III. Likewise, minor subroutines are described with the corresponding results throughout the thesis.

II.B. Recording Set-up and Peripheral Equipment

The basic recording configuration of the system eventually developed is shown schematically in Figure II.1. Individual components are discussed in detail in the subsequent sections, but the fundamental structure is as follows. A membrane-electrode gigaseal caused the currents flowing through channels in the patch to be transmitted up the electrode through an electrolyte solution. A silver wire, the tip of which was chlorided and in contact with the electrolyte solution, conducted the current to the amplifier headstage mounted on the microscope. A silver chloride reference electrode in the bath was also connected to the headstage and compared to the current from the patch electrode. The current signal was transmitted to the amplifier and converted into a voltage signal. The amplifier output was filtered at a frequency dependent upon the noise present in a particular recording and sent two ways. To monitor the recording on line, the signal was further filtered and displayed on an oscilloscope. The signal was simultaneously passed from the amplifier through an analogue to digital converter and stored on computer. The command voltages applied to the patch were generated on computer and conveyed, via a digital to analogue converter, to the amplifier. The command voltage was converted into a current signal which was transmitted through the electrode to the membrane patch. A photograph of an early version of the recording set-up is shown in Figure II.2.

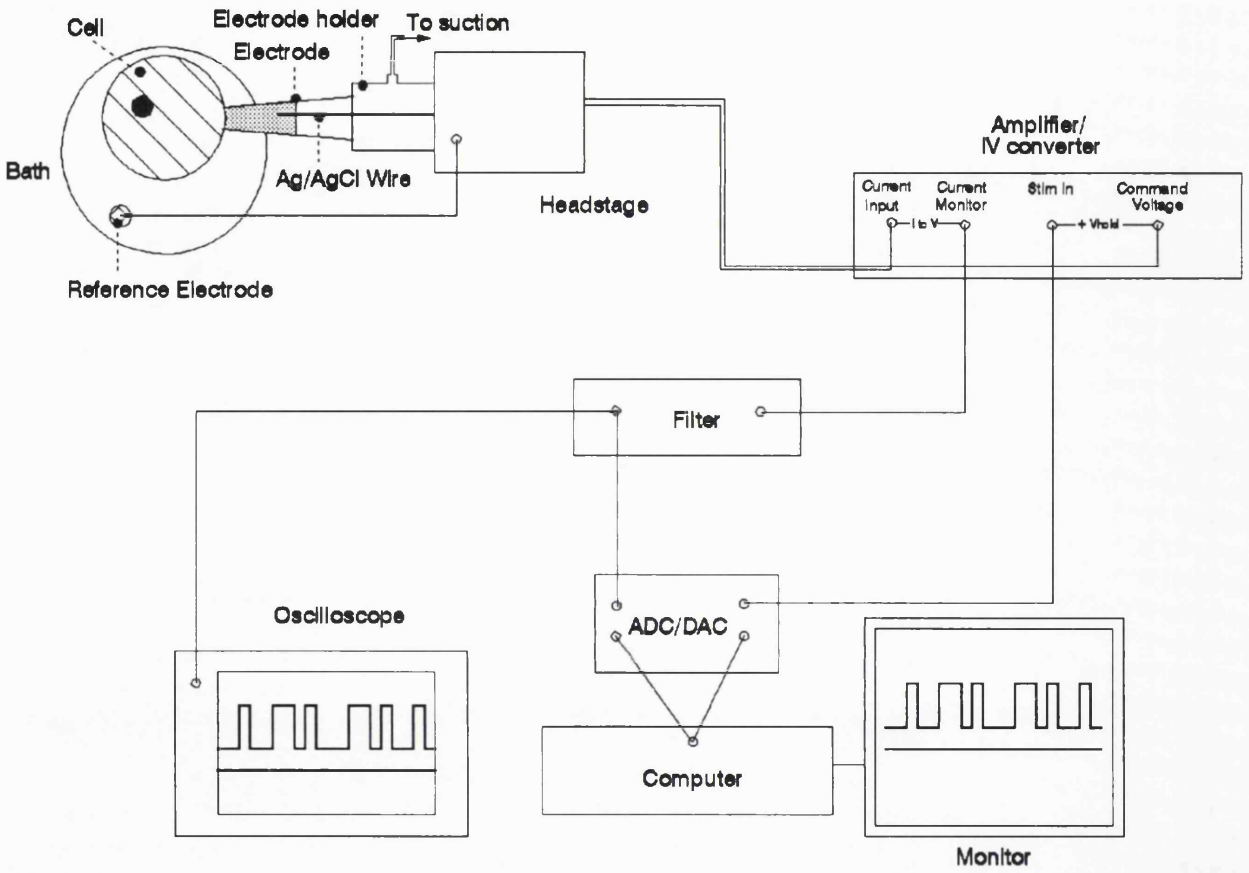

Figure II.1. Configuration of Recording System

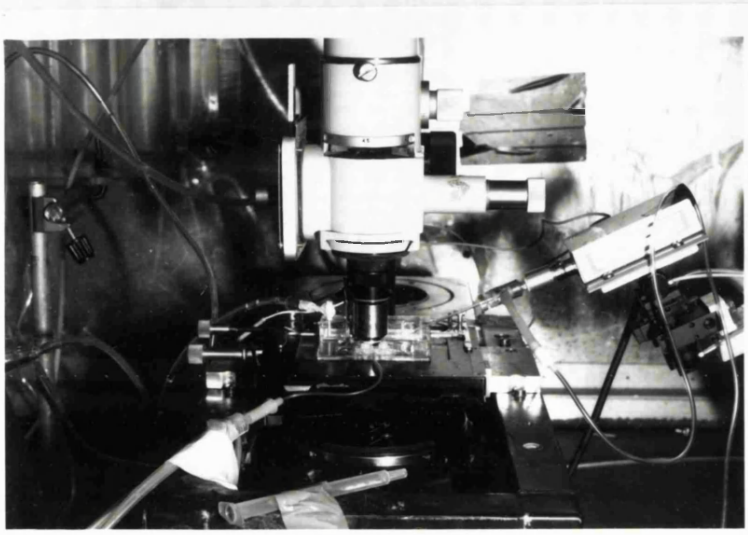

Figure II.2. The patch clamp recording system. An early form is shown, with an upright microscope and water-immersion objective. The electrode tip is attached to a bovine RPE cell.

II.B.1. Amplifier

An EPC-7 amplifier (List Medical, Germany) was purchased to monitor the currents passing through single channels over a range of potentials. The input resistance of the amplifier is high so, by Ohm's law, the small channel currents produce a large voltage change which is easily detected. To "clamp", or maintain a constant potential difference across the patch of membrane, feedback circuitry in the amplifier applies a current of equal magnitude but of opposite direction to the patch whenever a channel current is detected. The amplifier must be able to respond at high frequency to clamp the patch effectively as the transitions in current level occur within 10^{-7} sec. The amplifier controls the potential across the patch by holding the "extracellular" space within the electrode at a user specified command voltage. Thus a positive command voltage increases the potential difference across the patch and effectively hyperpolarizes the patch. The high resistance electrode-membrane

seal physically isolates the patch from the bath solution and electrically isolates the patch from the rest of the cell; a 10 mV change in the command potential across a 1 GΩ seal will produce a leak of only 10 pA. This is comparable to the current flowing through a single channel and thus the membrane patch is voltage clamped independently from the rest of the cell.

II.B.2. Electrodes

Correct electrode choice and fabrication was critical for successful recording because a) electrodes contributed to the inherent noise of the system and b) a smooth electrode tip with an internal diameter less than 2μm was necessary for gigaseal formation with the membranes of cultured RPE cells. The various parameters which control these factors were varied and eventually a combination was found which produced low noise gigaseal recordings with reasonable predictability.

II.B.2.a. Glass

The type of glass used to fabricate electrodes was found to contribute to successful gigaseal formation. No gigaseals were ever formed using electrodes pulled from soft flint glass Cee-Bee capillaries (Bardram Lab. Supplies, Birkerod, Denmark). As these were the first capillaries tried, it was unclear other factors contributed to the inability to form seals, but as other publications reported higher rates of seal formation with hard borosilicate glass (Corey and Stevens, 1983), thin walled capillaries GC150TF from Clark Electromedical (Reading, UK) were tested next. However, few gigaseals were formed with this glass either. Most of the data in this thesis was obtained with the Kovar sealing glass # 7052 from Garner Glass Company (Claremont, CA, USA), although the gigaseal formation rates were not as high as those reported by other researchers (Rae et al., 1988), and it was not possible to form multiple seals with the same electrode. Towards the end of this study, several weeks passed when no gigaseals were formed. The precise reason for this remains unknown,

but seals were eventually formed again when electrodes were made from thick walled borosilicate glass (GC150F, Clark Electromedical). Thick walled electrodes have been reported to have higher rates of seal formation than thin walled electrodes (Corey and Stevens, 1983).

The choice of electrode glass can influence the amount of background noise in the recording. A detailed comparison of the noise inherent in the different types of glass used in this study was not undertaken, but the conclusions drawn by other researchers influenced the choice of glass and agree qualitatively with the baseline noise found in the records presented here. The inherent noise present in 20 different types of glass was measured at 10 kHz by comparing the noise of the electrode with the tip exposed to air with the noise present when the tip was sealed with Sylgard 184 (Dow Chemicals, UK) (Rae et al., 1984b). The noise was found to be inversely proportional to the thickness of the electrode wall and the conductivity of the glass. Thus thick-walled electrodes made with borosilicate glass will produce less noise than thin-walled electrodes made with softer glass.

II.B.2.b. Electrode Fabrication

Electrodes were pulled in two stages on a List Electromedical vertical puller. The temperature of the heating coil during the second pull determined the diameter of the electrode tip. For the cell-attached recordings used in this study, the electrode component of the series resistance was not crucial. Instead, noise from the seal arises partially from the patch capacitance, which is proportional to the size of the patch (Rae et al, 1988). To minimise this noise, the heating coil temperature was chosen to give an internal tip diameter of approximately 1µm. This produced electrodes with a resistance of 7-10 MΩ when filled with a 120 mM KCl solution.

II.B.2.c. Coating and Polishing

A proportion of the electrode-membrane seal resistance is shunted

across the electrode wall. This can be reduced by increasing the thickness of the wall. Sylgard was used to coat the outside of the electrode and effectively increase the wall thickness. The electrode was mounted on a List Electromedical CPZ-101 pipette forge and Sylgard was applied under low magnification. The coating began approximately 100 µm from the electrode tip and extended 1 cm up the electrode to assure that no segments of uncoated electrode were in contact with the bath solution. The Sylgard was then cured with a 15 second blast of hot air. Sylgard was stored at -20 °C and kept at room temperature for 15 minutes before use to attain the correct viscosity.

The electrode tip was gently fire polished immediately after being coated with Sylgard. The tip was advanced under high magnification to within several microns of a thin platinum wire. A thin coating of glass along the wire prevented the discharge of metallic ions onto the electrode. Current was then passed through the wire for several seconds until the electrode tip darkened slightly. The degree of fire polishing necessary was determined by trial and error.

After coating and polishing, electrodes were stored in a covered dish and used within two hours. No gigaseals were ever formed with electrodes stored for longer than two hours; microscopic examination revealed the tips were covered with dust particles.

II.B.2.d. Electrode Filling

The electrodes used did not contain an internal capillary rod to fill the tip rapidly. Instead, electrodes were mounted into an old electrode holder with a side arm. The tips were submerged into the chosen electrolyte solution and suction was applied at the side arm to draw the solution into the tip. The remainder of the electrode was backfilled with a syringe fitted with a plastic catheter tube. Air bubbles were dislodged with a gentle tap. Solutions were passed through a filter with a pore diameter of 0.2 µm. Electrodes were filled immediately prior to use.

II.B.3. Electrode Holder

The electrode holder used for patch clamp experiments performs several functions. It transmits the current flowing through the electrolyte solution to the headstage via a silver-silver chloride connection. It must contain a outlet to control the pressure inside the electrode so that the gentle suction necessary for the formation of a gigaseal can be applied. Finally, the holder must grip the electrode securely to minimise vibration at the tip.

The choice of electrode holder can significantly affect background noise levels of the record system. In early experiments, an electrolyte-filled perspex holder with an internal silver-silver chloride half cell (#EH-2R, Clark Electromedical) was used, but recordings were plagued by high background noise. The contribution of the holder to this noise can be determined because the total noise is the sum of the variances of the separate noise sources. Thus, the RMS of the noise is the square root of the sum of squares of the individual noise sources:

$$RMS = \sqrt{(A^2 + H^2 + P^2)}$$

where A = amplifier noise

H = holder noise

P = pipette noise

The noise produced by this holder, and by the pipette it held, were compared with the noise produced by two other holders; a shielded and non-shielded Teflon holder from List Electromedical. The Teflon holders were considerably less noisy, and the pipettes contributed less noise when mounted in the Teflon holders. The shielded holder increases capacitance to ground and thus contributed slightly more noise than the unshielded holder. The unshielded Teflon holder was consequently used for most of the records presented here.

The Teflon holder transmitted signals with a silver wire which was silver chlorided and immersed into the electrolyte solution at one end. The other end

was dry and connected, via a BNC, to the headstage. In spite of an elaborate sequence of rubber O- rings, solution would occasionally creep up the wire and offset the electrode potential, as measured before seal formation. This was eventually controlled by cleaning the holder regularly with ethanol dried in an air stream, and using a Teflon coated silver wire.

II.B.4. Microscope

Originally, the patch clamp set-up was developed around an upright Zeiss microscope. The high-power water immersion objective used on this microscope allowed the electrode to be advanced at an angle only 20° from horizontal, but as the fresh RPE cells used in early experiments were approximately 10 µm high, this was sufficient. When it was eventually decided to use cultured RPE cells, this narrow approach angle made seal formation impossible. The flat cultured cells required a near- vertical electrode approach. The system was redesigned around an inverted Nikon Diaphot microscope.

Gigaseal formation depended upon the precise alignment of the electrode tip and cell membrane. Phase contrast was thus necessary in both microscope systems to visualise the location of the clear electrode. The relative transparency of the cultured cells made the use of phase contrast optics even more vital than it had been with fresh cells.

II.B.5. Manipulation

Precise control over electrode tip position was achieved by mounting the headstage, which was connected to the electrode holder and the electrode, on to a 3-D Narashigi hydraulic manipulator (Research Instruments, UK). The hydraulic manipulator was in turn mounted onto a 3-D Huxley manipulator. The electrode was advanced towards the cell to be patched in two stages. The Huxley manipulator was used to bring the electrode within 20 µm of the cell and the final approach was made with the hydraulic manipulator.

II.B.6. Vibration Reduction

Vibration was a recurrent problem in this system. The membrane-electrode seal was mechanically stable, and could remain intact under considerable force. However, the cultured cells were rigidly fixed to the bottom of the recording chamber, and the top surface of the cells was only 5 μm above the chamber floor. Slight vibration made gigaseal formation difficult and often ruptured any seal already formed, while even light contact with the equipment caused the electrode tip to knock against the chamber floor and break.

Several steps were taken to reduce vibration. The entire recording system was mounted on a vibration isolation table (Ealing Optical, UK). Air cylinders full of compressed nitrogen cushioned the system from most of the vibrations present in the laboratory. However, the elaborate complex of coarse and fine manipulators, headstage, electrode holder and electrode were originally attached to the table at the top of a single magnetic stand, and considerable vibration occurred at the electrode tip. Eventually, this entire complex was mounted directly onto the body of the Nikon microscope and the vibration that did occur in the recording chamber and electrode were more closely synchronised. The controlling unit of the hydraulic manipulator was mounted on a shelf isolated from the recording system. This further reduced the vibration transmitted to the electrode tip during the final stages of electrode advancement.

II.B.7. Faraday Cage

An aluminium Faraday cage was constructed to electrically isolate the recording system. The cage was hinged at several points to allow access to the interior, and was grounded through the amplifier. The majority of the synchronised noise was transmitted through the front of the set-up, but this area had to be kept accessible until the electrode tip-cell distance was within the range of the hydraulic manipulator. To prevent vibration at this critical stage, swinging aluminium doors were mounted on a shelf close to but isolated

from the main system.

II.B.8. Recording Chamber

Several perspex chambers were developed, but for the majority of experiments described here, a simple structure was used. A circular hole 3 cm in diameter was drilled into the centre of a flat, square block of perspex 1 cm high and 10 cm wide. The cultured cells used for recordings were grown in treated culture dishes 3 cm in diameter, and these dishes were simply placed into the central hole of the chamber. A series of small holes were drilled either side of the culture dish mount. Two small needles at opposite ends of the culture dish provided an inlet and outlet path for perfusing solutions. In order to hold the needles, and a silver chloride reference electrode in position, they were fixed onto cocktail sticks mounted into the small holes either side of the recording dish. The entire chamber was held in position with clips on the microscope stage.

II.B.9. Perfusion System

The recording chamber was perfused with a gravity fed inlet system while solutions was removed with the gentle suction provided by a flow pump connected to a nearby tap. Several features of the system were developed to reduce the noise and vibration levels during recordings.

Solutions flowed into the chamber from one of five bottles through Marprene tubing with an internal diameter of 0.8 mm. Solution change occurred with a system of three-way valves allocated to each of the five input lines. The valves were fixed onto a board mounted on a shelf separate from the recording system. This isolated any vibration produced by the solution change. The five input lines converged in a mixing well mounted 8 cm from the recording chamber. At the usual perfusion rate of 2 ml/min, a newly selected solution took 12.5 seconds to reach the chamber and solution change was complete within 45 seconds. In between these times, the cells were bathed in a

combination of the old and new solutions.

Early experiments indicated that the baseline noise increased when solutions flow transversed the Faraday cage. To eliminate this noise, the bottles containing the solutions were positioned inside the Faraday cage. When the upright microscope was replaced by the inverted microscope, however, the recording chamber was level with the solution bottles, and the solutions could not flow. Bottles were moved to an elevated shelf outside of the Faraday cage, and noise was reduced by grounding the mixing well.

The solutions were bubbled with 95% O_2 / 5% CO_2 and this caused substantial vibration. Originally, therefore, solutions could only be bubbled in between recordings. Removing the bottles to an outside shelf reduced the vibration transmitted to the chamber, and allowed the solutions to be bubbled continuously.

Most of the recordings presented here were performed at room temperature. Unitary channel conductance is only slightly affected by temperature (Q_{10} = 1.5) but channel gating and kinetics are more dependent upon temperature (Q_{10} = 2-4), as expected if the channel acts like an enzyme (Hille, 1984). In several later experiments, the solution temperature was raised to 35°C by surrounding the last 5 cm of the inlet tube with a wide tube internally perfused with hot water. No significant difference in channel kinetics was detected, but the comparison was limited by the small number of the recordings made at 35°C.

Solution was removed from the chamber by the gentle suction provided by a flow pump attached to a nearby tap. As mentioned above, the flow of ions through the Faraday cage was thought to produce electrical noise, so a two stage system was used. The flow of tap water through the pump was used to suck air out of an Erlenmeyer flash contained within the Faraday cage. This in turn created a vacuum which drew solution from the recording chamber into the flask.

II.B.10. Solutions

A variety of solutions were used in this study. The composition of solutions used in specific cases, for example tissue culture or drug testing, are detailed in the protocols found in relevant chapters. The composition of the core solutions used repeatedly in this study are listed in Table II.1. The potassium chloride and calcium chloride were obtained from BDH LTD (Poole, Dorset). Unless otherwise noted, all other chemicals used in this study were obtained from Sigma Chemicals (Poole, Dorset).

Table II.1. Solutions

	NaCl	KCl	$CaCl_2$	$MgCl_2$	Hepes	$NaHCO_3$	Glucose	EGTA
Control	124	5	2	1	10	16	5	-
High K	10	100	2	1	10	16	5	-
Low K	100	10	0.5		10	-	-	5

Ionic concentrations are given in mM.

Control solution is also referred to as mammalian, or MAM.

Solutions used for recording were bubbled with 95% O_2 / 5% CO_2. The pH was adjusted to 7.2 by adding 5 ml of 1M NaOH per 1 L of control solution, 5 ml of 1M KOH per 1 L of high potassium solution. Suction filtration was then used to remove any particles larger than 0.2 µm from the solution. Solutions were stored as x10 stock concentrations, but the glucose and $NaHCO_3$ were added only when working strength solutions were made to preserve the stock solution and prevent ions from precipitating out. Solutions were made fresh every two days, but the pH was checked regularly during the course of experiments. Little or no variation was ever found in the pH when the solutions

were continuously bubbled.

In solutions with [Ca^{2+}] = 2mM, deionised distilled water was used, but a calcium-free water was used to make up low Ca^{2+} solutions. EGTA and calcium were added to the working strength low Ca^{2+} solutions as EGTA did not readily dissolve at high concentrations. The concentration of free calcium present in these solutions is determined by the concentration Ca^{2+} and Mg^{2+} added and the amount of EGTA present to chelate the divalent ions. At pH 7.1, EGTA bind to Ca^{2+} 10^5 time more readily than Mg^{2+} and the calculations used to determine the precise amounts of Ca^{2+}, Mg^{2+} and EGTA required to yield a given concentration of free Ca^{2+} are complex (Caldwell, 1970). The values here are obtained from Mayer et al., (1990).

II.B.11. Gigaseal Formation

The technique used to form a gigaseal between the membrane and electrode is similar to that described previously (Hamill et al., 1981). Small potentials between the electrode tip and reference electrode were offset to zero with the non-inverting input of the amplifier when the electrode entered the bath. The resistance of the electrode was measured with a 10mV pulse applied at 5 Hz. Under high (x500) magnification, the electrode tip was advanced until it reached cell membrane. Gentle suction was then applied to the electrode and if conditions were right, the measured resistance increased dramatically and tight seal was formed. Seals typically ranged from 0.8 - 2 GΩ and formed within 20 seconds of the application of suction. Initially, the suction was produced by mouth; a small tube attached to the side arm of the electrode holder was held in the mouth and the amount of suction necessary was learned by trial and error. It was difficult to standardise the suction generated this way however, and occasionally the electrode would simply enter the cell. In later experiments, suction was produced with a syringe attached, via a tube, to the sidearm. Withdrawing the syringe 0.3-0.4 ml often produced a seal. The actual decrease in pressure produced was unknown.

II.B.12. Data Acquisition

The current flowing through the channels was visualised as a voltage signal on an oscilloscope after being processed by the amplifier. The data had to be stored, however, before amplitude and kinetic information could be quantitatively analysed. During early recording sessions, data was stored on a Racal Store-4 FM recorder. Data was acquired at a rate of 30 inches/sec (10 kHz) and relevant sections were played back onto a chart recorder at a rate of 3.75 inches/sec (1.25 kHz). The limitations of this system were readily apparent; at a sampling frequency high enough to preserve sufficient detail, the sheer volume of tape and paper was prohibitive, and the manual measurement of current values and kinetic information was impossible.

It quickly became apparent that the data needed to be digitally acquired and analysed and an IBM-compatible Liberty 286 computer was purchased. The s200 analogue-to-digital converter from Intracell Ltd. (Royston, UK) was chosen because of the flexibility of its single on-board add on card and its competitive price. The s200 had 8 ADC input channels an and 4 DAC output channels and operated with a 12 bit resolution, features that were more than adequate for single channel recording. However, the compatible software packages, Active and Satori, used to acquire, manipulate and analyse the data, were found to be inadequate in several respects. Specific difficulties will be discussed in later sections, but overall, the choice of the Intracell system substantially hindered the project.

Data was acquired on-line at sampling frequencies from 3 to 10 kHz, chosen to reflect specific experimental goals. Stimuli traces were stored with the data in files of 20 kbytes to 1 Mbyte and transferred to floppy disk for later analysis.

II.B.13 Voltage Clamp Stimuli

Originally, the command potential delivered to a patch of membrane was

manually chosen at the amplifier, and a simple stimulator was constructed to provide voltage steps of a desired size. The stimulator was connected to a Neurolog (Digitimer, UK) phase generator and delay-width timing circuit to control the timing and duration of the pulses. Pulses ranged from 0.1 - 2 V with divisions of 0.1 V, and were scaled by the amplifier before being added to the specified command potential. The manual control meant that the amplitude and timing of these pulses, and of the command potential, could not be adjusted quickly during an experiment.

When the recording system was converted to a computer-based process, it was possible to construct set stimuli protocols composed of various pulse duration and potential combinations with the Active software from Intracell. The DAC of the s200 board enabled these stimuli protocols to drive the amplifier and could thus control the command (holding) potential delivered to the patched membrane. Any current which flowed through the channel was recorded and synchronised with the stimuli trace.

All voltages given are the potential difference between the reference electrode in the bath and the interior of the pipette tip, and the sign is related to the pipette tip potential unless otherwise noted. Thus, in a cell attached recording with an electrode potential of -40 mV, the patch is depolarised by 40 mV with respect to the external surface of the cell membrane. It is impossible to determine the precise membrane potential of the cells used in this configuration, though of course, the changes in membrane potential induced by the clamp currents are the cause of the changes in the channel activity seen in this study. In order to separate data from inferences about the membrane potential, all data are given as the negative of the electrode potential.

II.C. Data Analysis

As mentioned in section II.A, the records of single channel activity contain two types of information; the amount of current which flows through the channel when the channel is open and the temporal characteristics of these

openings. There are several ways to measure both parameters and the particular attributes of each recording determine which is best. If the measurements are made over a range of conditions, this data can be interpreted to yield detail about microscopic channel mechanisms and the contribution of the channel to the cells macroscopic activity.

II.C.1. Current Amplitude Measurements

The amount of current which passively flows through a channel is determined by the electrochemical driving force on the ions present and the permeability of the channel to each of these ions. This is described by the Goldman constant field equation, as mentioned in Chapter I. The potential across the channel can be altered with patch clamp technique, and change in channel current with potential, the channel conductance, can be determined with accurate measurements of current size. The reversal potential, E_{rev} occurs when an equal number of ions flow in both directions across the channel and no net current is produced; i.e. the electrochemical forces are at equilibrium. E_{rev} is obtained by extrapolating the conductance, and if the concentration of ions on either side of the membrane is known, a ratio of ionic permeabilities is determined by calculated by the constant field equation. If two ion types, A and B, are considered;

$$E_{rev} = (RT/zF) \ln \frac{P_A[A]_o}{P_B[B]_i}$$

where $[X]_o$ and $[X]_i$ are the external and internal ion concentrations, respectively, P_X is relative permeability of the channel to each ion, and R is the gas constant, T the absolute temperature (K), F is the Faraday constant and z the ionic valance.

At atmospheric pressure and room temperature, algebraic manipulation gives:

$$P_A / P_B = ([B]_i/[A]_o) * e^{(E_{rev}/25.2)}$$

Physical and electrical barriers inside the channel pore also limit the rate at which ions can pass through the channel, and it is thus possible that two channels with identical ionic selectivity have different conductances. In addition, the constant field equation predicts that a channel bathed in symmetrical solutions will have a linear conductance, while a channel bathed in an asymmetric solution will rectify and the conductance will be larger when ions flow from the more concentrated side. If a concentration gradient exists, the channel will rectify and the current may not be linear but instead rectify and pass more current in one direction than the other. Many epithelial cells contain channels which do not agree with this prediction, however, and these channels suggest new models for channel gating (Rae et al., 1988).

In summary, accurate measurements of the amount of current flowing through a channel are used to characterise the channel in terms of its ionic permeability, conductance and rectifying properties. The remainder of this section concerns the different techniques used to measure the current flowing through channels.

II.C.1.a. Current Measurement Methods

In theory, the measurement of the amount of current which flows through a single channel should be straight forward; the channel alternates between conducting open states and non-conducting closed states and the transition between these states is marked by a vertical displacement of the current trace. As the current depends on the electrochemical gradient, the amount of current flowing when the channel is open should be constant, and can be measured as the difference between the open and closed current levels. However, several factors complicated the measurement of current size in this study. There was considerable variation in the open channel current levels within a single

opening and between openings even under constant conditions. This variation was compounded by the fact that channels were infrequently open at most of the potentials tested and a relatively small number of events occurred over several minutes. Usually, there was more noise present when the channels were open than closed, and this made it difficult to determine the precise current level of the open channel. In addition, sometimes the channels would partially close before returning to the fully conducting state.

The amplitude of channel current was measured in several ways, each dependant upon the methods available at the time and each with its strengths and weaknesses. When the data records were originally digitised, three basic approaches were possible. Quick measurements were made by plotting out a trace of date, and determining the baseline and open channel current levels by eye; the difference between the levels was the current amplitude. If the baseline was very stable and relatively noise free, and if there were many channels open for long enough periods of time, this method gave a reasonable estimate of the current size that was unaffected by brief closures. These conditions were rarely met, however, and measurements were subject to unconscious user bias.

Alternatively, an on-screen ruler was used to measure the difference between the current levels when the channels were open and closed and a histogram of the distribution of values was constructed. The measurements were subjective, like the method used above, but as they were made for each opening, these measurements more accurately represented the variation between openings. The values were not affected by brief closings, but there was only one value for every channel opening, and when the probability of opening was low, the current values were not distributed smoothly.

Automated measurements were possible with Satori software. An early version of the program (version 2) measured the current flowing through a channel by calculating the derivative of the current trace; opening transitions

gave positive values while closing transitions gave negative values. This approach was theoretically very powerful, for it was possible to determine if a channel opened and closed at equal rates, or if the transitions involved intermediary substates. In practice, however, it was very difficult to obtain an accurate measurement of the size of the channel current; if a channel did not open instantly, as was usually the case, the value obtained was only a fraction of the true current size. It was also impossible to calculate the amount of current flowing through the channel once it had opened; small fluctuations were measured as independent current values. The derivative of the current trace can provide much useful kinetic information, but it was of little use when measuring current amplitudes.

In February, 1991, an updated version of Satori was obtained which produced an amplitude histogram of all the current values of a record; referred to here as the all-point method. Because the current levels fluctuated as the channels opened and closed, the histogram produced peaks at the open and shut levels. Gaussian functions were fit to the distributions. For a single Gaussian,

$$f(x) = \frac{C}{(\sqrt{2\pi}) * \sigma} * \exp\left\{\frac{-(x-A)^2}{2\sigma^2}\right\}$$

where A = distribution mean

C = area of function

σ = standard variation.

Variables were fit to minimise the chi-squared values. The least squares method depends upon the size of the bin, and not the data itself, so bin size was chosen to produce a smooth distribution.

In some recordings, two identical channels were detected when the one current peak was twice the other, and further confirmed when this relationship

was seen at all holding potentials tested. In other records, two distinct channel types were present and the peaks were not integer multiples of each other, but when both channels were simultaneously open, a fourth peak equal to the sum of the other peaks was detected.

For some records, current levels were measured with both the on-screen ruler and data-point method. Both methods yield similar conductance values, but the values obtained with the on-screen ruler are slightly larger. This is probably because of the user-bias of the on-screen measurements; open current values were taken from the highest point of each channel opening and did not include information about the variation within each opening. The all-point method gave a more accurate measurement of the average current. It was obvious that the measurements from different records could only be compared if they were obtained by the same method. All records from cultured channels acquired before February, 1991 were thus re-analysed with the all-point method.

II.C.1.b. Filters

A greater variation in current size was seen for channel types that opened for a relatively small duration, and it was important to make sure this was not an artefact of data filtering. The shortest detectable channel open is determined by the corner frequency of the filter used on the data. For a Gaussian filter, the fraction of full amplitude attained by an opening of a given duration is:

$$P_a = 2.67 * f_c * w$$

where f_c is the -3dB frequency of the filter and w is the length of the opening (Colquhoun and Sigworth, 1983). The cut-off frequency varied with the background noise level of the recording, and in most cases was 1kHz. Thus, the minimum width necessary for the channel to reach 95% of its value is 0.3

msec. The shortest opening duration seen was 0.7 msec, so the variation in channel size is most probably an attribute of the channel itself.

II.C.2. Kinetic Analysis of Channel Activity

In addition to information about the size of the current step produced when a channel open or closes, the single channel trace also records when each transition occurs. This kinetic information has two main applications. The probability of finding the channel open, P_O, combined with the channel conductance and density along the membrane determines the contribution of the channel to cellular function. The rate at which the transitions occur provides information about the processes which control channel gating. This thesis is concerned with contributions made by individual channel types to the RPE, and therefore most of the kinetic analysis has involved channel open probabilities. However, in a few records, attempts were made to correlate observations with changes in transition rates and thus a brief description of relationship between transition rates and gating processes is included in the next section. The practical approaches to kinetic analysis used in this study are discussed in section II.C.3.b.

II.C.3.a. Transition Rates and Probability Distributions

It is thought that a channel acts as an enzyme, and that transitions between channel states occur with an overall frequency described by the rate constant of the reaction. If the channel is considered to have just two states, open and closed, then the probability of a transition occurring depends upon the rates of the reaction that opens or closes the channel, R_O and R_C. The channel has no "memory" and the probability of a transition occurring is independent of its past history; the behaviour is described as a Markov process. The probability that no transition has occurred thus decays exponentially with time, and the distribution of these probabilities is determined by the overall rate constants of the reaction (Colquhoun and Hawkes, 1983).

This theory is applied to the analysis of single channel records as follows. The distribution of opening durations is determined by the rate of channel closing. If this distribution decays as a single exponential function, then the transition is determined by a single rate constant, and involves at least one single step. If the distribution decays as the sum of two exponentials, then at least two intermediate steps are involved before the channel closes. The number of exponential functions gives only the minimum number of states because it is always possible that the transitions between several states may occur at a similar rate.

II.C.3.b. Practical Approach to Kinetic Analysis

Before the kinetic characteristics of a channels behaviour can be described, channel openings must be detected and duration of each opening must be recorded. The temporal attributes of the data in this thesis were determined with the semi-automated analysis routines of the Satori program. The open and closed channel current levels were estimated by eye. An opening was detected when the current trace crossed a threshold set at 50% of the open channel amplitude. The information was stored as the time that the transition occurred and the state destination of the transition, in this example "open". Each fit was checked for validity before the information was accepted for analysis, and errors caused by a noisy baseline and openings of short duration were minimised. It was possible to detect crossings of more than one threshold. Thus, if two channels were present on the record, each could be analysed providing the amplitude of the open current of the larger was more than twice the smaller. If the difference between the current levels was less than this, it was not possible to obtain an accurate measurement of the close times. However, small sections of the record containing only one of the channels could be analysed, and the probability of channel opening could be determined for each channel.

Probability distributions for the duration of open and close states were

plotted and the histograms were fit with an exponential function;

$$f(t) = (1/\tau) * \exp^{(-t/\tau)}$$

Values were chosen for the maximum likelihood of the function describing the data by accumulating the conditional probabilities of observing the events (Colquhoun and Sigworth, 1983). If, for example, the data was very noisy, but additional filtering would interfere with event detection, the distribution was corrected for missed events, by excluding durations smaller than a specified value from the fit.

II.D. Summary

This chapter has discussed the development of the patch clamp system used in this study; the mechanical set-up and electrical configuration, the essential protocols used to record from channels and the ways in which these recordings were analysed. The development of the system has been discussed in detail to reflect the time and effort that was necessary to establish a working system. Inexperience undoubtedly led to inappropriate choices. However, the system was eventually successful and I was able to obtain the single channel data described in this thesis.

Chapter III. Single Channels of Bovine RPE Cells

III.A. Introduction

Until recently, the majority of studies on the transport mechanisms of the RPE have been done on non-mammalian tissue. The bullfrog (*Rana catesbeinana*), in particular, has been the source of much of the information about RPE transport. However, the effect of light on the RPE of higher animals, such as birds, reptiles and mammals, is more complex than in frog RPE. Electrical changes generated at the basolateral membrane are responsible for the fast oscillations and light peak of higher animals (Gallemore et al., 1989). These changes do not occur in frog RPE, and it is possible that the transport mechanisms may differ in other respects. Information about the RPE transport mechanisms is ultimately practical if it can be used to treat the diseased human eye, and if fundamental differences exist between amphibian and mammalian transport mechanisms, this ultimate goal is best achieved with the study of mammalian tissue. Bovine tissue was chosen because the cells were relatively large and thus a larger area was available for the formation of gigaseals. Bovine eyes were also readily available and inexpensive.

When the studies on bovine cells were first attempted, the information available on the transport mechanisms was sparse (Joseph and Miller, 1986; Miller et al., 1988). Recently, however, several thorough reports have been published and it is now possible to produce a comprehensive model of bovine RPE transport (Miller and Edelman, 1990; Joseph and Miller, 1991; Joseph and Miller, 1992; Edelman and Miller, 1991).

The bovine RPE cells had the additional advantage of being fresh. I am not aware of any work to date which describes the activity of single channels on fresh RPE of any species. Information on the fresh tissue is preferable to that from cultured cells because it is more relevant to the in vivo state.

The information obtained from experiments on bovine RPE cells is limited. Records were always very noisy and "classic" single channel activity

was rarely observed. The bovine cells were used for the first attempt at patch clamp recording with the newly established set-up, and initially it was thought that the inability to obtain good records was due to a fault in the recording system itself. However, subsequent work on cultured human cells showed that the system was adequate (see Chapter V) and for some time it was thought that the preparation itself was faulty.

Recent experience has suggested another explanation. The activity of a large conductance channel masked other smaller, less active channels. As a result, the small proportion of original records which were not discarded were reanalysed and some basic information was extracted. The results confirm the findings of cultured cell experiments and emphasise a new possibility which may have important implications for RPE physiology.

III.B. Methods

III.B.1. Dissection

Bovine eyes transported on ice from a local abattoir and usually arrived between 4-6 hours post-mortem. An incision was made just posterior to the *ora serrata* and the anterior portion and vitreous were discarded. The eyecup was filled with calcium and magnesium- free phosphate-buffered saline PBS (CMFPBS, see Table II.1) and the retina was gently peeled away from the underlying RPE and snipped as closely as possible to the optic nerve head with fine scissors. Occasionally, patches of photoreceptor outer segments remained attached to the RPE. A Pasteur pipette was used to create a gently flow of solution directed at the outer segments and the outer segments detached. The eyecup was then rinsed twice with calcium magnesium free PBS (CMFPBS) to ensure all retinal fragments were removed.

RPE cells were removed from the underlying Bruch's membrane by gently brushing the eyecup with a Pasteur pipette. The tip of the pipette was fire-polished to prevent the sharp edges from puncturing Bruch's membrane; if cuts were made, collagenous fibrils from the choroid contaminated the

preparation and interfered with the electrode tip when to recording. After removal, the RPE cells were placed in a test tube. Microscopic inspection at this point revealed sheets of cells, indicating the tight junctions were still intact.

III.B.2. Enzymatic Cleaning

Adult cells are covered with connective tissue and extracellular contaminants which prohibit the formation of the high-resistance electrode-membrane seal necessary for successful single channel recording (Hamill et al., 1981). Enzymes are used to remove this debris and permit seal formation. The precise combination of enzymes varies with species and cell type as the composition of the extracellular debris differs (Spector, 1983).

Bruch's membrane contains a high concentration of collagen and several forms of collagenase were tested. Collagenase 1A (Sigma, UK) gave the best results. Collagenase 1A (2 mg) was dissolved in 4 ml CMFPBS which had been preheated to 37°C. RPE cells were added, and the mixture was incubated at 37°C for 10 minutes. The mixture was gently agitated halfway through the incubation, and had settled to the bottom of the test tube by the end of the incubation period. The enzyme solution was carefully removed and replaced with control solution. The cells were then triturated through the mouth of a fire-polished Pasteur pipette twice, and placed in the recording chamber. The cells settled to the bottom of the chamber within 3 minutes, after which the chamber was perfused with control solution and broken cell particles were washed away. Most of the cells remaining were isolated.

Although this protocol was found give the highest rate of seal formation, good recordings were not frequently achieved, and continuous attempts were made to improve the protocol. As the incubation time was increased, the cells appeared to be less healthy and a higher percentage of the cells ruptured; as it was decreased, the rate of seal formation decreased. A similar relationship was found when the concentration of collagenase was altered. Hyaluronase has been used to clean the surface of frog RPE cells for whole cell recording

(Hughes and Steinberg, 1990). However, in this study, the inclusion of hyaluronase in the incubating mixture caused many of the cells to rupture, and reduced the polarity of pigmentation used to identify the basal membrane (see below). Both of these effects made it difficult to record from cells, and both effects were less pronounced as the concentration of hyaluronase was decreased (from 5mg/ml to 0.5mg/ml).

Several other enzymes were tested alone and in various combinations; collagenase type II and IV, papain, trypsin and DNAse (all from Sigma, U.K.). The effects of papain and trypsin were similar to those of hyaluronase. The other enzymes had no detectable effect on the rate of seal formation or the quality of the records. When a large proportion of the cells were ruptured, inclusion of the DNAse reduced the viscosity of the cell mixture. However, better results were obtained by reducing the proportion of ruptured cells by triturating the cells more gently and keeping the enzyme concentration to a minimum.

III.B.3. Cell Selection

It was impossible to approach the apical surface of the cells without the electrode tip coming into contact with numerous microvilli. Microvilli often entered the electrode tip, and as the diameter of the microvilli was considerably less than the electrode, it was impossible to form any gigaseals. Consequently, attempts were only made to patch clamp basal portions of the membrane.

A mixture of melanotic and amelanotic cells were brushed from the eyecup and plated in the chamber. Many of the cells were a combination of the two, and pigment was concentrated in the apical side of the cell. Identification of the basal membrane was possible under low magnification, and cells with a pigment-free section facing the side of the chamber that the electrode approached from were selected. It is unclear whether the channels found on the basal side of isolated cells would be found there in vivo. The distribution of pigment suggests polarity was maintained to some extent. However the tight-

junctions are responsible for separating the components of either membrane, and once they are removed, membrane-bound proteins including ionic channels can flow through the semi- liquid membrane.

III.B.4. Recording Technique

The basic technique used to obtain recordings from the single channels of bovine RPE is essentially the same as that outlined in section II.B. Figure III.1 shows the electrode and cells in recording configuration.

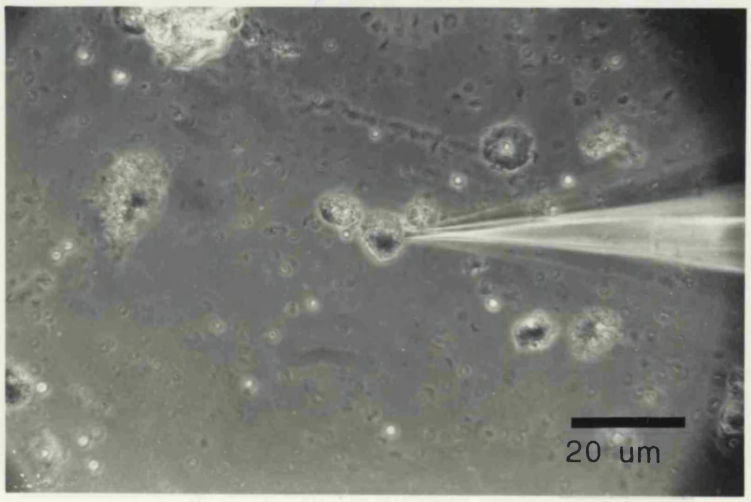

Figure III.1 Photomicrograph of Bovine Recording. The patch electrode had sealed onto the cell membrane.

III.B.5. Data Analysis

Three methods of data analysis were used to obtain data about the single channel currents.

1) Amplitude histograms. The large number of channels and the considerable background noise present in most of the patches present made it impossible to obtain any information about channel amplitude by constructing histograms of the current levels. A typical histogram is shown in Figure III.2. Filtering the traces at a variety of frequencies did not clarify the distributions.

2) Manual analysis at a constant potential. Distinct opening and closing

transitions were periodically visible in the large majority of records. The amount of current flowing through the channel during these openings was measured by fitting horizontal cursors to the current record at the level of the baseline and channel open levels. Long stretches of data were examined to confirm the placement of these cursors. It was not possible to fit more than ten horizontal cursors at a time, and frequently, more levels were present. However, this method gave reproducible results. This method was particularly well suited for the measurement of flickery, noisy currents, like those present in the bovine channels; a histogram would include all the currents less than fully open and consequently give a value less than the true open level.

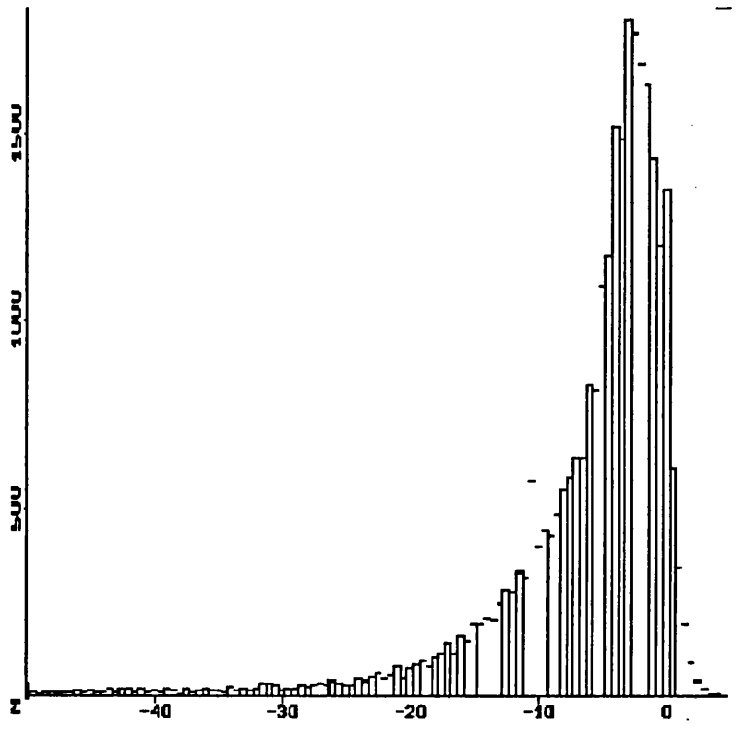

Figure III.2. Amplitude histogram of all currents flowing through a patch at -60 mV. In this cell-attached recording, the electrode and bath contained control solution. This distribution shows the continuous changes in current size that made it impossible to use amplitude histograms in the analysis of bovine data.

3). Manual analysis of voltage ramps. The inability to detect channel events clearly led to the repeated use of ramped voltage protocols* during the bovine experiments. These ramps allowed the general characteristics of the patch to be detected easily. An on-screen current ruler was used to measure the size of individual openings. The on-screen current ruler recorded the holding voltage present at the point where a difference in current was measured. This method also avoided an underestimation of the current flowing through flickery channels.

In both cases of manual analysis, conductance values were determined by plotting all of the current-voltage information together. It was not possible to distinguish channels by visual examination on the basis of their amplitude or kinetic characteristics. Therefore, data points were grouped together when the line which passed through them produced the regression coefficient closest to one. The slope of this line was the channel conductance. This selection criteria is based upon the assumption that all conductances were Ohmic. In eight cases, so many channel levels were present that it was not possible to fit a regression line to the data.

III.C. Results

III.C.1. General Observations

Once the protocols had been adequately developed, it was possible to form tight electrode-membrane seals on a regular basis. Typically seals ranged from 1 to 5 gigaohms. Most of the recordings were performed in the cell-attached configuration. Although several attempts were made to record in the inside-out configuration, the seal was usually lost shortly after patch excision.

All patches showed some form of activity; the patch was usually so active that distinct transitions were difficult to detect. Figure III.3 shows an example of currents obtained from bovine cells, and Figure III.4 shows how cursors were fit to the channel to obtain current information. The slope-fitting process described above was used to convert current values from a variety of potentials into channel conductance.

* Ramps went from +100 mV to -100 mV in 5 seconds.

Many of the early records contained considerably more noise than this. The inability to recognise this activity as usable channel information led to the destruction of over 70% of the records obtained. The remaining records were later analysed for conductance and selectivity information. Because of this subjective selection, no claims about the frequency of encountering a particular channel type have been made.

A quantitative kinetic analysis of these records was not attempted because the patches usually contained a large number of frequently open channels. The situation was made worse by the noisy large conductance channel. The opening of the other channels could not be reliably distinguished from this noise.

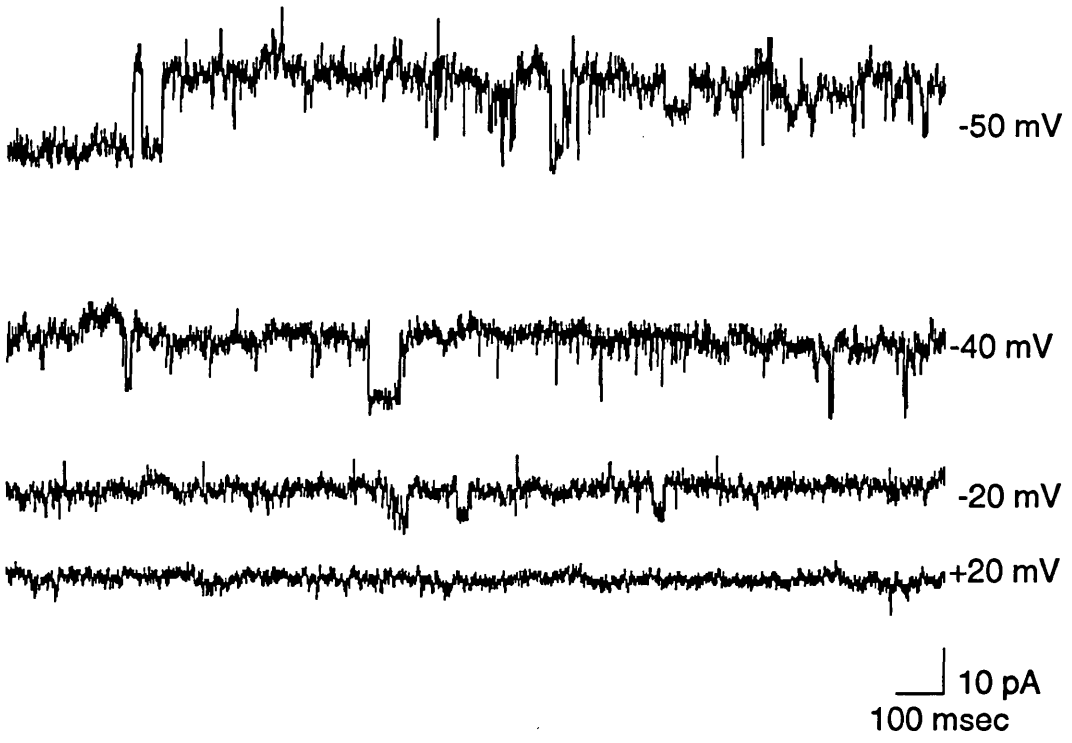

Figure III.3. Current trace from a noisy, large-conductance channel in bovine cells; this channel had a conductance of 292 pS. These traces show unusually clean transitions. The electrode and bath contained control solution. - Vp is shown to the right of each trace and upward deflections indicate outward current through open channels.

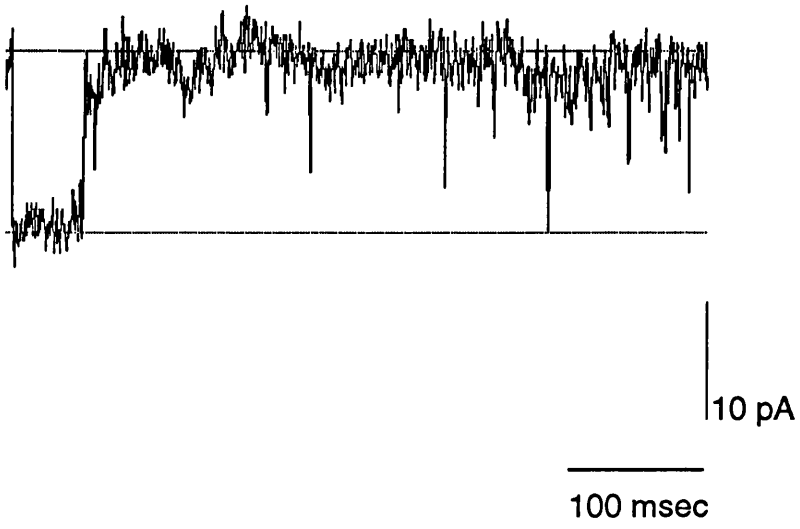

Figure III.4. This cell-attached trace shows how cursors were fit to the current records to obtain the value of the current steps. The bath and electrode contained control solution and the patch was hyperpolarized by 40 mV with respect to the membrane potential.

III.C.2. Channel Grouping

When a frequency distribution of the conductance values was constructed, it became clear that it was not possible to divide the channels based upon their conductance. Figure III.5 shows this histogram. There appear to be three conceivable groups between 50 pS and 150 pS, but the small number of records and the variation in these records means that it impossible to separate the channels accurately. The only channel group it is possible to distinguish was the noisy high conductance channel type. It had a mean of 228 pS, but a large variation (SD = ± 35 pS). The mean reversal potential of this group when the electrode contained control solution was 11.0 ± 11.8 mV; in other words nothing can be concluded about the selectivity of this channel. The conductance values and calculated reversal potentials for all bovine records

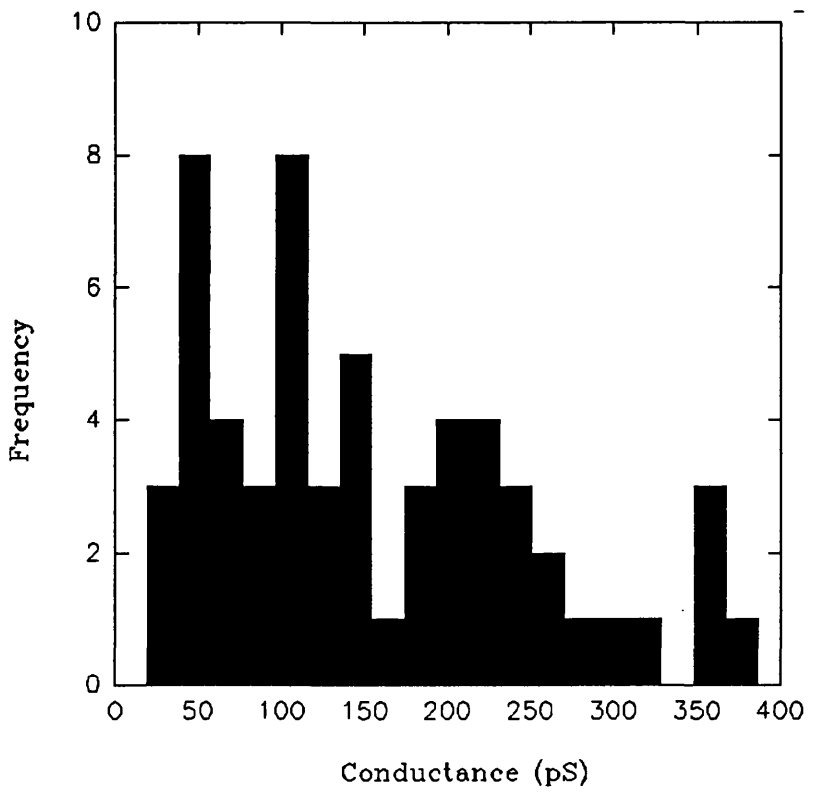

Figure III.5. The distribution of conductances seen in bovine records with both control and high potassium solution in the electrode. Three groups are suggested between 50 and 150 pS, while there is clearly a fourth group at 220 pS. The histogram contained 30 bins.

analysed are shown in Figure 1, Appendix 1.

The conductance values used for the distribution in Figure III.5 were obtained from experiments with control solution and experiments with high potassium solution in the electrode. Initially, it was thought that pooling the conductance values from these different experiments together caused the lack of clear channel groups. However, it was not possible to distinguish groups when the conductances were separated by their electrode solution, either.

III.D. Summary

These experiments provide the first description of ionic channels present on fresh mammalian RPE cells. Channels were seen which had conductances

ranging from 24 pS to over 300 pS, and there appeared to be channel groups with at 55 pS, 106 pS and 147 pS. However, the large variation made it difficult to classify these groups with certainty. The only clearly distinguishable group was the noisy channel with a mean conductance of 228 pS.

This variation may have resulted from a natural distribution, or it may have been caused by the methods. For example, the used of cell attached configuration meant that neither the membrane potential nor the intracellular ion composition was controlled. Any fluctuation in these values between cells might have led to inconsistent measurements.

The choice of stimulation protocols and analysis methods may have effected the results. The ramping voltage protocol would select for channels whose voltage and time dependent activation and inactivation combined to give channel activity. Small conductance records were undoubtedly missed because records were dominated by large noisy currents; small openings would be expected to produce current deflections close to the size of the noise seen in the large openings.

The presence of a noisy, large conductance channel prevented the use of traditional methods of channel analysis. Because of the less rigorous methods of channel analysis, the small numbers of values in each cluster and the large variation in these values, I do not want to make any definite conclusions at this stage. However, later studies on cultured cells indicate that some of the conductance groupings suggested by this study may be correct.

Chapter IV. Cell Culture

IV.A. Introduction

The majority of this thesis concerns single channels of cultured human RPE cells. These cells were chosen for several reasons. 1) Traditionally, cultured cells had been used for single channel recording because the dissociation procedure required for good culture leave the cell membrane free of connective tissue and other extracellular debris (Spector, 1983). Thus, cell membranes require no additional enzymatic cleaning for the formation of a gigaohm electrode-membrane seal and avoids the short-term disruption of channel function associated with enzymes such as trypsin (Lamb and Ogden, 1985). 2) The cultured cells were grown in the same building, thus avoiding the delay involved with trips to the abattoir and allowing greater control over experimental schedules. These factors combined to reduce the "post-mortem" time of the cells used for experiments from a minimum of four hours to only minutes. 3) The only other report on the single channels of the RPE involved cultured human cells (Fox et al.,1988), demonstrating that these cells were amenable to the patch-clamp technique and therefore providing a valuable reference point. At this point of the project, it was still unclear if the failure to obtain clean records of single channel activity was due to a real property of the fresh bovine cells, or whether the recording system had been incorrectly assembled. The first patch clamp recordings from cultured RPE cells showed the current level changing in clean rectangular steps. It was now possible to fine-tune the recording system and begin to accumulate data which could be properly analysed.

IV.B. Basic Techniques and Morphology
IV.B.1. Methods
VI.B.1.a. Cell Donors

Standard tissue culture techniques based on those of Dr. M. Boulton of the University of Manchester were used to ensure a supply of cultured cells. Cultured human RPE cells provided by Dr. Boulton were transported frozen

after reaching the second passage and maintained in liquid nitrogen until needed. All the results in this work are from RPE cells from one of four donors, with characteristics as outlined in Table IV.1 below.

Table IV.1 Characteristics of Cultured Cell Donors

Culture Number	Donor Age	Donor Sex	Passage on Arrival
2021	7 yrs	male	2
2023	65 yrs	male	2
2017	76 yrs	male	2
730	68 yrs	female	3

IV.B.1.b. Basic Culture Technique and Cell Maintenance

To avoid contamination of the cells, all handling of medium and cells took place in a vertical laminar flow hood using sterile technique. The stock supply of cells were grown in 75 ml cell culture flasks, and subcultured into 35 mm petri dished for patch recording. Medium was changed twice a week. The cells were maintained in the following medium;

Composition of Growth Medium (100 ml).

20 ml foetal calf serum.
10 ml F10 nutrient medium (x10)
0.4 g glucose
0.24 g NaHCO3
0.5 ml fungizone
0.0014 g l-glutamine
0.001 g kanamycin sulphate
0.006 g benzyl penicillin
0.001 g streptomycin sulphate

The mixture was made up to 100 ml with sterile deionised distilled water, and had a final pH of 7.4. The foetal calf serum (FCS) was heat-inactivated at

57°C for 45 minutes before use. Any unused portions were stored frozen at -40°C. The antibiotics, glutamine and fungizone were frozen in single use aliquots. The medium was made up in 200 ml volumes at a time and usually lasted 2 weeks. The medium was sterilised by filtering through "millipore" filters with pores of 0.2 micron diameter to remove bacteria and other contaminants.

Most of the cells used in this study were grown in 20% FCS to ensure that the all the growth factors necessary for protein expression and epithelioid morphology were present. Occasionally, single channel records were obtained from cells grown in 15% or 10 % FCS. These cells appeared identical to those grown in 20% FCS, when viewed under the light microscope. Although this does not necessarily reflect a similarity in the distribution of channels, no major differences were observed in the behaviour of single channels.

IV.B.1.c. Subculturing Techniques

Cells were usually sub-cultured when the cells became confluent; approximately once every two weeks. The rate of subculturing was varied somewhat, however, depending upon the need for cells in experiments.

The basic protocol used to subculture cells is as follows. Cells firmly attached to the flasks were washed twice with sterile phosphate-buffered saline (PBS) then filled with 1.5 ml of trypsin solution (see below). Nearly all the cells detached and rounded-up within 5 minutes. The enzyme solution containing the suspended cells was placed in a sterile centrifuge tube, with 3 ml of the growth medium added to halt trypsin activity, and spun at 700 RPM for 7 minutes. The supernatant was discarded and the pellet resuspended in 1ml growth medium. Usually, half of this was plated in a flask and the other half plated into ten 3mm sterile plastic petri dishes. Additional growth medium was then added to the cells. The petri dishes were used directly in single channel experiments. If, for some reason the experimental dishes were not needed, the remaining cells were either plated in another flask or frozen.

Composition of phosphate-buffered saline (PBS)

NaCl	0.8 g
Na_2HPO_4	0.115 g
KCl	0.02 g
KH_2PO_4	0.02 g

Made up to 100 ml with sterile distilled water and filter sterilised.

Trypsin solution

Trypsin type III (Sigma)	0.25 g
EDTA	0.02 g

Made up to 100 ml with sterile PBS and filter sterilised. Final trypsin concentration = 0.25% ; final EDTA concentration = 0.02%.

IV.B.1.d. Freezing Cells

Cells were periodically frozen to maintain stocks. After trypsinising and spinning, cells were resuspended in 1ml of growth medium containing 10% DMSO. The mixture was slowly frozen in stages by leaving it at -20°C for 2 hours, -40°C for 4 hours and -80°C for 12 hours. Cells were stored in a cryogenic container containing liquid nitrogen. When needed, cells were defrosted in a water bath at 37°C. The defrosted cell suspension was mixed with 3ml growth medium and spun at 700 RPM for 7 minutes. The pellet was plated as in a standard subculturing. A large percentage of cells usually survived freezing and attached to the flasks, but occasionally the success rate was low. This could have been due to the formation of ice crystals in the cells which had frozen too rapidly, causing the cells to rupture, for there was a high concentration of loose melanin granules in these cases.

These methods and solutions are based upon those of Dr. M. Boulton.

IV.B.1.e. Cell Plating

Cells were normally used for single channel experiments 1-10 days after plating, but occasionally cells plated up to 3 weeks previously were tested. No difference in channel activity or density was detected with the time since subculturing but the number of recordings was too low to sufficiently test for any effect. Qualitative observations suggest that the rate of gigaseal formation did decrease, however. This is most likely caused by the increase in microvilli and the cell expansion (see section IV.D.2). Cells were plated on sterile 35 mm petri dishes. These dishes were transferred directly to the recording set-up and placed in a perspex chamber designed specifically to hold them. The density of cells in each experimental dish varied slightly, but averaged 5×10^4 / cm^2.

IV.B.2. Results

The cells used in these experiments were identified by the presence of pigment granules. They were usually spindle shaped and averaged 8 µm wide and 15 µm long. They contained a central nucleus of approximately 4 µm in diameter. The nuclear area of the cells was usually surrounded by a ring of melanin pigment granules. The density of these granules decreased with cell passage but granules were always near to the nucleus. Most cells contained only one nucleus, but the proportion of cells containing more than one nucleus increased with successive passages. Increased polyploidy with passage has been noted in cultured RPE cells (Basu et al. 1983). Only cells containing one nucleus were used for patch clamp experiments. Recordings were performed on cells up to and including the 7th passage. After this point, concentration of pigment in the cells was considered too low and the cells became much more spread out. Typical cells are shown in Figure IV.1.

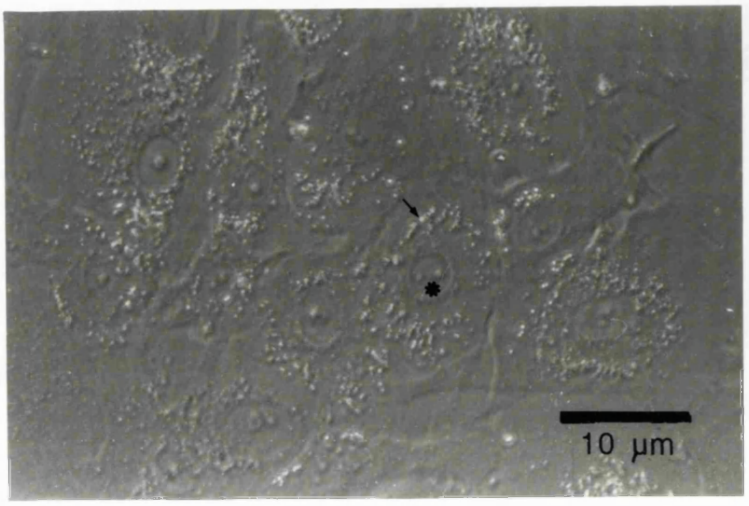

Figure IV.1 Micrograph of cultured cells under phase contrast. Stubs are indicated with an arrow, the nucleus is shown with * .

When viewed under phase contrast microscopy, the central nuclear of the cells appeared thicker than the rest of the cell. In addition to a general elevation, small "stubs" were just discernible under phase contrast. These stubs were found in the same region as the pigment granules.

IV.C. Primary Cultures

Several attempts were made to raise my own line of cultured human cells for variety of reasons. One would expect the electrophysiological characteristics of cells from primary cultures to be close to those in vivo. Secondly, it seemed statistically important to increase the number of donors for the RPE cells used in this study. In addition, using cells from donors of a variety of ages might reveal information about the ageing of the RPE.

IV.C.1. Methods

Human eyes from donors ageing from 74 to 95 years old were obtained between 26 and 32 hours post-mortem. Cells were isolated using a protocol based upon the method of Basu et al.(1983) with a few variations.

1. The anterior segment was removed at the ora serrata and the vitreous and retina were gently removed.
2. The eyecup was filled with 0.25% trypsin, 0.02% EDTA and was incubated at 37°C for 30 minutes.
3. The cells were loosened with solution flowing through a Pasture pipette, removed, and placed in a test tube with 2 ml of growth medium containing 20% FCS. This was to halt trypsin activity.
4. The cells were spun in a centrifuge at various speeds for 5 minutes (see below).
5. The supernatant was removed and the cells were resuspended in 2 ml growth medium.
6. 1 ml of the cell suspension was placed into one of the wells of a sterile multiwell plate.

IV.C.2. Results

Four attempts were made to get cells to grow. Initially, the cells were centrifuged at 400 RPM but this resulted in a dense pellet that was difficult to separate. When the speed was reduced to 100 RPM the cells appeared to be healthy, densely pigmented and round, with only a very few loose melanin pigment granules surrounding them; i.e. evidence of little damage. In each of the three sets of platings from such cells, 4-8 cells per well attached to the substrate, as indicated by the prominence of the cell nucleus and the enlargement of the cell surface area. Half the volume of medium was changed twice weekly to avoid disturbing any cells that had attached. However, no more than 8 cells ever attached per well in the 4 weeks of observation. The most probable reason for the lack of success was the fact that between 26 and 32 hours had elapsed between the donors' death and receipt of the eyes. The attachment of several cells seems to indicate that the protocol was adequate,

but that the vast majority of cells were no longer able to attach.

IV.D. Electron Microscopy

Good patch clamp recording requires a high resistance seal between electrode tip and cell membrane. This requires that the cell membrane be clean and smooth. As the apical surface of RPE cells in vivo is covered with numerous projections, it was important it was important to get a closer view of the cell surface. Scanning electron microscopy (SEM) was used to obtain Images of the membrane at different times after sub-culturing. This demonstrated the development of membrane projections and the overall condition of the cell surface.

IV.D.1. Methods

The 35 mm culture dishes routinely used in patch clamp recordings were too large for several of the stages of SEM; cells used for SEM were thus grown on "thermanox" plastic coverslips for tissue culture cut into 1cm^2 pieces.

SEM was performed on two groups of cells, one fixed three days after plating onto the coverslips, the other fixed 15 days after plating. Both trials utilised cells in the third passage from donor 2021 (7 year old male). The cover slips were prepared for SEM inspection with the following procedure:

1. Growth medium was washed off cells with Ca^{2+} and Mg^{2+} free PBS.

2. Fixing

A. Cells were fixed in the following gluteraldehyde solution for 30 minutes at room temperature.

Gluteraldehyde solution
0.1 M Na Cacodylate
0.005 M HCl
0.3 M gluteraldehyde
10^{-5} M $CaCl_2$

B. Cells were washed 3 times with Cacodylate/sucrose buffer

Cacodylate/sucrose Buffer

0.25 M Na Cacodylate

0.012 M HCl

0.22 M sucrose

10^{-5} $CaCl_2$

C. Cells were post fixed in 2% Osmium overnight (16 hr.)

2% Osmium Solution

0.2 M Na Cacodylate

0.01 M HCl

0.08 M Os O_4

Care was taken to keep the cells moist at all times during these solution changes.

3. Dehydration

A. Cells were washed briefly in 20% ethanol.

B. Cells were suspended in 20% ethanol for 10 minutes.

C. Cells were suspended in 50% ethanol for 10 minutes.

D. Cells were suspended in 70% ethanol for 10 minutes.

E. Cells were suspended in 90% ethanol for 10 minutes.

F. Cells were suspended in 100% ethanol for 10 minutes.

4. Cells placed into a critical point dryer to avoid the destruction of the membrane which occurs when fluid evaporates.

5. Cells were gold coated and placed in the scanning electron microscope.

IV.D.2 . Results

Figure IV.2 shows the surface of the nuclear region of an RPE cell fixed three days after plating. The central bulge, which indicates the position of the nucleus, can be seen. Surrounding the nuclear area are many short, cylindrical "stubs" projecting out from the membrane. These stubs were present on nearly every cell and were always found close to the nucleus. They occurred equally

in the central area of the culture dish, where the cells were approaching confluence and in the peripheral, subconfluent areas. The cell membrane away from the nucleus appears smooth but thin and was devoid of stubs. The stubs are approximately 0.5-1 μm in diameter. They appear approximately spherical, and thus can project up to 1 μm from the membrane surface.

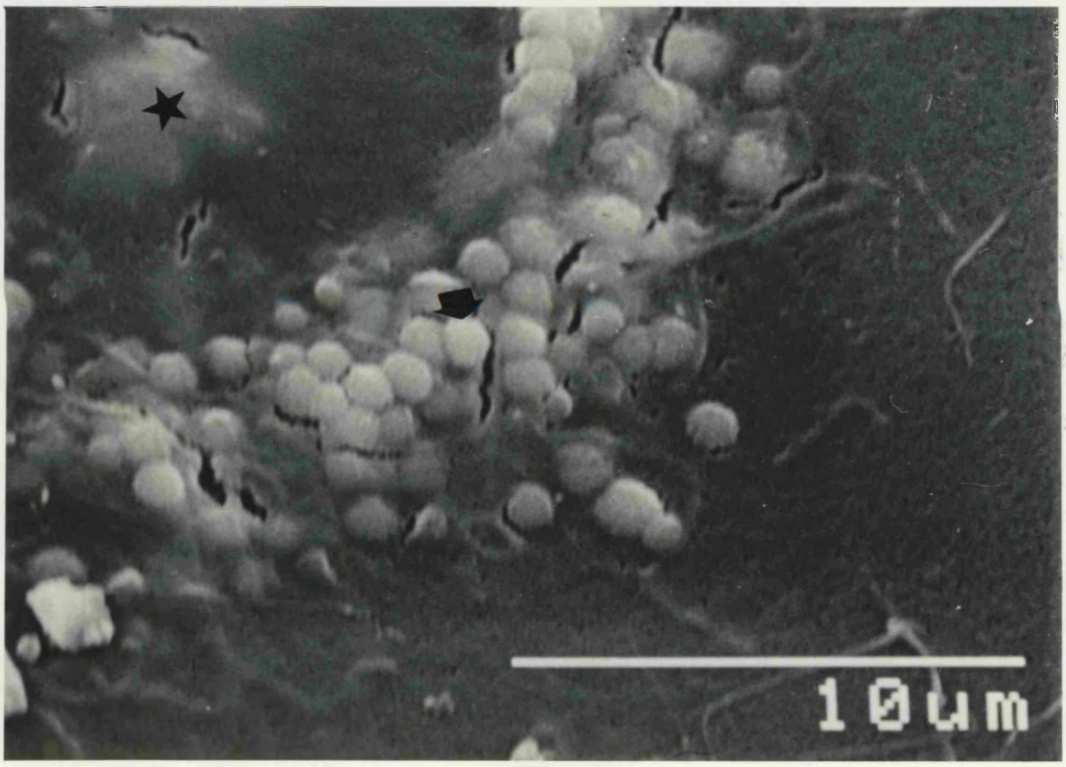

Figure IV.2. Scanning electron micrograph of a cultured RPE cell taken three days after the cell was plated onto the substrate. The arrow shows a stub and the nucleolus is indicated with a ★ .

Figure IV.3 shows a SEM of a confluent cell fixed 15 days after plating. The stubs on these cells were less prominent, but it is unclear whether this is due to the fact that the stubs are receding, or because the remaining cytoplasm

has partially engulfed them. The reduction in stub number in this preparation, when compared to cells fixed only three days after plating, is unlikely to be an artefact of the SEM preparation as this trend was also noticed in a number of preparations under the light microscope.

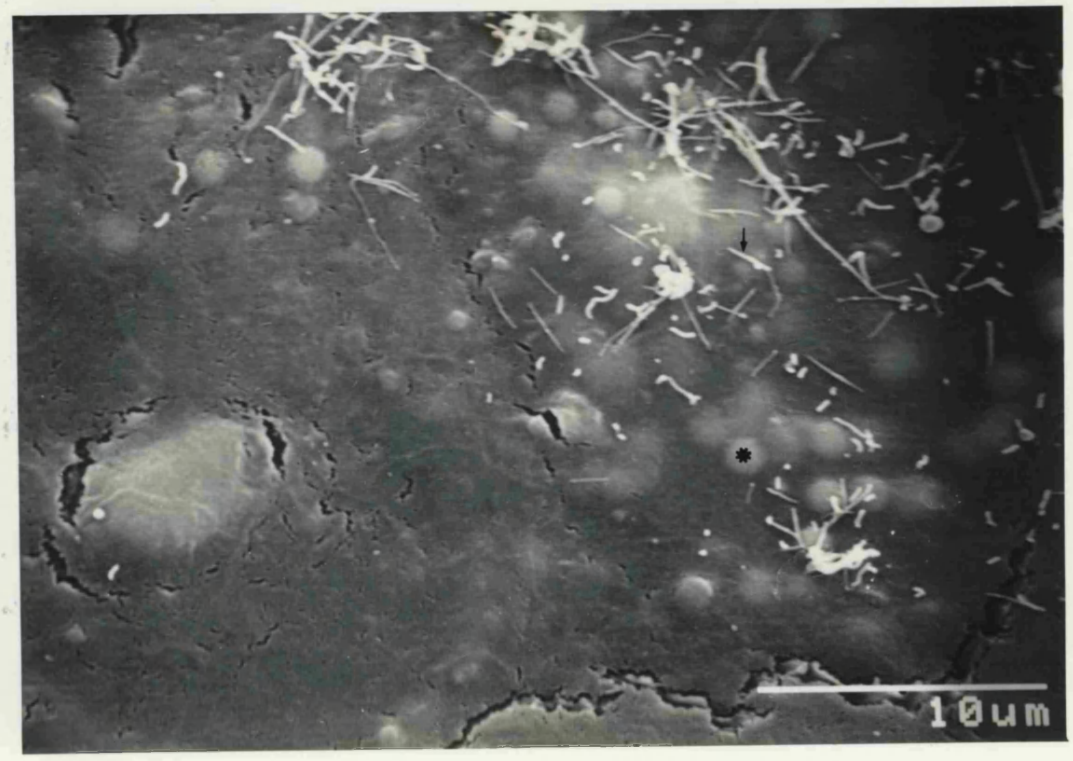

Figure IV.3. Scanning electron micrograph of a cultured cell fixed 15 days after plating. Microvilli are shown with an arrow and a stub is indicated by a ✱ .

In confluent cells fixed 15 days after plating, a second type of projection was detected. This can be seen in the higher magnification micrograph in Figure IV.4. This closely resembles the microvilli commonly reported (Basu et al., 1993). These microvilli were approximately 0.1 µm wide and 1-2 µm high. They were only present on confluent cells, but often extended further from the nuclear region than the larger stubs. Both types of projection often occurred at the same place. The thinner microvilli were never seen on the cells fixed 3 days

after plating.

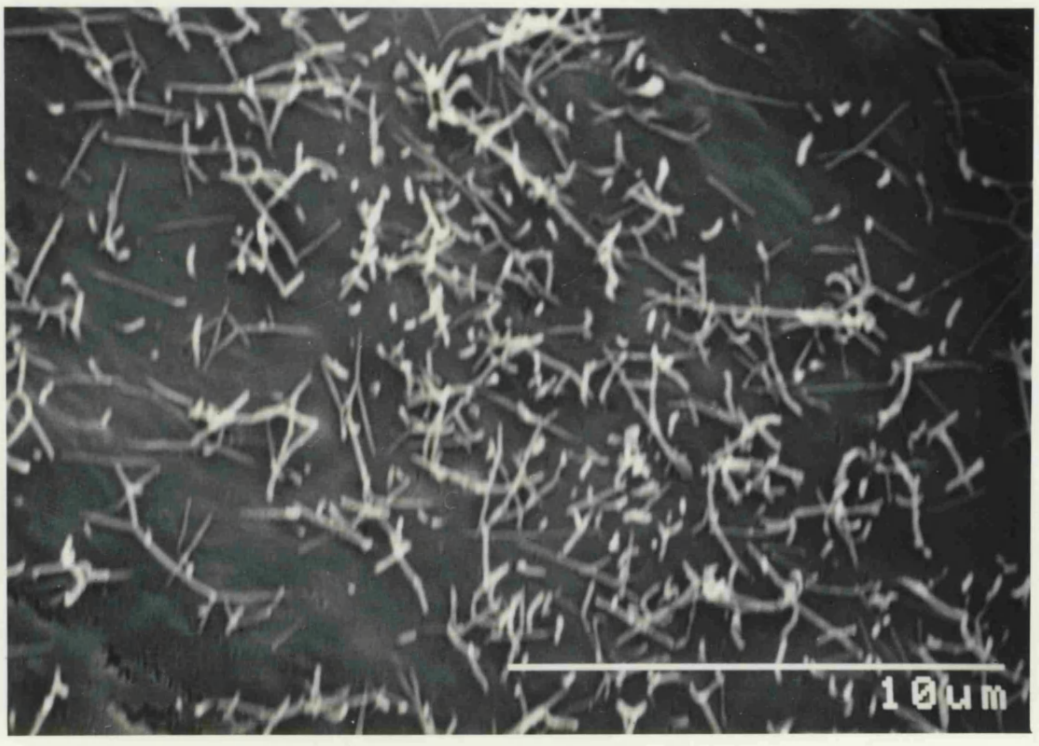

Figure IV.4. Scanning electron micrograph of a cultured cell fixed 15 days after plating. The feather-like extensions were present in a region away from the nucleus

Cell membranes from both preparations cracked in places; viewing the cells under light microscope after each successive stage indicated that the cracking occurred in the critical point dryer. It is possible that the pressure dropped too quickly and the extreme thinness of the cells made them vulnerable to this. The cracking does not appear to have affected the overall cell structure.

IV.E. Recording Protocol

Cells from passage 4-8 were used for patch clamp recordings.

Although the basic method of gigaseal formation described in section II.B.11 was followed, I adjusted the protocol based upon my experience during the experiments. The thickness of the cells greatly affected the rate of successful gigaseal formation. In the flatter portions of the cells, away from the nucleus, seal attempts were marred by the presence of synchronised 50 Hz noise. This noise was never detected when the electrode was positioned elsewhere in the recording bath, and was not caused by the incomplete grounding of components inside the Faraday cage. The 50 Hz interference was detected when the electrode approached the membrane at the thinnest point of the cell, and increased as a seal was formed. The highest resistance seal ever formed with the membrane in this peripheral area was only 0.5 GΩ and seals were never maintained for longer than 1 minute. It is hypothesised that the thinness of the membrane made it difficult to compensate for the 45° angle of electrode attack; in a cell region with a thick layer of cytoplasm, the membrane can mould around the slight angle. in a flat region no such adaptation is possible and the electrode often breaks on the surface of the underlying substrate before both edges have reached the membrane.

A second aspect of cultured cell morphology that interfered with gigaseal formation was the presence of cytoplasmic stubs covering the thickened regions of the cells. Many more than 200 attempts were made to form a gigaseal onto one of these stubs; only 3 short lived seals were ever formed. As mentioned above, these elevations were clearly visible under phase contrast microscopy and thus could be avoided when advancing the microelectrode towards the cell.

It quickly became apparent that gigaseal formation on thin cell regions was impossible, but the presence of membrane stubs on the elevated sections of the cells also hampered seal formation. Successful recording thus depended upon finding the combination of an area of elevated membrane devoid of microvilli stubs.

When subconfluent cells were used, the rate of obtaining successful seals increased. This is most likely because the number and density of the stubs was less in subconfluent cells, providing a greater area of smooth, patchable membrane between the stubs. Sub-confluent cells were also preferred in the only other report of patch clamping from cultured RPE cells to date (Fox et al., 1988) although the reasons for this were not expanded.

V.F. Summary

The results presented in this chapter suggest that the cultured cells used in this study were healthy. The continued presence of melanin granules indicates that a certain level of differentiation was maintained. Melanin levels have been are reported to be reduced in proliferating cultures of RPE (Pfeffer, 1991) and pigmented ciliary epithelial cells (Cilluffo et al., 1993), but return with time. The possible implication of these results to cell polarity and the degree which these cells might mimic those in vivo is discussed in Chapter VI.

It is unclear what the larger stubs are. When cultured cells are challenged with rod outer segments or bacteria, a thick projection of similar dimensions quickly forms and attaches itself to the foreign body (Boulton and Marshall, 1986). The absence of either substance make this explanation unlikely, however. These stubs did not resemble the bleb protrusions seen in other cultured epithelial cells (Peterson and Mooseker, 1993). It is more probable that these stubs are formed by pigment granules. Several attempts were made to relate the position of pigment granules and the stubs by moving the phase contrast ring; the elevations were usually associated with pigment .

The small diameter projections seen in SEM resemble the microvilli previously reported in RPE cultures (Basu et al., 1983). The observation that these microvilli were only seen in confluent, established cultures reinforces the idea that these microvilli reflect a more differentiated state.

It was possible that some of the features seen under SEM were artefacts of the Thermanox coverslips. Both the standard perspex petri dishes and the

Thermanox coverslips were " treated for tissue culture " by the makers but it was not possible to discover what each treatment entailed. The cells looked identical under the light microscope. As neither surface was permeable nor coated with laminin or other treatment reported to alter cell behaviour, it is reasonable to assume that the pattern of membrane projections observed under SEM occurs in cells grown on the petri dishes.

It is not obvious why none of the primary cultures of human RPE cells were successful. The most likely explanation involves the high donor age and the long post-mortem time. The attachment of several cells in each attempt indicates that the protocol was adequate but the vast majority of cells were no longer able to attach.

The relevance of cultured cells to those in vivo and the question of membrane polarity are discussed in Chapter VI.

Chapter V. Single Channels of Cultured Human RPE Cells

V.A. Introduction

The ability to voltage clamp small patches of membrane means that the single channel technique can theoretically provide precise information about the activity, selectivity and location of the channels which contribute to a cell's physiology. Although not electrically excitable, the RPE undergoes a series of potential changes in response to light and by examining the effect of changes in potential on individual channels, the contribution of these channels to the entire response can be more thoroughly understood.

Several whole cell studies, and one single channel study, have been undertaken in which channels of the RPE have been voltage clamped, and have been mentioned briefly in Chapter I. Several voltage-dependent currents were described from the whole cell work, including inwardly rectifying and outwardly rectifying potassium currents (Hughes and Steinberg, 1990; Fox and Steinberg, 1992; Wen et al., 1993). However, none of the potassium channels identified in the single channel study showed any sign of voltage activation (Fox et al., 1988).

The purpose of this chapter is examine the activity of single channels from cultured human RPE cells. The normal parameters by which channels are characterised, such as conductance and selectivity were analysed, and the relationship between voltage and channel activity was investigated. The channels in this study were found to be voltage-activated.

V.B. Methods

The basic experimental set-up for these experiments has already been described in Chapter II, and the protocols used for the culture of RPE cells are discussed in Chapter IV. Specific techniques used in this chapter will be explained as they arise.

Channel conductance is defined as the slope of the single channel

current-voltage (i/V) relation. The i/V plot for each channel was fitted with a first order regression equation to determine the slope which best described each data set. Most patches were clamped to test potentials from -60 to 120 mV and observed for spontaneous activity, but activity was rarely seen at all potentials within this range. Consequently, the conductance values were not all determined from the same range of potentials. In some records, the amount of current flowing through a particular channel type did not increase, or even decreased, when the patch was depolarised beyond a certain potential (see section V.C.1.c below). The unitary conductance of such channels was calculated up to the point of inflection in the i/V curve.

V.C. Results

The data below were obtained from the RPE cells of 3 donors, but the cells were subcultured onto several hundred experimental culture dishes. Between 10 and 20 attempts at making seals were made from each dish. The rate of success varied considerably: in some preparations, a seal was made at each attempt, but sometimes weeks went by without a successful recording. The final analysis was made on some 73 experiments. Cells from passages 4-8 were used, and were plated between 2 and 35 days before being used for experiments. The passage number, donor, and age since plating is shown in Table 1, Appendix II, for all recordings.

In approximately 10% of successful seal attempts, channel activity was observed at the membrane potential (i.e. at a pipette potential of 0 mV) during the first few seconds after seal formation. After this time, no further activity was ever seen in such patches even though they were polarised to a range of positive and negative values up to ± 150 mV. It was not possible to obtain sufficient data within the short space of activity to characterise these channels.

V.C.1. Channel Conductance

It is obviously important to discover the number of different channels present on the membrane and if it is possible to and group the channels by certain criteria. Only after the channels are grouped can the characteristics of a population be assigned to particular channel type. As mentioned previously, two basic types of information are available from single channel analysis; the amount of current flowing through a channel and the temporal aspects of channel activity. It is theoretically possible to distinguish between channels of different type on the basis of both of these characteristics, but historically the amount of current flowing through a channel and the way in which this current changes with the potential across the membrane has been used most frequently to both distinguish and describe different channel types. In this study, channels were separated on the basis of their current amplitudes because this was the most consistent of the measured attributes. However, even the conductance values within hypothesised channel groups varied considerably. Because of this variation, it was necessary to obtain as many records as possible. Thus much of this study involved a single type of experiment, the recording of spontaneous activity in channels over a range of potentials under identical conditions.

This basic experimental protocol was performed with both control and high potassium solution in the electrode. The concentration of sodium and potassium bathing the extracellular face of the channels was considerably different in the two situations; $[Na^+]$ = 145 mM and $[K^+]$ = 5 mM in control solution, $[Na^+]$ = 35 mM and $[K^+]$ = 100 mM in high potassium solution (see Table II.1). The results presented here are from 50 cell attached records with control solution in the patch electrode and 23 cell attached records with potassium internal solution in the patch electrode. The results from these two types of experiments will initially be dealt with separately.

V.C.1.a. Control Electrode Solution

For each recording showing channel activity, the unitary conductance was calculated. The distributions of channel conductances was plotted as a histogram and is shown in Figure V.1. There appeared to be 3 major conductance peaks; the simplest possible interpretation is that there were three channel types present. However, the populations overlap, so it was first necessary to show that more than one population of channels was present.

The distribution was fitted with a single Gaussian function, or the sum of several Gaussian functions;

$$f(x) = (a/(\sigma * \sqrt{(2\pi)})) * e^{-0.5[(x-\mu)/\sigma]^2}$$

where a = height; μ = mean; σ = standard deviation. Deviations of the data from the function were calculated by the least-squares method. For a single Gaussian, the residue was 6.69: for two, the sum of squares fell to 5.39, and they fell considerably further with three Gaussians factors to 1.25. The sum of squares remained 1.25 when the number of Gaussian factors was increased to four. This strongly suggests that there are three channel types present when grouped by their conductances. The three channel types identified in this way had mean conductances of 26.4 ± 6.7 pS, 54.4 ± 7.0 pS and 91.7 ± 12.0 pS.

When the sample size is small, the choice of class interval can effect the value of mean conductance when these are determined by a fit to a frequency distribution. To remove this influence, records were divided by their conductances into the three groups at points suggested by the distribution. Group A contained records whose conductances were less than 40 pS; G_A < 40 pS. Likewise, groups B and C were defined as 40 pS < G_B < 80 pS and G_C > 80 pS. The mean value of the conductances for group A was 24.4 ± 8.5 pS, 58.7 ± 10.0 pS for group B and 95.6 ± 9.7 pS for group C. These values are all well within the standard deviations of those found by fitting the distribution with the sum of three Gaussian, and thus the choice of class interval did not

significantly distort the mean conductance values for each supposed group. The channel types observed with control solution in the electrode will be referred to as the 24 pS, the 59 pS and the 96 pS channel types.

The grouping of channels effects a variety of parameters in this analysis. Because the variation in both conductances and actual current size within each group was considerable, further tests were performed to assure the groups were distinct. The Statgraphics software package was used to perform an unpaired t-test to compare the conductance values of the 24 pS with those of the 59 pS types, and compare the 59 pS types with the 96 pS types The results are shown in Table V.1. Assuming unequal variance in all groups, the groups were significantly different, with $p < 0.001$ in both cases.

For each channel type, the current values measured at a given potential were averaged (Appendix III, Table 7.) The resulting i/V for all three channel types when the electrode contained control solution is shown in Figure V.2.

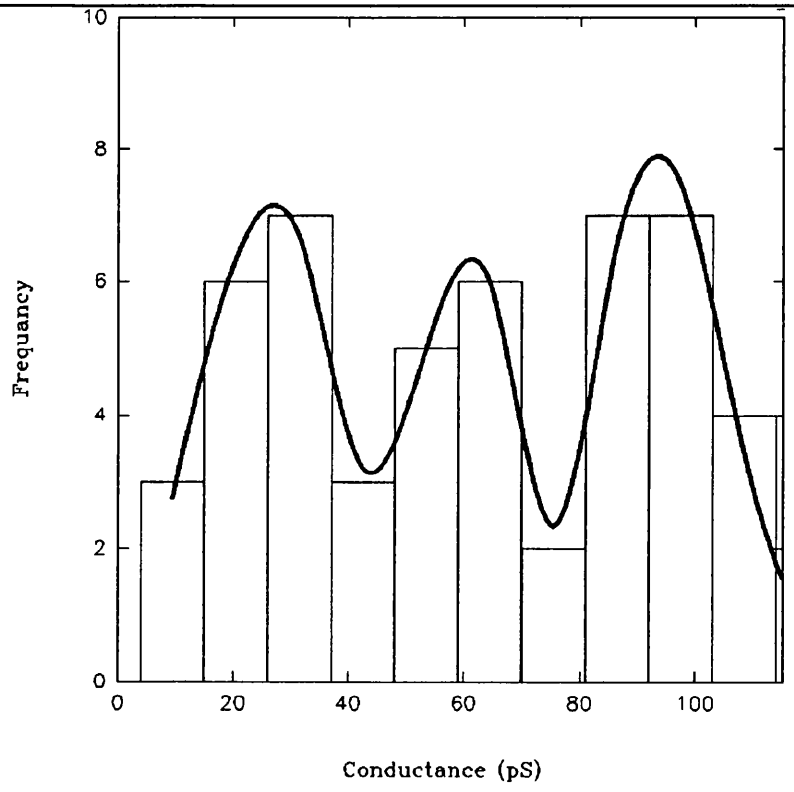

Figure V.1. The distribution of conductances of channels observed when the electrode contained control solution. The distribution was fitted with the sum of three Gaussians.

The three conductance values obtained in various ways are all roughly multiples, and thus it is important to reiterate that the conductance values were taken from amplitude measurements that clearly represented single channel openings. They do not represent double and triple openings of the same channel type. This question is examined more thoroughly in section V.C.6.

The above arguments make it extremely probable that at least three distinct channel types were present on the top surface of cultured human RPE cells. An example of the 24 pS channel type is shown in Figure V.3; the 59 pS channel type is shown in Figure V.4., while the 96 pS channel type is shown in Figure V.5. The conductance, reversal potential and other characteristics of each record grouped into channel types are shown in Appendix I, Table 2. The actual current flowing through these channels over the range of potentials tested is shown in Appendix III, Table 1.

A small number of records did not appear to fit into any of the groups. There are several possible reasons for this but to avoid error these records were excluded from all groups.

The 96 pS channel type was most frequently encountered (37% of all channels analysed); 31% of the channels seen were the 59 pS type and 24% were the 24 pS type . Only 8% of channels were unclassified.

V.C.1.a.i. Non-linear Conductance Values

In eight records of the 96 pS channel types, the conductance decreased, fell to zero or even became negative as the patch was depolarised by more than 50 to 100 mV. Initially, it was thought that this observation was merely an artefact of the protocol used to measure the current amplitudes; if the channel became more flickery with depolarization and the rate of transitions towards the baseline increased, then mean current obtained from an all points histogram would decrease in value. However, these records were carefully reanalysed and it was found that the reduction in current value was real. Figure

V.6 illustrates this phenomenon.

Three important observations relate to this decrease in current value. First, the channel activity was not effected. The probability of finding the channel open, and the average duration of each opening continued to increase with depolarized potential over the range which caused a drop in current. Second, this effect was never seen when the electrode contained the high potassium solution. Finally, this effect was seen more frequently and to a greater extent as the passage number of the culture increased.

Table V.1. Unpaired T-Test of Mean Conductances of Each Channel Group

Control Solution in Electrode

	24 pS vs. 59 pS	59 pS vs. 96 pS
Difference between Means	35.35	36.05
Ratio of Variances	0.734	0.804
t Statistic	8.97	10.17
Significance Level	p<0.001	p<0.001

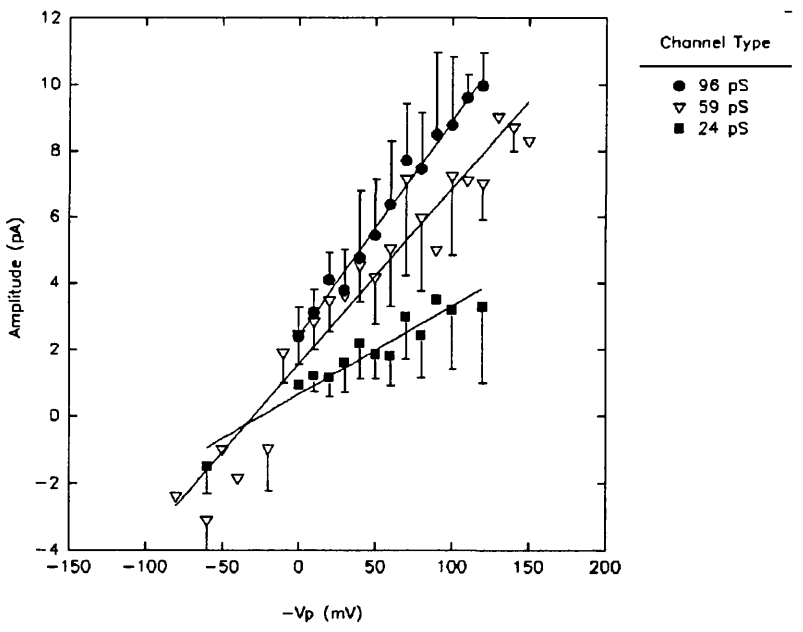

Figure V.2. Mean Current Voltage Relationship - control solution in bath and electrode. The current values at each potential were averaged for each channel type and the curves were fitted with a first order regression.

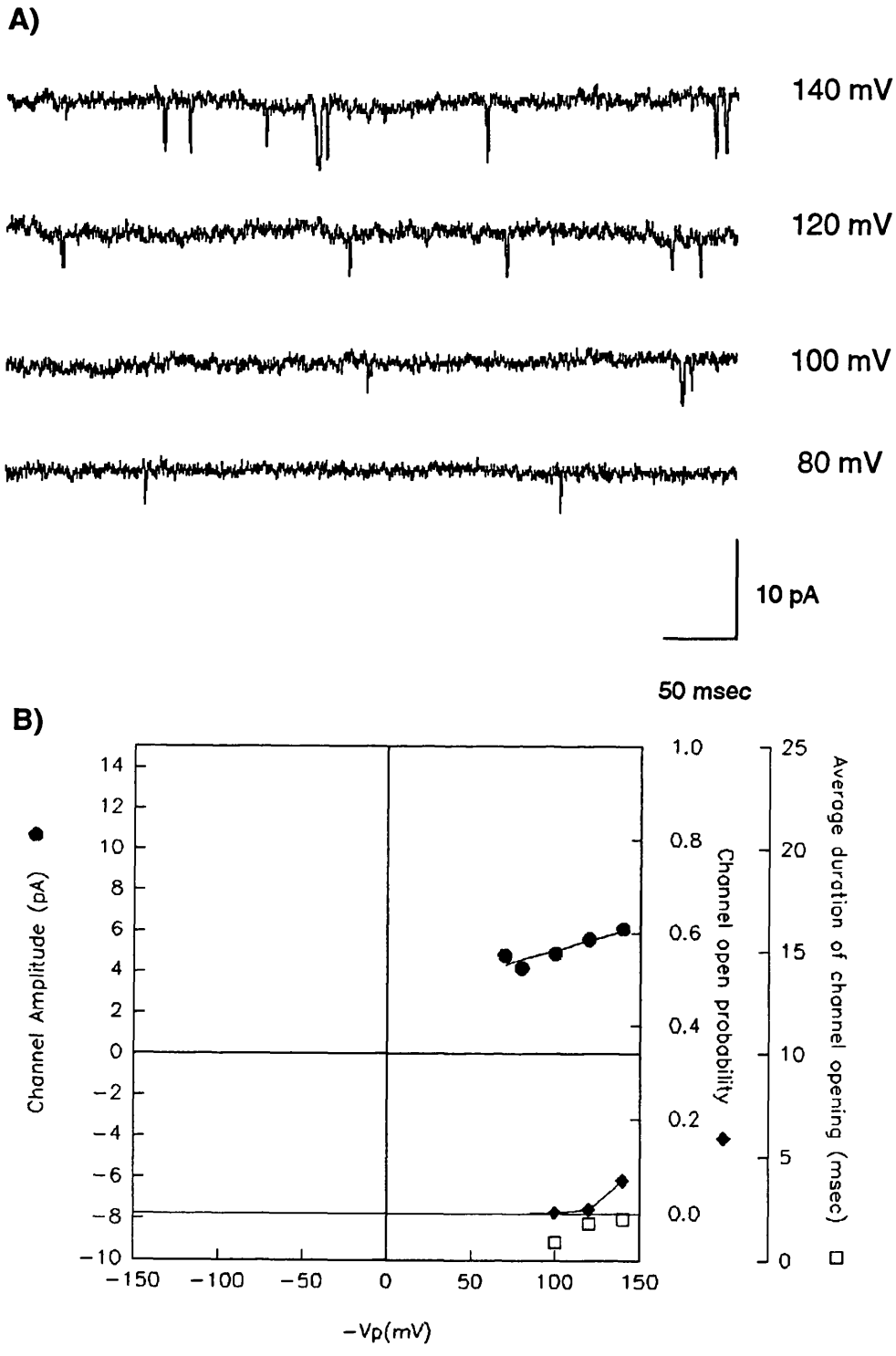

Figure V.3. Example of the 24 pS channel type observed when the electrode contained control solution. In A, the current trace activated at different potentials is shown. Downward deflections are outward current through open channels. In B, the current voltage plot is shown. Information about the kinetic attributes is included. All potentials given as -Vp with respect to membrane potential.

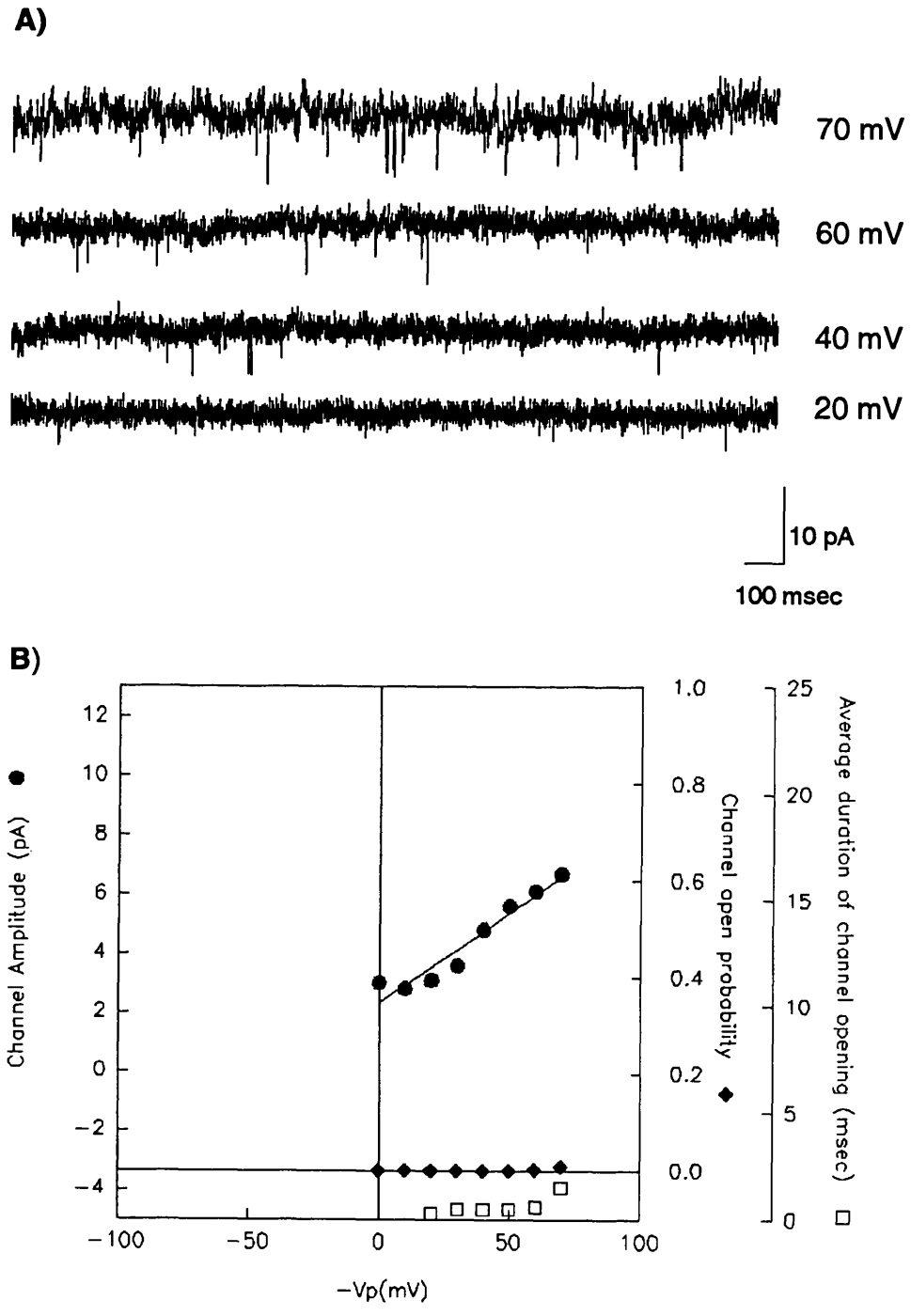

Figure V.4. Example of the 59 pS channel type observed when the electrode contained control solution. In A, the current trace activated at different potentials is shown. Downward deflections represent outward current through open channels. . In B, the current voltage plot is shown. Information about the kinetic attributes is included. All potentials given as -Vp and are with respect to the membrane potential.

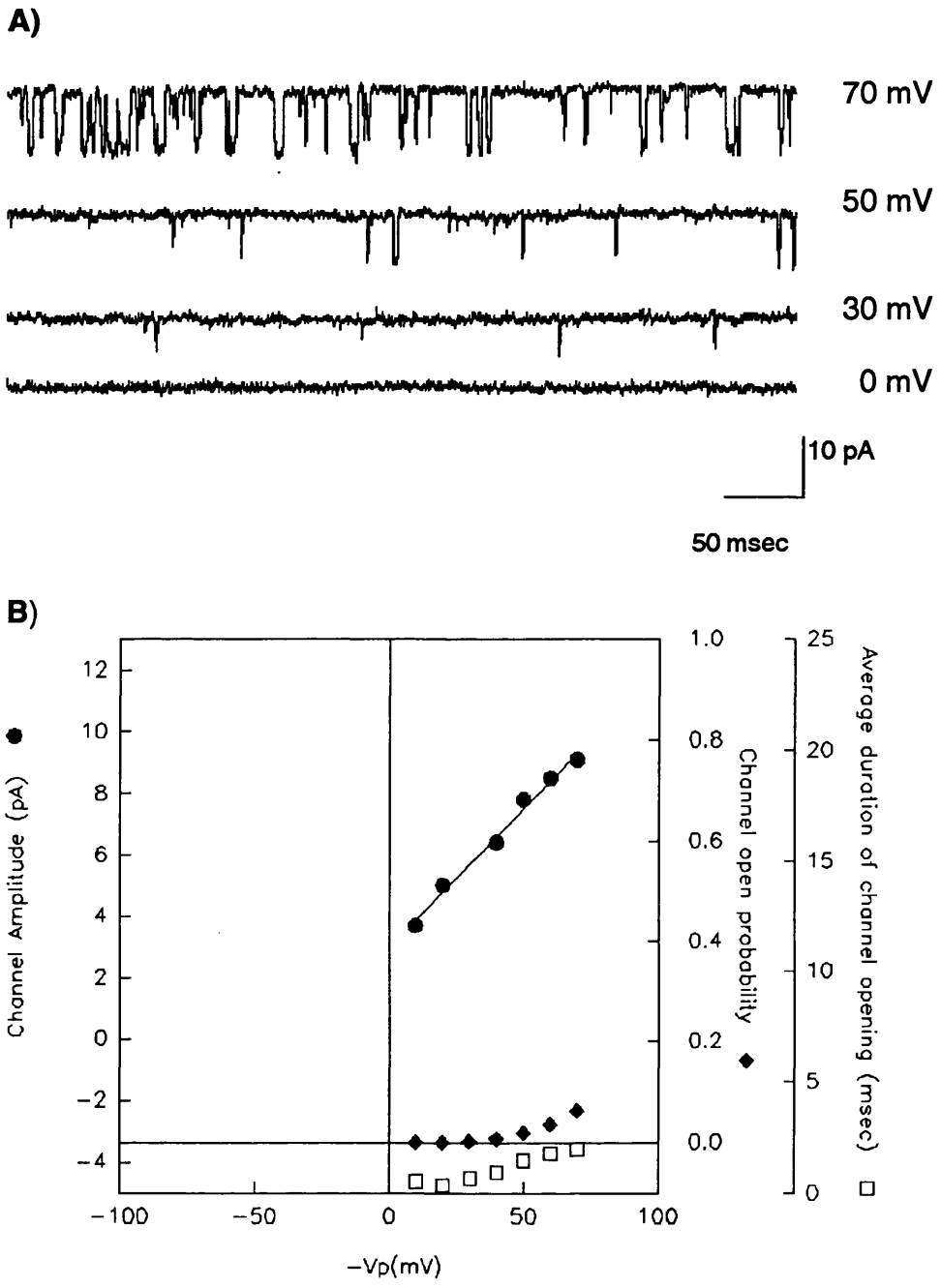

Figure V.5. Example of the 96 pS channel type observed when the electrode contained control solution. In A, the current trace activated at different potentials is shown. Downward deflections indicate outward current flowing through an open channel. In B, the current voltage plot is shown. Information about the kinetic attributes is included. All potentials given as -Vp and are with respect to the membrane potential.

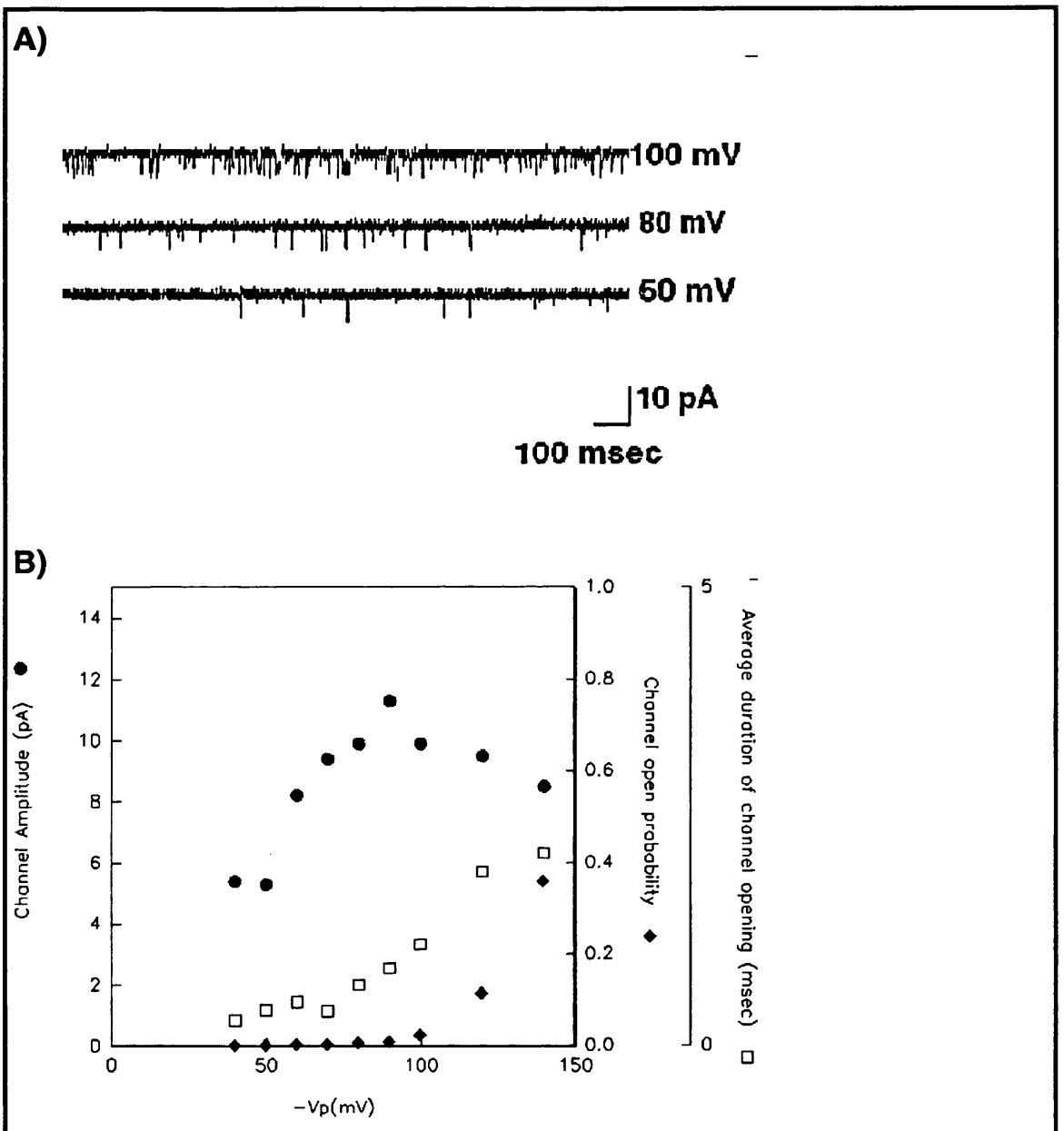

Figure V.6. A) Single-channel data from a 96 pS channel type showing a drop in conductance as the patch is depolarized by 100 mV. Downward deflections indicate outward current through open channels. **B)** Results of kinetic and amplitude analysis for this record over a range of potentials, showing that the drop in amplitude is independent of the voltage-dependent increase in channel activity. The electrode and bath contained control solution.

V.C.1.b. High Potassium Electrode Solution

At least three channel types were evident when electrode contained high potassium solution. The first was distinguished by conspicuous inward rectification; the conductance of this channel increased as the patch was hyperpolarized. An example of this channel is shown in Figure V.7. The remaining records were separated on the basis of their conductances. A distribution of the conductances of these channels is shown in Figure V.8 ; the inward rectifier channel types have been excluded from this histogram. A procedure similar to that used in section V.C.1.a.i was followed and the distribution was fitted with one Gaussian function or the sum of several Gaussian functions. The sum of the squares of the residuals was less with two Gaussian functions, and did not substantially decrease when three terms were added. The two Gaussian functions had peaks at 53 pS and 157 pS. The conductances were grouped according to this fit.

To compensate for any effect of bin number, the groups were separated, as suggested by the histogram above, and the mean conductance of each group was calculated. This yielded values of 47.0 ± 19.2 pS and 145.3 ± 41.0 pS. The conductances of these groups were compared with an unpaired t-test and found to be significantly different, with $p < 0.001$. The three channel types observed when the electrode contained high potassium will be referred to as the 47 pS type, the 145 pS type and the inwardly rectifying type. An example of the 47 pS channel type is shown in Figure 9, and of the 145 pS channel type is shown in Figure V.10. The mean conductance of the inwardly rectifying channels was 108.3 ± 29.3 pS, although the nature of rectification means that this value is determined by the particular range of points which make up each conductance value.

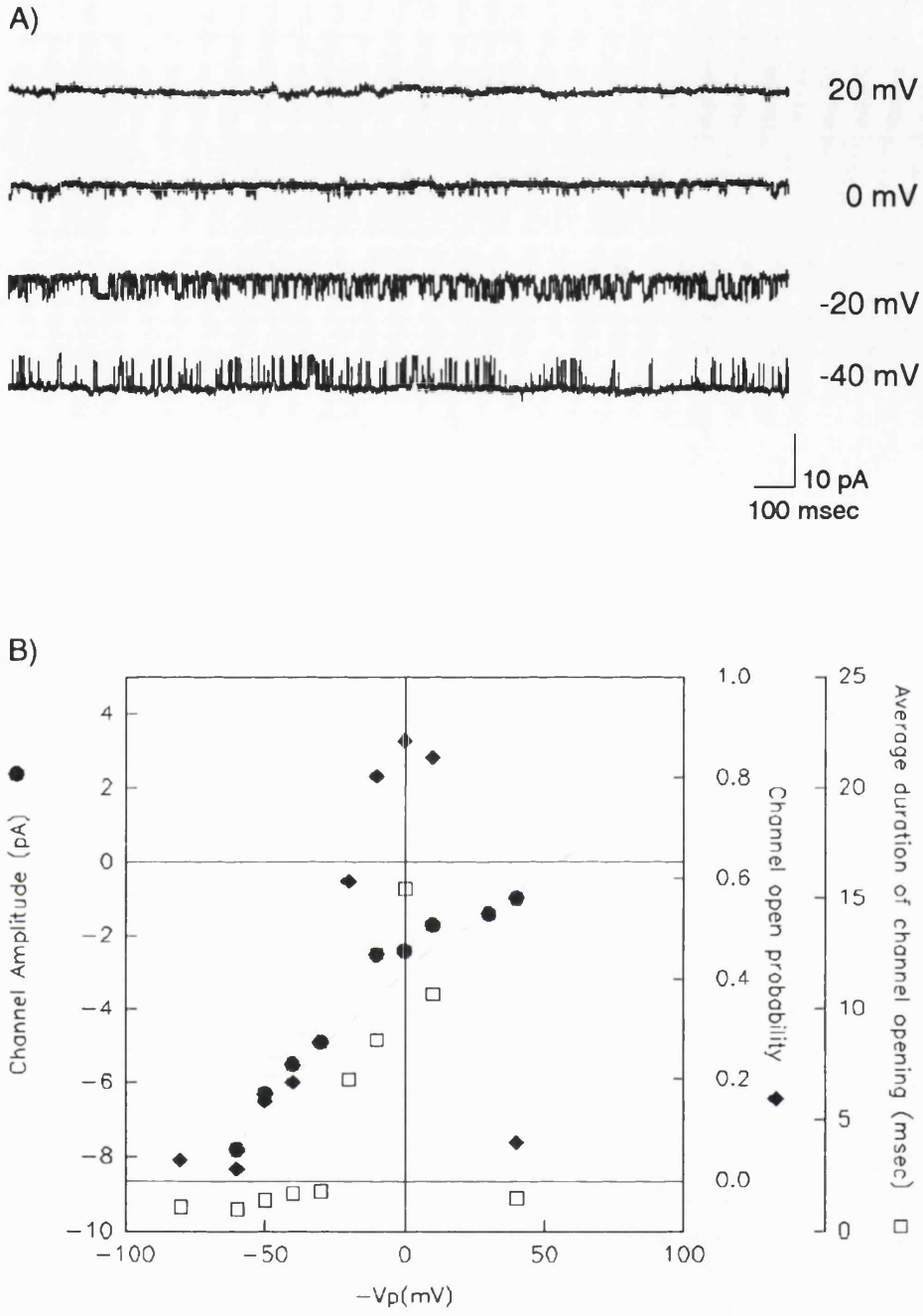

Figure V.7. Example of the inwardly rectifying channel type. This activity was only observed when the electrode contained high potassium solution. In A, the current trace activated at different potentials is shown. Upward deflections represent inward current through open channels. In B, the current voltage plot is shown. Information about the kinetic attributes is included. All potentials given as -Vp and are with respect to the membrane potential.

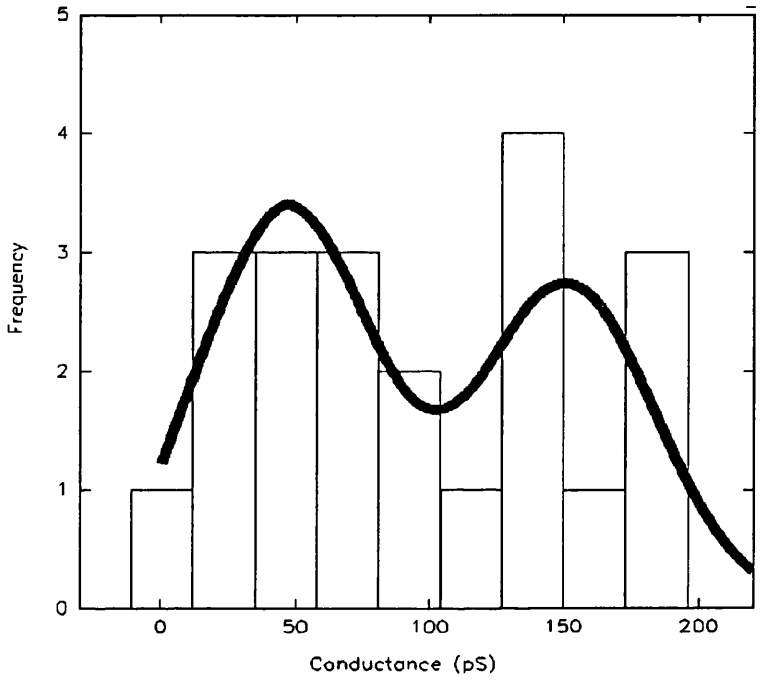

Figure V.8. Distribution of the conductances observed when the electrode contained high potassium solution. The inward rectifier records are excluded. The distribution is best fit with the sum of two Gaussian functions.

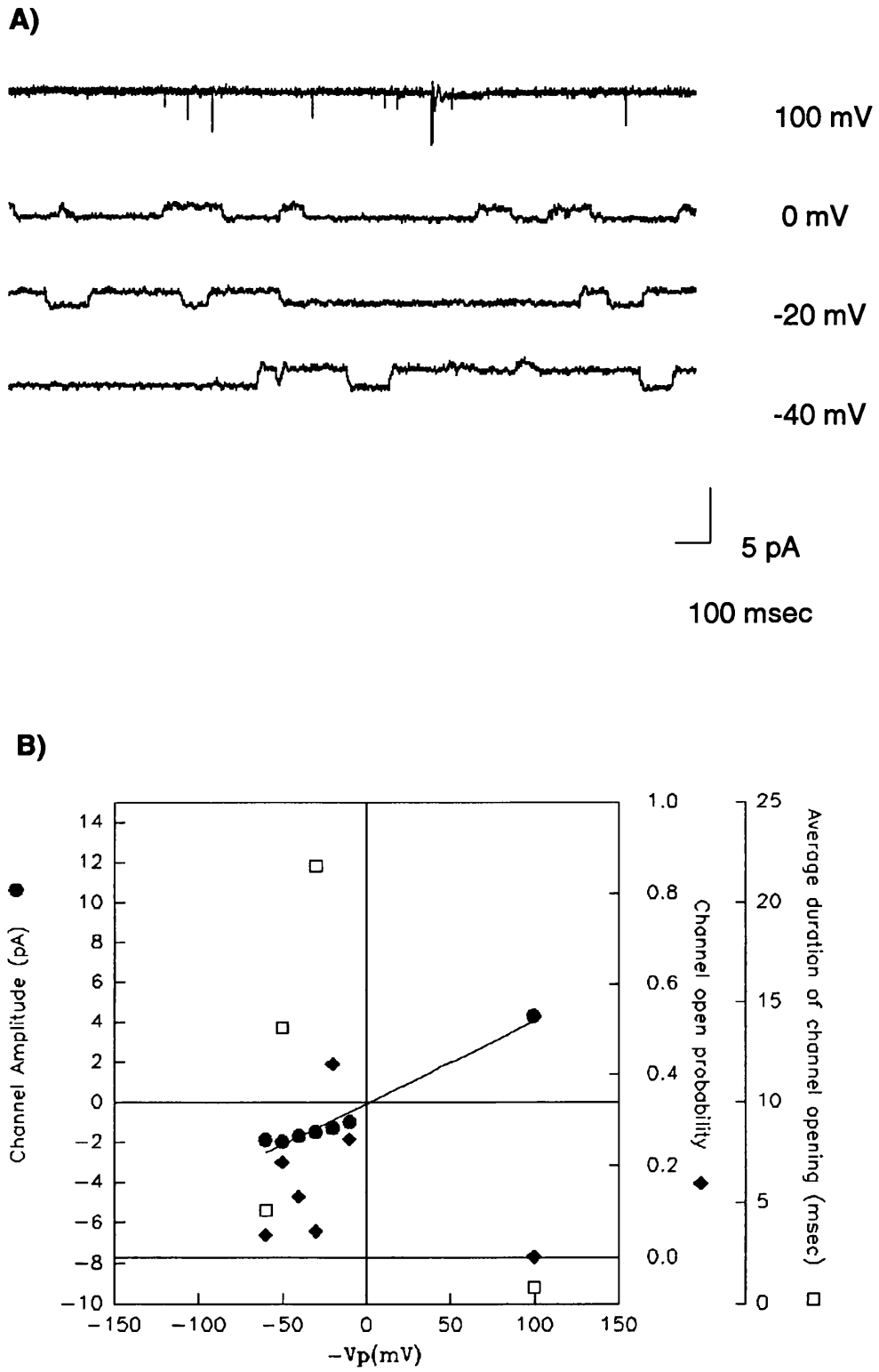

Figure V.9. Example of the 47 pS channel type observed when the electrode contained high potassium solution. In A, the current trace activated at different potentials is shown. At 100 mV, downward deflections are outward current through open channels; at all other potentials upward deflections indicate inward current. In B, the current voltage plot is shown. Information about the kinetic attributes is included. All potentials given as -Vp and are with respect to the membrane potential.

A)

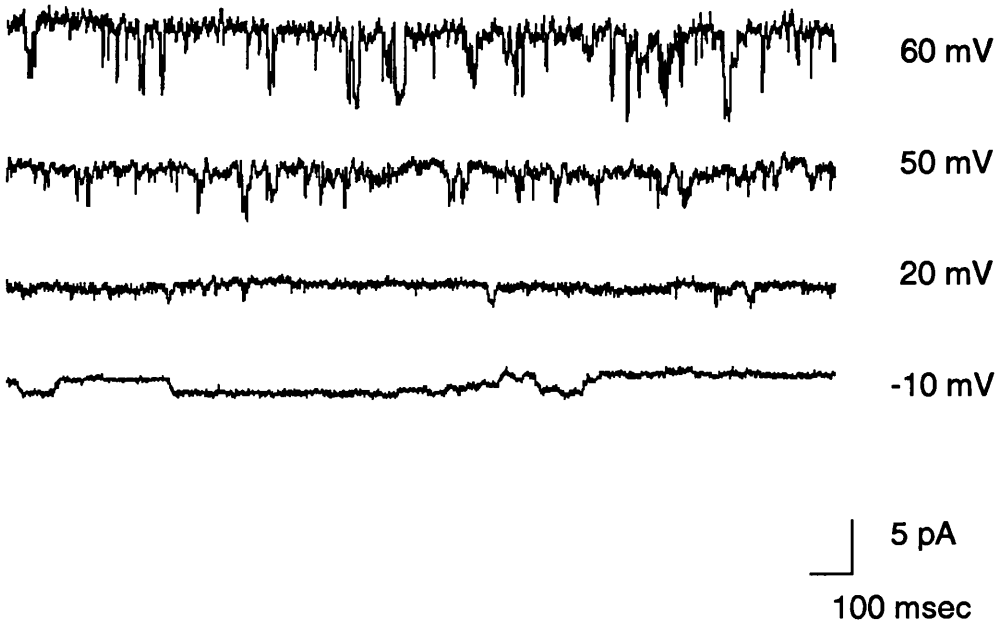

B)

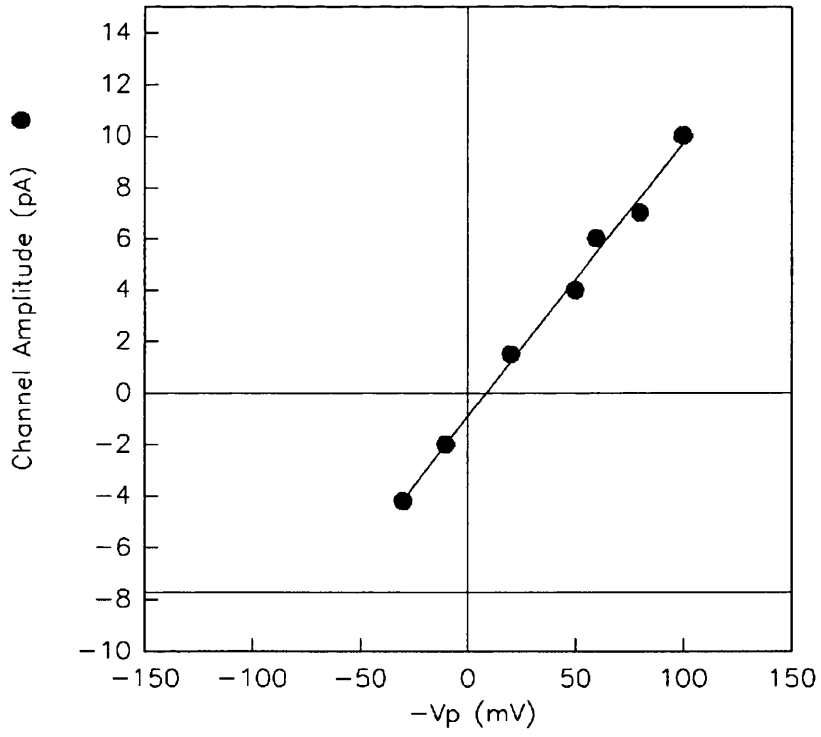

Figure V.10. Example of the 145 pS channel type observed when the electrode contained high potassium solution. In A, the current trace activated at different potentials is shown. At 60, 50 and 20 mV, downward deflections are outward current through open channels; at -10 mV upward deflections indicate inward current. In B, the current-voltage plot is shown. All potentials given as -Vp and are with respect to the membrane potential.

The average current values at a given potential for each channel type are plotted in Figure V.11. (see also Appendix III, Table 8.) The curves were fitted with a second order regression because the sum of squares of the residuals was smaller than when this line was fit with a first order regression.

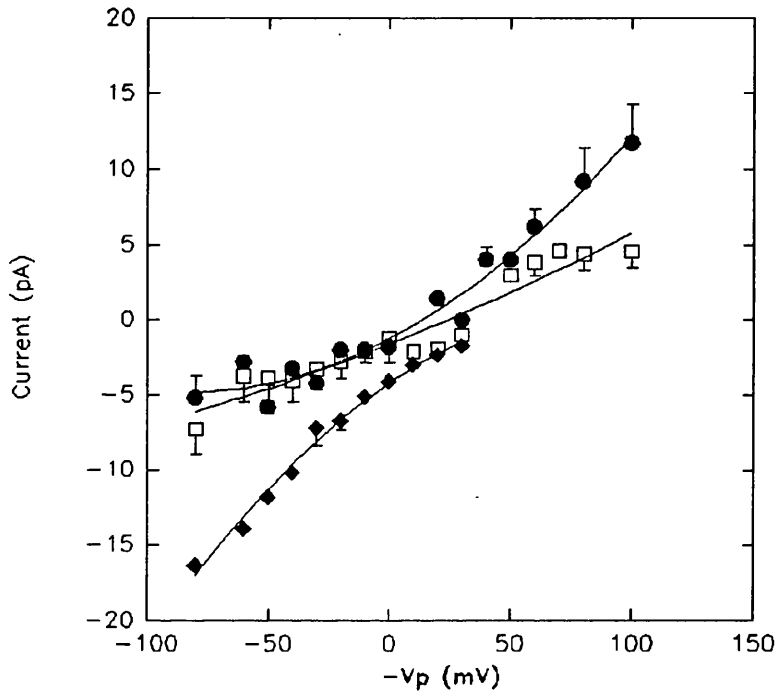

Figure V.11. Mean Current-Voltage Relationship. The electrode contained high potassium solution and the bath contained control solution. The current values at each potential were averaged for each channel type and the curves were fitted with a second order regression.

The 145 pS channel types were encountered most frequently (50%), followed by the 47 pS types (38%). The inwardly rectifying channel was seen in 12% of the records.

The conductance and reversal potential for all the channels observed when the electrode contained high potassium is shown in Appendix I, Table 3 The actual current at each potential is in Appendix III, Table 2.

V.C.2. Reversal Potentials

The potential at which the current flowing through a channel reverses, V_{rev} can theoretically provide valuable information about the permeability of that channel type to specific ions when the ionic composition on either side of the channel is known. Even when experiments are performed in the cell attached mode, as was necessary in this study, information about V_{rev} can roughly indicate a selectivity of one ion over another provided that the predicted Nernst potentials for the ions in question are widely separated. By its very nature, however, the potential at which no current flows cannot be measured with the patch clamp technique, and this value must be interpolated from the potentials for which current information is available. In several of the records in this study considerable baseline noise was present that may have obscured small currents. In addition, nearly all of the channels in this study were open less that 0.1% of the time at the resting membrane potential, and this also made it difficult to detect and reliably analyse the currents at this point. Consequently, V_{rev} often had to be interpolated over > 40 mV, and any small variations were thus magnified.

V.C.2.a. Control Electrode Solution

The first step in analysing the reversal potential was to determine if V_{rev} changed with conductance. The relationship between V_{rev} and conductance for each individual record is shown in Figure V.12. The only conclusion is that the variation in V_{rev} increases as the conductances falls. It was clearly not possible to subdivide channel types in terms of their V_{rev}, or reinforce the classification based upon conductance values.

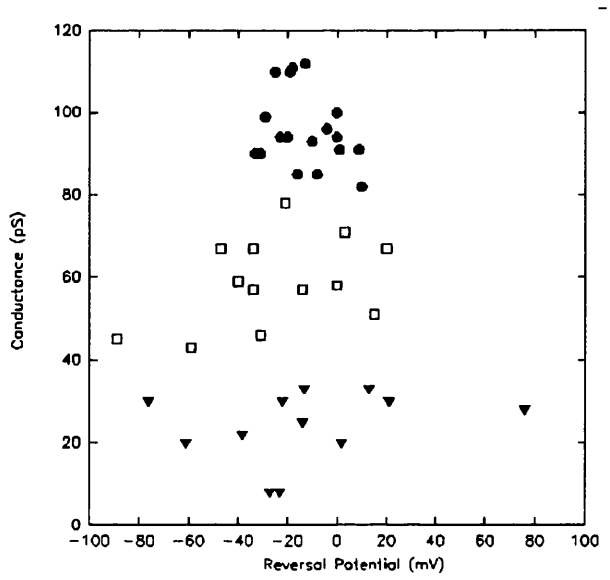

Figure V.12. When the electrode contained control solution, there was no trend relating channel type, and reversal potential, except the variation in reversal potential was inversely proportional to the conductance.
24 pS type (▸); 59 pS type (□); 96 pS type (●)

In order to limit the effect of individual variation, the reversal potential for each channel type was calculated from the averaged current information presented in Figure V.2. The 24 pS channel reversed at -23.5 mV; the 59 pS channel reversed at -28.8 mV and the 96 pS channel reversed at -26.2 mV. As the experiments were performed in the cell attached mode, these values are with respect to the resting membrane potential.

V.C.2.b. High Potassium Electrode Solution

Similar variations in the calculated reversal potentials were present with the channels observed when the electrode contained high potassium solution. Figure V.13 shows that there is no clear relationship between conductance and reversal potential.

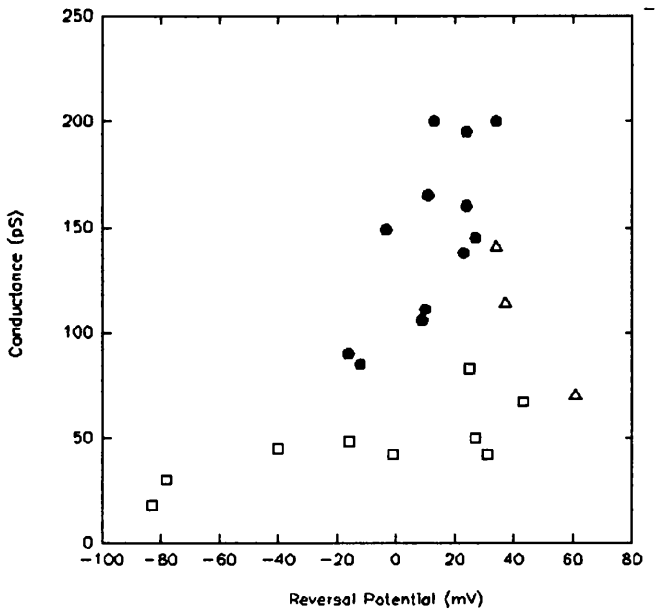

Figure V.13. When the electrode contained high potassium solution, there was no clear relationship between conductance and reversal potential for the 47 pS and 149 pS channels, except that the variation in reversal potential increased as conductance decreased. The inwardly rectifying channel reversed at more positive potentials.

Inwardly rectifying type (Δ); 47 pS type (□); 145 pS type(•).

Reversal potential values were calculated from the averaged current information shown in Figure V.11. The 47 pS channel reversed at 20 mV, the 145 pS channel reversed at 1 mV and the inward rectifying channel reversed at 33 mV. Again, these values are with respect to the membrane potential. While analysis did provide a reversal potential for the inwardly rectifying channel, the channel was never seen to reverse.

Table V.2 summarises the conductance, reversal potential and other information for the channel types seen with control and high potassium solution in the electrode.

Table V.2 Mean Conductances and Reversal Potentials for Each Channel Type

Conductance ± SD (pA)	24 ±9	59 ±10	96 ±10	108±29	47±19	145±41
Electrode Solution	Control	Control	Control	High K Inward R	High K	High K
Vrev (mV)	-24	-29	-26	38	23	14
Number	12	14	18	3	9	12
% of Channels	24	31	37	12	38	50

Reversal potentials are with respect to the membrane potential.

V.C.3. Ionic Selectivity

The information about the relative permeability of a channel to certain ions is best determined when the composition of the solutions bathing both the intra- and extracellular face of the channel is known, controllable and different. Unfortunately, the inability to achieve dependable inside-out recordings in this study made this impossible (see section V.C.5.). Alternatively, the extracellular potassium bathing the cell can be raised to intracellular levels; in this configuration the membrane potential and E_K are approximately 0 mV, and only potassium selective channels will reverse at 0 mV. At the time these experiments were performed, however, it was felt that the best way to deal with the variation in conductance and reversal potential values was to increase the

number. This meant repeating experiments under identical conditions; i.e. with control solution in the bath and electrode. Under these conditions, the ionic selectivity of the channels can be predicted if certain assumptions about the membrane potential and intracellular ion concentration are made.

The Goldman equation predicts that the current flowing through a channel is determined by difference between the membrane potential and the equilibrium potential for each ion, and by the relative permeability of the channel to each of the ions. Consequently, the relative permeability to different ions can be calculated by comparing the reversal potential to the equilibrium potential. However, the equilibrium potential depends upon the internal and external ionic concentrations, and in the cell attached recording mode it is not possible to determine the internal concentrations. Only the concentration of chloride inside fresh bovine RPE cells has been directly measured with ion selective microelectrodes and found to be 65 mM (Joseph and Miller, 1991). The intracellular concentration of potassium in bovine RPE has been estimated at 100 mM (Joseph and Miller, 1991). The "typical" sodium concentration in nerve, 30 mM, has been used to calculate E_{Na} as the mean levels in RPE are unknown (Kuffler et al, 1984). The equilibrium potentials for the three major ions when the cell electrode solution contains both control and potassium internal solution are in Table V.3.

Table V.3 Estimated Nernst Potentials

	Equilibrium Potential (mV)	
	Control	K
E_K	-75	0
E_{Na}	40	4
E_{Cl}	-20	-19

Based on the assumption that $[K]_i$ = 100 mM; $[Na]_i$ = 30 mM and $[Cl]_i$ = 65 mM

One further assumption is necessary to obtain relevant information about channel selectivity. In the cell attached recording mode, potential measurements are all made with respect to the true membrane potential, but there is no way of measuring the membrane potential directly. Repeated attempts to record in the whole cell mode, where it is possible to measure this value, were unsuccessful. Thus, to convert the reversal potentials into a true potential, a membrane potential of -45 mV was added to the pipette potential. It was previously reported that the average membrane potential of cultured human RPE cells was -45 mV (Fox et al, 1988) Thus, the "true" mean reversal potential is obtained by adding -45 mV to the values given in Table V.2. The "true" reversal potentials of all three channel types with either control or potassium "internal" solution in the electrode are displayed in Table V.4.

Table V.4. Adjusted Reversal Potentials

Channel Type	Vrev(mV)	Channel Type	Vrev(mV)
Control		High K	
24 pS	-69	In Rect	-7
59 pS	-74	47 pS	-22
96 pS	-71	145 pS	-31

Based upon the assumption that Vm = -45 mV.

When the values in Table V.4 are compared with those in Table V.3., it is clear that when the electrode contained control solution, the reversal potential of all three channel types was very close to the estimated equilibrium potential for potassium. This strongly implies that all three types were primarily

permeable to potassium.

When the electrode contained high potassium solution, the reversal potential of all three types dropped considerably, but all reversed at potentials considerably more hyperpolarized than the calculated E_K or E_{Na}. There are several possible reasons for this. The most obvious is that when the electrode contained high potassium solution, the cell membrane potential was more positive than -45 mV. If, for example, the membrane potential was only -20 mV, then the 47 pS channel would reverse at 0 mV, very close to the estimated E_K. This might have been caused by potassium flowing out of the electrode around the cell before a seal was formed. This is supported by the fact that two of the channel types reverse at a potential more negative than the equilibrium potential for and major ion. It is possible that the permeability of the channels changes with the ionic concentration bathing the external face of the membrane. It is also possible that this reflects a permeability to Cl^- although this is not very likely because two of the adjusted reversal potentials were more negative than E_{Cl}. Because of the uncertainty surrounding the reversal potentials from high potassium electrode solution, they shall not be dealt with further. Permeability calculations based upon these reversal potentials shall be performed for the experiments made with control solution only.

It was not possible to use the simplified form of the Goldman equation commonly employed in inside-out experiments to determine the relative ionic permeabilities because both sides of the membrane are bathed in both sodium and potassium, . Instead, a more complete form of the equation shown below was used, with the assumption that the channels were only permeable to sodium and potassium.

$$V_m+V_{rev}= 25.5*\ln \frac{a[K^+]_o+(1/a)[Na^+]_o}{a'[K^+]_i+(1/a')[Na^+]_i}$$

where a = the relative potassium permeability; ions moving from outside inwards;
thus 1/a is the relative permeability to sodium,
a' represents the permeability for potassium moving outwards,
1/a' - the permeability of the channel to sodium moving outwards,
and V_m+V_{rev} is the "true" reversal potential of the channel.

A simplification was made: that a=a', i.e. the channel did not rectify. When the equation was solved using the values of membrane potential and internal ion concentration mentioned above, (V_m= -45 mV, $[K^+]_i$=100mM, $[Na^+]_i$ = 30 mM) the relative permeability of each ion could be calculated and is presented in Table V.5.

Table V.5 Relative Cation Permeabilities

Channel Type	P_K/P_{Na}
24 pS	10
59 pS	22
96 pS	12

The relative permeabilities of potassium over sodium (P_K/P_{Na}) for the three channel types with control solution in the electrode. Calculations are based upon the assumption that $[K^+]_i$=100 mM, $[Na^+]_i$ = 30 mM and Vm=-45 mV.

The calculations above shows that all three channel types are primarily permeable to potassium. The precise values in Table V.5. should be taken only

as a rough indication because the membrane potential and internal ion concentrations had to be approximated. This makes it difficult to sort the channel types in terms of their $P_K/P_{Na,}$, or to use this information to further strengthen the classifications based upon conductance. However, it can be concluded that, when the electrode contained control solution, all the channels were potassium selective.

V.C.4. Correlation of Channel Types.

It is important to determine how the channels observed when the electrode contained control solution related to those observed when the channel contained high potassium solution. Three lines of evidence support the hypothesis that they are the same types of channels.

Firstly, three channel types were detected regardless of the electrode solution. A change in electrode solution would be expected to alter the characteristics of the channels present, but not to change the expression of particular channel types.

Secondly, the relative frequency of encountering the 24 , 59 and 96 pS channel types was qualitatively similar to that of the inward rectifying, 47, and 145 pS types, respectively (see Table V.2). The greatest difference occurs with the inward rectifying. This rectification would make it more difficult to detect this channel type close to the membrane potential and at depolarised potentials, where the greatest effort was made to detect channels. This would decrease the apparent frequency of the inward rectifying channel, and increase the likelihood of encountering the 47 and 145 pS channels.

Thirdly, the relative conductances of types of the 59 and 96 pS channels correspond to the 47 and 145 pS channels. The considerable difference between the two largest conductances is not unprecedented, for the conductance of large conductance channels such as the maxi-K increases as the extracellular potassium concentration is elevated (Yellen, 1984*b*). Although

the conductance of the inward rectifying channel is proportionally larger than the 24 pS channel, the conductance of inwardly rectifying channels is proportional to the square root of the external potassium concentration (McKinney and Gallin, 1988).

It is thus probable that the 24, 59, and 96 pS channel types observed with control solution in the electrode are the same as the inwardly rectifying , 47 and 145 pS. The conductance and reversal potential varied within each group, and it is possible that this variation reflected the presence of additional channel types. This question is dealt with in more detail in Chapter VI. At this point, however, the channels will be considered to be the same.

V.C.5. Inside-out Recordings

Ionic channels can be more completely characterised if the solutions of known composition can be chosen to bathe both the inside and the outside face of a channel. Traditionally this is possible with the form of patch clamp recording referred to as the inside- out variant (Hamill et al., 1981). In this mode, the electrode is slowly withdrawn from the cell into a bath solution which contains a low concentration of Ca^{2+}. The electrode-patch seal is mechanically stable and persists after the patch is torn from the remaining cell. As the electrode solution is on the "outside" of the channel and the chosen bath solution is on the cytoplasmic face of the channel, the ionic composition of solutions on both sides of the channel are known.

Many attempts were made to excise a patch of membrane into a low calcium solution, but in most of the experiments, patch withdrawal was accompanied by a sudden drop in seal resistance and the electrode-membrane seal broke down completely within 1 minute. During the interval between the excise of the patch and the loss of seal, the trace was extremely noisy, and although channel openings were sometimes detected, they were usually superimposed upon a current baseline so variable that it was impossible to

accurately determine the size of the current. The ionic composition and calcium concentration of the electrode solution had no detectable effect upon seal retention.

On four occasions, channels visible while cell-attached disappeared when the patch was excised, even though the seal resistance did not drop. The patch was held over a range of potentials, but activity was never detected. Loss of activity after patch excision has been associated with the formation of a vesicle, and channel activity observed after the vesicle was ruptured (Hamill et al., 1981). However, loss of seal occurred after the electrode was briefly held in the air.

Occasionally, channels were seen after the electrode was withdrawn, but with a distorted shape. This was probably caused by the formation of a membrane vesicle at the electrode tip; the large increase in membrane area caused an increased in the capacitance and this interfered with the transition times recorded by the electrode (Hamill et al., 1981). Vesicle formation occurred when the patch was excised into both control (2mM Ca^{2+}) and low Ca^{2+} solutions. When a vesicle formed, the electrode was quickly passed through air, as this has been reported to partially rupture the vesicle and produce a proper inside-out patch. In most cases this led to an immediate loss of seal, but occasionally, an inside-out patch was formed. However, the resistance of the seal was usually reduced to less than 0.3 GΩ and it was impossible to obtain records sufficiently stable and free of noise to be analysed. The inability to break the vesicle successfully has been reported by others (Rae et al., 1988).

V.C.6. Channel Demographics

V.C.6.a. Channel Distribution

In < 10% of the recordings made after the formation of a seal larger than 1GΩ, no activity was seen at any potential tested. In the rest of the patches,

spontaneous activity was only seen when the patch was substantially depolarized or hyperpolarized. This was especially true with control solution in the electrode. In patches which showed activity, only 32% contained only one channel. Two similar channels were found in 42% of the patches, two different channels were found in 22% of the patches and more than two channels were found in 4% of the patches showing activity (Table V.6). In patches which contained both a small conductance and a large conductance channel, only the large channel was analysed as the smaller current levels could not always be discerned with certainty. In some of the recordings, the baseline noise level was great enough to interfere with the detection of channels with a very low conductance, or in which the current was low for any other reason.

Table V.6. Distribution of Channels in a Patch

# in Patch	1	2 Same	2 Different	>2	Total
N	23	31	16	3	73
%	32	42	22	4	100

The presence of two identical channels was detected by the occurrence of a double opening; the current level rose in a step- wise fashion to a value equal to twice that of a single channel. However, as most of the channels found in this study were not open very frequently, there was always a probability that a patch contained two channels without showing a double opening. In order to discover if this possibility affects the records, a theoretical analysis was undertaken. The probability that a patch contains two channels but the two do not open simultaneously is given by:

$$P_b = \{1/[1 + 0.5(m_o/m_s)]\}^n$$

(Colquhoun and Hawkes, 1983). This value is determined by the average length of time for which the channel is open, m_o, the average time for which the channel is closed, m_s, and the number of openings that have occurred during the period of observation, n. The equation above applies only when $m_o << m_s$. For many of the channels in this study, $m_s > 300$ msec and $m_o < 1.5$ msec, thus >1900 openings, or more than a 10 minute stretch of record without double openings was necessary before $P_b < 1\%$. This was not often practical, as a 10 minute stretch of data obtained at a sampling rate high enough to resolve individual openings (3 kHz) required 4.3 Mb of disk space. It was more useful to polarise the patch to the point when the probability of opening was increased, and simply to check for double openings. However, in nearly half of the records where only one channel was seen, the largest average duration of channel opening seen at any potential tested was less than 1.5 msec. It is thus possible that the percentage of patches containing only one channel is overestimated, and may be as low as 21%, while the percentage of patches containing two identical channels could be as high as 53%. The percentage of patches containing two different types of channel and more than two types remain at 26% and 4% respectively.

The number of channels per patch depends upon the area of the patch, i.e. on the tip size of the electrode, and using electrodes similar to mine, Fox et al (1988) found that only 6% of the patches in their study contained only one channel, 20% contained two different channels and the remaining 74% of patches contained more than one channel of the same type. This distribution of channels per patch agrees qualitatively with the data presented here. This suggests that in both studies channels of the same type cluster together on the membrane- for reasons which are discussed later in the thesis. Such clustering

has been reported in other ocular epithelia (Rae and Levis, 1984*a*).

V.C.6.b. Uniqueness of Channel Types

When the electrode contained control solution, the three channel types were separated only by their conductances. All three types shared comparable selectivity for potassium over sodium and the voltage-dependence of channel activation of the three types was also similar. As the conductances, 24 pS, 59 pS and 96 pS, are roughly multiples it was important to prove that the channel types identified in this study were distinct and the higher conductance values were not caused by two or three 24 pS channels open simultaneously.

Several lines of evidence support the identity of distinct channel types. First, records exist where only type was observed. The 24 pS channel was seen alone on two occasions, the 59 pS channel on five occasions and the 96 pS channel on eight occasions. All three channels had a low probability of opening over most of the voltage range and it is highly unlikely that in the 59 pS and 96 pS records, two or three channels respectively opened simultaneously and never alone.

This argument is extended quantitatively with the use of the binomial theorem. If channels are assumed to be identical and act independently, then the probability of a double or triple opening can be determined with the binomial theorem. The general form of the theorem is as follows;

$$P_r = \frac{N!}{r!(N-r)!} * P_o^{\,r} * (1-P_o)^{N-r}$$

where
N = number of channels present
P_o = probability of a single channel being open
r = the number of channels simultaneously open (r = 0,1,..N)
P_r = the probability of r channels being simultaneously open
(Colquhoun and Hawkes, 1983)

If it is assumed that only two small channels are present, then the binomial theorem cannot be used to determine the probability of finding both of the channels open, for this involves dividing by 0 (N-r in the equation above) . However, as the probability of channel opening is very small, the theorem is simplified and the probability of finding both channels open simultaneously is

$$(P_o s / 2)^2$$

$P_o s$, the measured value for open probability of the smaller conductance channels, is divided by two to determine the P_o for each of the assumed two small channels. $P_o s$ is only an approximation. The true probability, $P_o S$, may be higher than the estimated $P_o s$ if a considerable proportion of time had been spent in a double opening; each channel's contribution to this higher level would have been ignored. In normal circumstances this can be calculated by simply adding the time spent in the higher level to the single level duration before dividing. Such a procedure could obviously not be followed in this case as it formed part of the conclusion.

The activity of small and medium channels at 60 mV (negative Vp) from record C150491b (see Appendix III) was used for the first part of this analysis. The calculated P_o of the small channels, $P_o S$ was 0.0017 and that of the medium channel $P_o M$ was 0.0015. If only two channels were present the $P_o M$ predicted by the above equation was 0.00005. This is substantially smaller than the 0.0015 measured and thus it is very unlikely that the higher current level in the record was produced by the simultaneous opening of two smaller channels.

If it is assumed that three small channels are present, then the binomial theorem can be used and in this case predicts that the probability of finding a double opening is 0.0001. Again, this is substantially smaller that the measured

P_oM of 0.0015 and it is very unlikely that the medium conductance channel is two small conductance channels.

The activity of the medium and large channels at 20 mV from record C230690d (see Appendix III) was used to determine the existence of the large conductance channel. In this case P_oM was 0.203 and P_oL was 0.034. The probability of a the medium channels producing a double opening was 0.010. If it is assumed that three medium channels were present, then the binomial theorem predicts the probability of a double opening as 0.012. It is thus unlikely that the large conductance channel is actually two medium conductance channels.

It was only possible to apply the Binomial theorem analysis to a small number of records because two different channels were seen together infrequently. However, this supports the hypothesis that the three channels types are different.

V.C.7. Kinetic Information 1: Steady State

A knowledge of how the open probability of a particular channel type changes in response to fluctuations in membrane potential or other stimuli will help explain how the whole cell responds to that stimuli. As this thesis is concerned with relating single channel activity found on RPE membranes with the integrated response of the entire tissue, information about P_o is of considerable importance.

Although there was more variation in the kinetic measurements than with the size of the currents in the channel seen, it was very possible to see patterns. Most of the patches used in this study contained more than one channel, and this limited the amount of kinetic information obtainable from the records. However, it was usually possible to calculate the probability of finding the channel open, P_o. Although this type of data does not reveal the details of channel gating transitions, it does allow single channel activity to be correlated with currents found in whole cell recording and the macroscopic channel functions.

V.C.7.a. Control Electrode Solution

In most of the recordings obtained with electrodes containing control solution, the probability of finding the channel open, P_o, was low near the resting membrane potential and increased as the patch was depolarised. This voltage - dependence of open probability is emphasised in Figure V.14, which plots P_o against patch potential for all the records obtained when the electrode contained control solution (see also Appendix III, Table 3). It also shows that some of the 96 pS type channels were open a much higher proportion of the time. These records make up 22% of the 96 pS types seen under these conditions. The reason for this increase in open probability is unclear.

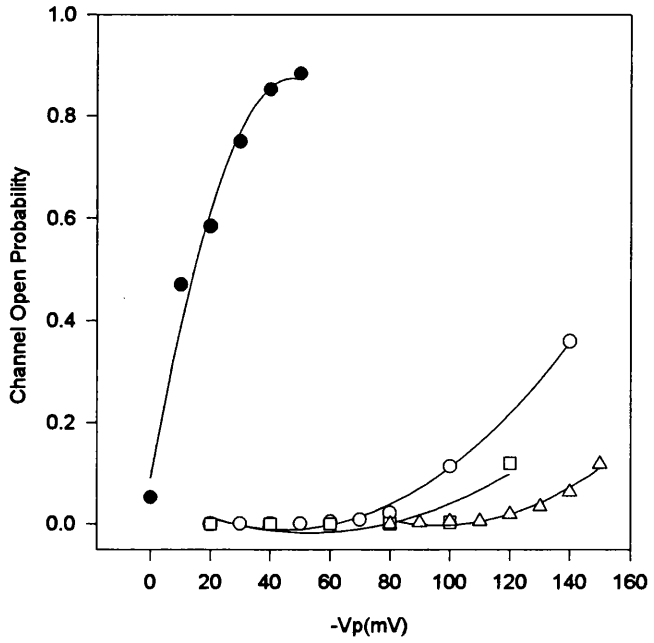

Figure V.14. The Voltage Dependence of Channel Activity. The increase in open probability as the patches are depolarized is shown by the hollow circles, squares and triangles, which respectively represent the 96 pS, 59 pS and 24 pS channel types seen when the electrode and the bath contained control solution. The solid symbols show an example of a 96 pS channel type with greatly increased probability of opening.

To quantify the voltage dependence of the increase in P_O, the relationship was fit with a sigmoidal function ;

$$f(x) = 1/\{1+e^{[k^*(Vm - Vm50)]}\}$$

where Vm = membrane potential (mV); Vm50 = the potential at which channels were open 50% of the time; and k = amplification constant. Vm50, was used to describe the relationship. A sigmoidal function was chosen because, (a) the gating process of many channel types is thought to behave as an enzyme and as an enzyme, is fit by the sigmoidal Michalis-Menten relationship; (b) in the few cases when the P_o of a channel rose from near 0 to near 1, P_o increased in a sigmoidal manner with voltage; and (c) when only the rising tail of the P_o/ potential relationship was available, a sigmoidal function appeared to fit. In many of the records, P_o did not rise above 0.2 even though the patch was depolarised over 100 mV. In these cases, the function has to be extrapolated over many millivolts to the point where the channel was expected to open 50%

of the time (V_m50). Obviously, it was not possible to test if the P_o would continue to increase in a sigmoidal way past this point, or if another function would describe the relationship more accurately. P_o would eventually approach 1. It was clear that for most of the channels, P_o increased with potential in a non-linear fashion. Thus the V_m50 provided a way to quantify the general relationship between P_o and potential.

P_o did not change in a predictable way with potential in 33% of the 24 pS channel type , 27% of the 59 pS channel type and 11% of the 96 pS channel type (see Appendix I, Table 2). The remaining records showed a clear increase in P_o with depolarising potentials, and were fit with a sigmoidal function. Of these, V_m50 was at least 90 mV more depolarised than the resting potential in 75% of those from the 24 pS channel type, 73% of the 59 pS channel type and 88% of the 96 pS channel type. The dependence of P_o on potential can be directly seen in Figure V.4 and Figure V.5, which are typical of the records showing this response. These results strongly indicate that the activity of all three channel types is voltage dependent and activity is greatly increased at depolarized potentials.

Four records of the 96 pS type channel, the open probability was very high (0.4 - 0.9) when the patch was depolarized by 0 to 50 mV. These records have been distinguished in Figure V.14, and an example of such a record is shown in Figure V.15. It is unclear why the activity of these channels was so much higher than that of the remaining population.

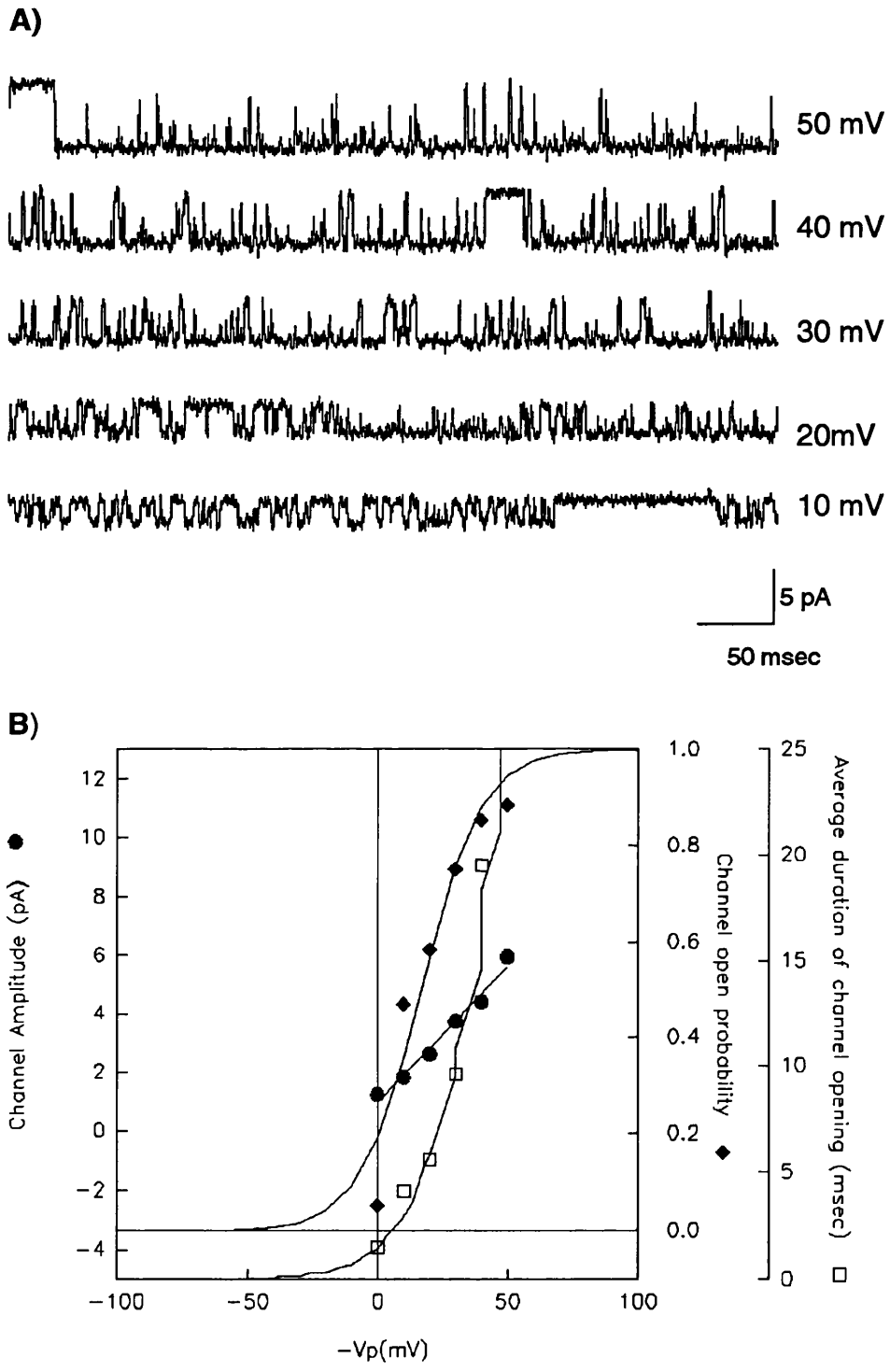

Figure V.15. Highly active large-conductance channel . A. Current traces at various potentials show the channel open a large proportion of the time. Downward deflections reflect outward current through an open channel. B. The relative increase in channel activity is seen by comparing this graph with Figure V.5.B. All potentials given as -Vp and are with respect to the membrane potential. The electrode and bath contained control solution.

V.C.7.b. High Potassium Electrode Solution

When the electrode contained high potassium solution, no clear trend between potential and P_o was apparent (Appendix III, Table 5). Only 33% of the 145 pS type channels and only 44% of the 47 pS type channels could be fitted with a sigmoidal function. These channels were generally open more frequently at all potentials than when the electrode contained control solution. It was only possible to analyse the kinetic attributes of two inwardly rectifying channels; both of these channels were open more than half the time at all potentials tested. They attained a maximum P_o near the membrane potential (i.e. pipette potential was 0 mV) and decreased when the patch potential was either hyperpolarized or depolarised. This large P_o helped reinforce the distinction between the inwardly rectifying channels.

V.C.7.c. Time Constants

A channel usually goes through several transition states before it fully opens or closes, and each transition has its own individual rates. If a distribution histogram is constructed of, for example, the amount of time the channel is open, it is possible to detect the number of transitions the channels goes through before finally closing by examining the exponential decay of the distribution. If the decay is best fit by two exponentials, then the channel goes through at least two transitions before closing (Colquhoun and Hawkes, 1983).

The presence of more than one channel in a patch made it impossible to determine precisely the distribution of the open and closed times, and thus information about the transition rates between these states is limited to only few records. The information available from these records was limited further because a large number of openings were necessary before a smooth histogram could be constructed. Consequently, histograms were only constructed for two records containing the 96 pS channel type, and only when the channels were depolarised by 120 mV. In both of these records, the distribution

of open times and closed times were best fit with two exponentials. Although variation does exist between the values of these two channels, the analysis does show that both the open and closed state consist of at least two transition states. The same is true for the 59 pS channel type. The time constants themselves are shown in Appendix III, Table V.9.

V.C.7.d. Open Verses Close Rates

It was not possible to estimate the number of transition states that underlaid each opening or closing for most of the recordings because of small event number and the presence of multiple channels. However, it was possible estimate frequency of channel opening and closing. The number of times a particular channel type opened per second, n, was recorded, and the average duration of these openings, D_o, was calculated. The number of events was proportional to the frequency of channel opening, while the average duration of channel opening was inversely proportional to the frequency of channel closing.

The P_o is the product of the average duration of channel opening, D_o, and the frequency of opening, n;

$$P_o = n * D_o.$$

As described above, P_o increased with potential for the majority of channels seen when the electrode contained control solution. It was important to determine whether this increase was caused by an increased frequency of channel opening or a decrease in the frequency of channel closing. This was done in several steps (Figure V.16). First, the change in number of events (per second) with potential was compared with the change in the average duration. However, to normalise the data, each value was calculated as a percent of the value obtained at the most hyperpolarized potential. Finally, the percent change in duration was divided by the percent change in event number per second for each potential for which there was data for, and this plot was fitted with a first

order regression. If, for example, the percentages of both parameters increased, but the regression was horizontal, then both parameters increased at the same rate and contributed equally to the increase in P_o. However, in 70% of the 96 pS type channels analysed, the regression was negative; the number of events per second was increasing at a faster rate than the average duration of opening. This implies that, for these channels, an increase in the frequency of opening is largely responsible for the voltage dependent increase in P_o.

A similar analysis was performed for the other two channel types as the data from both of these groups showed evidence of a voltage dependence of channel activity. Although some channels did show a negative regression when the data was processed in this way, the results were not consistent. This may have been caused by the smaller size of the current, and consequent variability in the measurement, or may reflect a true difference between the channel types.

V.C.8. Kinetic Information 2: Temporal Dependence

The voltage dependence of channel activity described in the previous section was readily apparent when recording, for it was usually necessary to depolarise patches considerably before openings could be detected. The normal voltage protocol consisted of holding the patch at potentials depolarised by 10 mV at as time and checking for channel activity. The potential was steadily increased and the currents flowing through the channel at a particular potential were recorded. Occasionally, this protocol would be interrupted and the patch would be held at or near 0 mV (i.e. the membrane potential) before returning to the depolarised value. When this happened, channel activity was greatly increased soon after the sudden depolarisation and slowly returned to steady state levels.

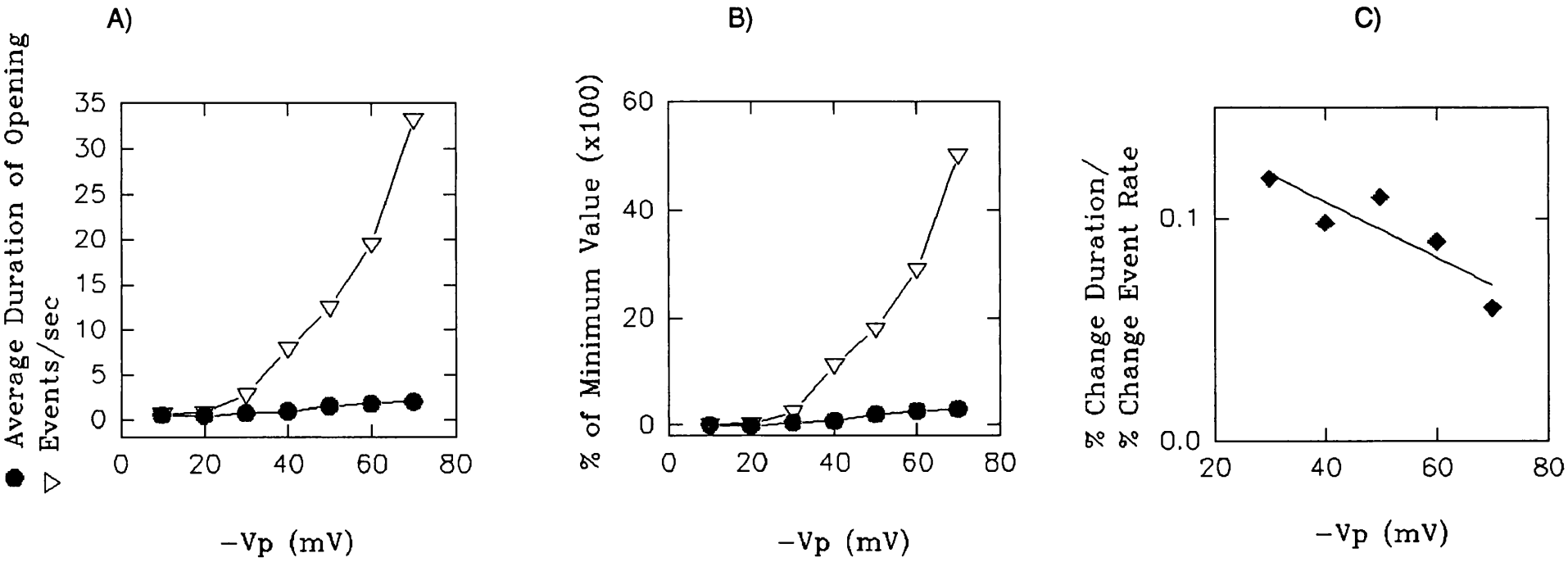

Figure V.16. The event rate, symbolising the channel opening rate, and the average duration of channel opening, representing the channel closing rate, from a typical 96 pS channel type are analysed to indicate possible mechanisms behind the increase in channel activity with patch depolarization. A) The actual measurements are shown , and indicate that both parameters increase as the patch is depolarized. B) When the two parameters are normalised , it is clear that the number of events per second increases much faster with potential than the average duration of openings. C) The relative contributions of the two parameters show that the event rate, and thus the channel open rate, is largely responsible for the voltage-dependent increase in channel activity. -Vp is given with respect to the membrane potential.

The increased activity after sudden changes in potential meant that special care had to be taken when measuring P_o. If the channel activity had not reached a steady state, the P_o value would be high and a smooth relationship could not be found. Aside from causing inconvenience, this observation suggested that the channels were in fact time- and voltage- sensitive.

Evidence of time- and voltage-gated activation was clearly seen in seven different records. The increase in channel activity began within 10-20 msec after the onset of a depolarizing pulse and this increased activity inactivated 2-4 seconds after the pulse began. An example of a typical recording is shown in Figure V.17. The kinetics of activation were not analysed further, but the characteristics of the inactivating component are shown in Appendix III, Table 10.

Although it was not possible to conduct a complete investigation into the temporal dependence of channel gating, several patterns are suggested by the inactivation data. The values of τ, the time constant of inactivation, were remarkably constant when the test potential was 100 mV for the four channels tested from both channel types. The effect of changing the holding potential was not tested. However, τ did vary with the test potential; the channel inactivated more quickly at larger depolarizations. This observation is important, for it shows that the temporal gating is not an artefact. If the effect was related to patch capacitance, τ would increase as the change in potential increased. While inacitivation was observed in both the 96 pS and the 59 pS channel types, it was not possible to compare the values of τ because of the small number of records tested for temporally gated activity.

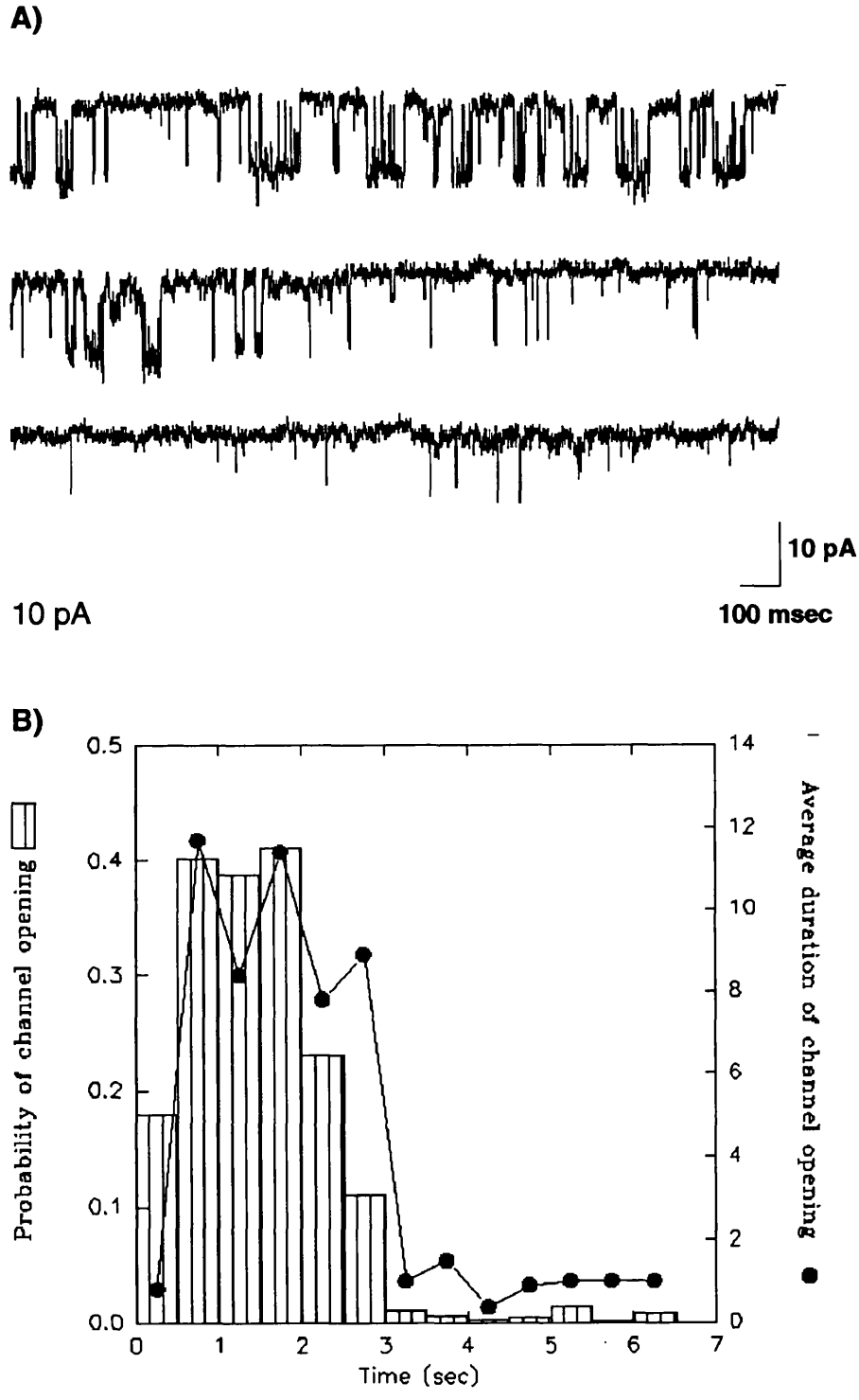

Figure V.17. Time and Voltage Dependance of Channel Activity. In A, the patch was rapidly depolarized from a -Vp of -60 to -100 mV (with respect to the membrane potential). The decline in the activity of this 96 pS channel during these three consecutive traces is apparent. Bath and electrode contained control solution. B) The decline in open probability corresponded to a decrease in the average duration of channel opening.

V.C.9 Calcium

The activity of several types of potassium channels is modified by the concentration of calcium. The channel types show a range of conductances and are commonly found in a variety of secretory and absorptive epithelial cells including pancreatic acinar (Maruyama and Petersen, 1983) and the distal colon (Loo and Kaunitz, 1989), The best known of these channels, the large conductance BK or Maxi-K channel, has been reported in several ocular epithelial cells including chick lens (Rae et al., 1990) and the non-pigmented ciliary epithelium (Barros et al., 1991). Whole cell recording has also shown the presence of a calcium-sensitive potassium current ($I_{K(Ca)}$) in the pigmented ciliary epithelium (Jacob 1991), a cell type developmentally related to the RPE. The widespread distribution of calcium-sensitive potassium channels in epithelia suggested that one or more of the potassium channels found in the RPE might also be modified by internal calcium. Although technical difficulties made it impossible to carry out a rigorous study of the calcium sensitivity of the potassium channels found in the RPE, the results below suggest that the largest of these channels is activated by calcium.

V.C.9.a. Methods

Low external Ca^{2+}

The low concentrations of calcium are required in the external solution were obtained by using the Ca^{2+} chelator ethylene glycol bis (ß-aminoethyl ether)N,N,N',N'-tetraacetic acid (EGTA). The amount of free calcium in a solution of a given Ca^{2+} and EGTA concentration is determined by numerous factors including the temperature, pH and magnesium concentration (Caldwell, 1970). The calculations are complex, and for the experiments here, the values of Mayer et al. (1990) were used. Table V.7 shows the concentration of EGTA and CaCl added to the control solution for these experiments.

Table V.7. Composition of Low Calcium Solutions

Free Ca^{2+} (M)	$[Ca^{2+}]$ (M)	[EGTA] (M)
$5x10^{-6}$	$1.9x10^{-3}$	0.002
$5x10^{-7}$	$1.6x10^{-4}$	0.002
$5x10^{-8}$	$6.7x10^{-4}$	0.002
$5x10^{-9}$	$4x10^{-4}$	0.01
0		0.001

Ca^{2+} Ionophore

The efficient intracellular buffering of Ca^{2+} and the presence of intracellular stores of Ca^{2+} make it difficult to know how long it takes intracellular free Ca^{2+} to fall after Ca^{2+} is removed from the bath solution. These factors also make it impossible to do the reverse experiment, and effectively increase intracellular free Ca^{2+} by merely increasing Ca^{2+} in the bath. A more precise method of changing intracellular calcium while recording in the cell attached mode is by including a calcium ionophore in the buffered extracellular solution. The ionophore overrides the cells ability to buffer Ca^{2+} by increasing the membrane permeability to Ca^{2+}.

A series of experiments were performed in which the ionophore A23187 was added to control solution containing 2mM Ca^{2+} and to solutions containing $5x10^{-7}$ and $5x10^{-6}$ M Ca^{2+}. A23187 was dissolved at a concentration of 1 μM in a mixture containing 50% ethanol and 50% distilled water. A final A23187 concentration of 0.1 μM was produced by adding 1mL of the stock A23187 to 99ml control solution. A solution containing 0.5% ethanol in control solution was found to have no effect on channel activity.

VI.C.9.b. Results

Low external Ca^{2+}

The majority of the Ca^{2+}-sensitive K^+ channels are controlled by the concentration of intracellular Ca^{2+}. The most direct way to show that the activity of a channel is calcium sensitive is therefore to excise the patch so that the solution bathing the cytoplasmic face of the channel can be controlled. The effect of a change in the concentration of "intracellular" Ca^{2+} on channel activity can then be determined. Unfortunately, the low-resistance of the electrode-membrane seal in these experiments meant that patch excision nearly always resulted in seal loss, and attempts to test for Ca^{2+}-sensitivity in this way were not successful.

Ca^{2+} sensitivity was tested indirectly by recording in the cell-attached mode and reducing the calcium in the solution bathing the cells. A typical recording from such an experiment is shown in Figure V.18.

A change in $[Ca^{2+}]_o$ was shown to effect channel activity in four recordings containing a large conductance channel. These results are summarised in Table V.8.

In record C150491d, the electrode contained Ca^{2+}-free solution while in records C240491l and C260591k the electrode contained control solution with 2mM solution. This indicates that the presence of Ca^{2+} in the electrode was not sufficient to prevent a drop in activity. Nor was it necessary to remove all of the external Ca^{2+}; the test solution used in records C150491d and C240491k was nominally Ca^{2+}-free but $Ca^{2+}{}_o$ was reduced to only 5×10^{-6} M in record C260591k.

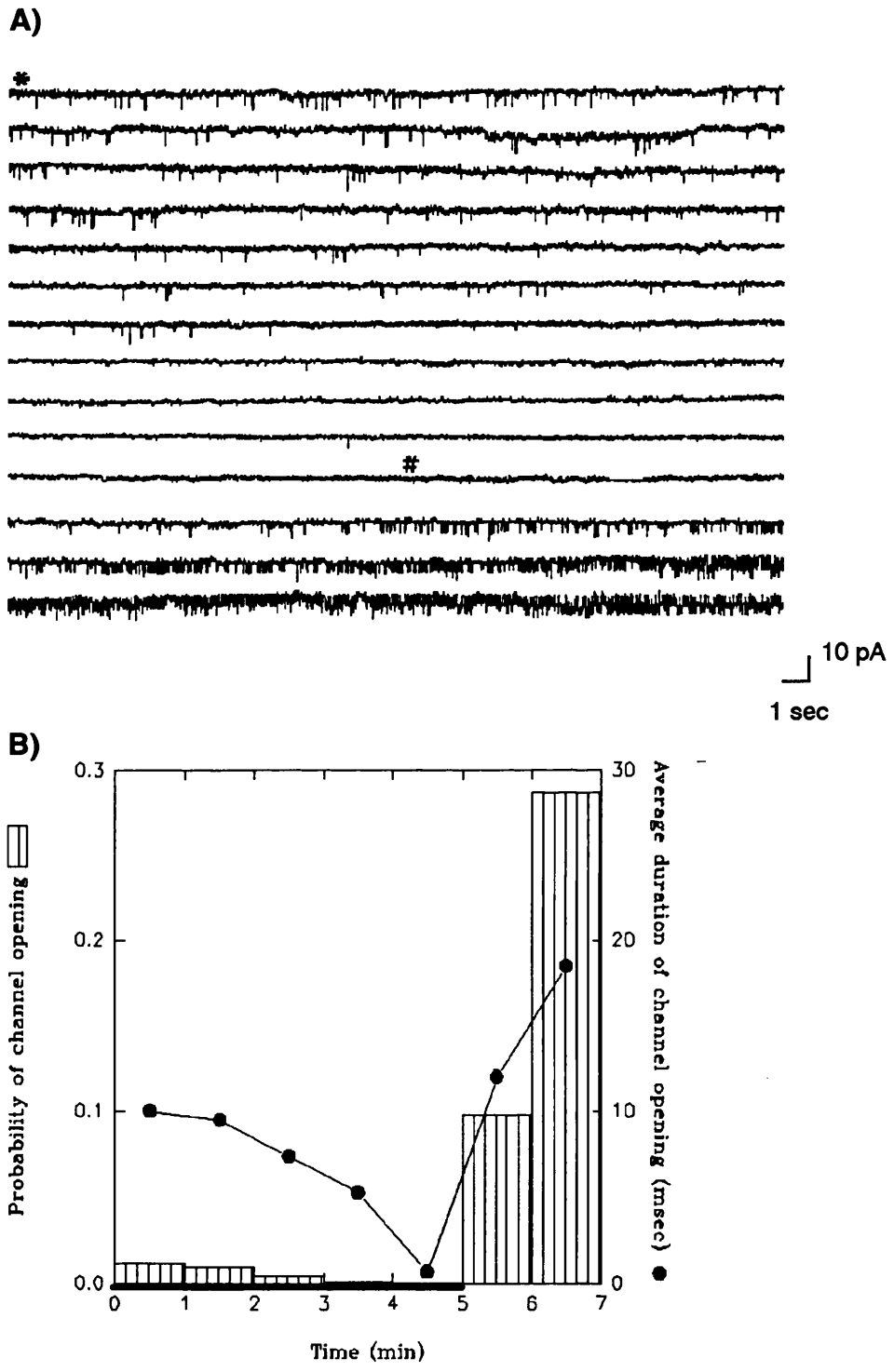

Figure V.18. A) Consecutive recording from a cell attached patch depolarized by 50 mV with respect to the membrane potential. At the point marker *, the solution bathing the cell was switched from control with 2 mM to one which was nominally Ca^{2+} free. At #, control solution was returned to the bath. In B, the resulting decline in channel activity is shown. Upon return to control solution, this channel overshot original activity levels. The black bar represents time the cell was in Ca^{2+}-free.

Table V.8. Effect of External [Ca^{2+}] on Channel Activity

		Control		Test			Return		
Record	-Vp(mV)	I(pA)	P_O	I(pA)	P_OM	P_OE	I(pA)	P_OM	P_OE
C150491d	40	6.4	0.015	6.4	0.021	0.018	6.3	0.218	0.012
C240491m	50	4.3	0.045	4.2	0.002	0.072	4.1	0.038	0.065
C250691k	40	4.9	0.015	4.0	0.002	0.013	4.4	0.44	0.015
C181191f	80	9.9	0.005		0.001			0.005	

P_OM = measured probability of channel opening

P_OE = estimated probability of channel opening based upon IV/P_OV plot in control conditions

It was not possible to know how long it would take for internal Ca^{2+} to fall. The patch potential was therefore kept constant for the duration of the experiment so that only one variable was altered and the change in channel activity in response to low external calcium could be calculated. In control conditions, channel activity occurred at detectable rates only when the patch was depolarised with respect to the cell interior. If a decrease in channel activity caused by low Ca^{2+} was to be detected, the channel needed to be active in control conditions. Thus, the patch was depolarised by a constant value throughout the experiment.

A considerable delay existed between the reduction of external Ca^{2+} and a change in the activity of the channel. In record C240491m, activity

remained constant for 230 seconds before beginning to fall and reached a steady rate 400 seconds after the solution had been changed. In record C250691k, these times were 360 and 680 seconds respectively and in record C181191f, these values were 180 and 230 seconds respectively. In one early experiment of this type (C150591d), the cell was in a Ca^{2+}-free bath solution for only 125 seconds before the solution was returned to control. No decrease in channel activity was seen during the test period, but activity increased to 14 times greater than pre-test levels within 20 seconds of the return to 2mM Ca^{2+}_o solution. This indicates that the low Ca^{2+}_o initiates a series of intracellular changes which require at least about 230 seconds before they cause a produce a drop in channel activity.

Upon return to control solution, channel activity substantially overshot pre-test levels in two of the four channels showing a calcium effect. In these records the overshoot occurred began within one minute of the return to control Ca^{2+}. Activity was not seen to return to pre-test levels after this; one record was continued for 3 minutes after return to control solution and the other for 8 minutes. In the records not showing an overshoots, the activity levels remained relatively constant at pre-test levels for 4 minutes (150591d) and 4.5 minutes (C181191f).

The activity of these channels was strongly voltage dependant, and the true potential across the patch in a cell attached recording is the sum of the patch potential and the membrane potential. It is therefore necessary to prove that the drop in channel activity was not an artefact produced by a hyperpolarization of the membrane potential caused by the decrease in external Ca^{2+}. This can be shown clearly by comparing the amount of current flowing through the channel during periods of high and low activity (Table V.8). For example, the mean current flowing through the channel in record C240491m while the cell was in control solution was 4.3 pA. After Ca^{2+} was removed from the bath, the P_o fell close to zero, but when the channel did

open it passed 4.2 pA. If the channel conductance and internal $[K^+]$ is assumed to remain constant, this indicates a cell membrane hyperpolarization of 3 mV. However, if one extrapolates from the iV/P_oV plot for this channel in control conditions, the P_o at the new potential would be 0.086, while the measured P_o is 0.005. Thus the drop in channel activity is not caused by a change in membrane potential. In all the patches tested, the current flowing through the channel during periods of altered activity remained within 10% of control values and was not sufficient to explain the change in activity.

It was observed that the rate of channel openings decreased dramatically when the P_o declined, and increased when the P_o rose following return to control solution. The duration of channel opening was calculated over the course of the experiment and was found to fall when the P_o decreased and rise when the P_o increased (see Figure V.18). These observations suggest that a fall in internal Ca^{2+} leads to a drop in opening frequency of the channel.

In one preliminary cell attached experiment on a 90 pS channel, epinephrine was added to the bath at a concentration of 500 µM. Channel activity transiently increased, with the P_o rising from 0.0045 to 0.007 in 150 seconds. The P_o then fell to below control levels, 0.003, where it remained for three minutes.

The effect of a decrease in Ca^{2+}_o on the 59 pS channel was tested on only one occasion. Fluctuations in the P_o meant it was not possible to conclude anything.

Calcium Ionophore A23187

Unfortunately, no data is available from the experiments in which calcium ionophore A23187 was added to bath solution. These tests took place over a three week period towards the end of the experimental period during which time no gigaohm seals were formed. The lack of and viable recordings means

that it is unknown whether the protocol would have been effective.

VI.D. Summary

Three main classes of potassium channels were identified in this chapter. The classification of channels was based upon conductance, which is frequently used to characterise channels; it was also used here because it was the only parameter which showed signs of clustering. The validity of this grouping was supported by several statistical tests, and reinforced by the observation that the channel types were often observed alone. When different channels were seen together in the same patch, independence was shown with the binomial theorem. Experimental design increased the validity of channel classification. For example, the possible effect of ion concentration upon conductance was eliminated by separating the records obtained with different solution. In addition, the comparatively low levels of channel activity meant that this activity was easily detected. This contrasts with the channels observed in bovine records which were obscured by the frequent presence of large, noisy currents.

It is possible that the method of analysis led to an underestimation of current amplitude. When the "all-point" method of current measurement was used, the mean duration of each channel is low and the sampling frequency is low, it is possible that some of the rising and falling portion of the current event was included in the measurement. The analysis methods tries to avoid this problem, but it remains a possible source of current underestimation.

The conductance histogram was fit with a Gaussian function to eliminate subjectivity. However, the histogram illustrated the considerable variation in the conductance values. It is possible that this variation reflected the existence of more than one channel type per identified group, but without additional information, this cannot be validated (but see Chapter VI). The channels were not always active at the same potentials so the range over which the

conductances were calculated varied. This would effect measurements if the conductance was not the same over the entire range of potentials. The conductance of the 96 pS channel type occasionally decreased at very depolarized potentials; it is possible that this type of a decrease caused some of the variation observed in conductance values.

The variation in reversal potential measurements could reflect a variation in the cell membrane potential and the intracellular ion concentrations. The lack of channel activity near this reversal potential may also have lead to errors, as the conductance line must be extrapolated or interpolated over a considerable distance. This extrapolation/interpolation would tend to magnify any error made in determining the conductance. However, the precise ionic selectivity of a channel is itself variable and can depend upon a particular combination of solutions and conditions (Rae and Levis, 1984*a*).

There is strong support for the theory that the activity of these channels is voltage dependant. Although the exact relationship between channel open probability and potential varied, the voltage dependence was steep. This means that a small shift in the cell membrane potential could substantially alter the Vm50. However, this variation in kinetic behaviour might be an inherent property of the channels; large variation in the Vm50 has been reported in Maxi-K channels from pancreatic B cells, even though these measurements were made from excised patches, where the potential and ion concentration can be controlled (Cook et al., 1984).

The small number of appropriate records limited the analysis into the mechanism behind voltage dependence. The data suggested that, for the 96 pS type channels and perhaps the 59 pS type channels, the channels open more frequently and are less likely to close as the membrane is made more depolarized. The analysis of the temporal aspect of voltage activation was limited by the low number of results, and by the variation in parameters such as holding potential and test potential. The application of a standard voltage

protocol might have clarified this. However, although insufficient analysis prevents the characterisation of the mechanisms responsible, the data clearly show that channels inactivate in a time-dependent manner in response to depolarizing steps.

The results from the calcium study are restricted because they rely upon indirect changes in the internal calcium level. However, the reduction of external calcium has been shown effective in reducing levels of intracellular calcium in smooth muscle cells (Mayer et al., 1990). This is supported by results which show that lowering external calcium does not effect the amount of current flowing through the channels, and presumably, the membrane potential. The observed effect on channel gating is thus probably direct, although confirmation requires further experiments on excised patches.

In summary, the data from cell-attached recordings shows the existence of at least three types of channels in cultured human RPE cells. When cell-attached recordings were performed with control solution in the electrode, the mean conductances were 24, 59 and 96 pS. When the electrode contained high potassium solution, the conductances were 108, 47 and 145 pS respectively. Reversal potentials show that all three channel types were primarily permeable to potassium. When the electrode contains control solution, the probability of finding all three channels open was low at the membrane potential, but increased when the patch was depolarized. The 59 and 96 pS channel types displayed a time- and voltage-dependent increase in opening. The 96 pS channel also seems to be activated by elevations in internal calcium. When the electrode contained high potassium solution, no clear relationship between open probability and potential could be found. The implications of these findings are discussed in Chapter VI.

Chapter VI Discussion

VI.A. Introduction

This thesis has described the characteristics of ion channels on cultured human and bovine RPE cells. It is necessary to examine these characteristics closely and to compare them with one another, with those reported for other cell types, and with the currents previously reported in single channel and whole cell studies of the RPE. The conclusions can be used to predict several possible contributions of these channels to RPE physiology. In particular, they should help clarify a dynamic model of transport with mechanisms co-ordinated by voltage and other stimuli.

VI.B.1. Comparison of Channels in Bovine and Cultured Human Preparations

One of the big issues to be addressed is whether the channels identified cultured human cells are the same as those found in fresh bovine cells. Although it was not possible to distinguish discrete groups of channels with conductances below 200 pS in bovine cells, values did cluster near 55 pS and 106 pS (Fig. III.5). These are similar to the values found for the 59 pS and 96 pS channels in the cultured cells (Fig V.1). Although no cluster of bovine channels was found to compare with the 24 pS group identified in the cultured preparation, there were bovine records of a 24 pS and a 35 pS channel. This might be reflect an additional group. The detection of small conductance channel types in bovine cells was complicated by the presence of the large and noisy channel. It is thus possible that additional examples of a small conductance channel types were simply obscured. It must be stressed at this point that a similarity in conductances between the two preparations was not due to any operator bias. The methods used to measure the channels found in the bovine RPE and calculate the conductances were as objective as possible; all the channel amplitudes were measured and the regression lines fit before the distribution of conductances, and thus similarity, was discovered. Records

from the two tissue types differed considerably in appearance and initially no similarity was expected. These values are also very similar to those reported previously for cultured human RPE cells : 27 pS, 45 pS, and 99 pS (Fox et al., 1988).

Nothing resembling the 228pS channel found in bovine cells was ever seen in the cultured cells used in this thesis. The 147 pS channel in bovine cells also appears to have no counterpart in the cultured cells. The reason for this is unclear, but it was the least frequently encountered channel type in this study. It is possible that transitions to this level represented subconductance levels of the 228 pS channel in bovine records. The methods used to determine current size would not have been able to distinguished between a full conductance and a subconductance level as long as some of the transitions to the subconductance level were from the closed level. Fox et al. (1988) reported that their 300 pS channel had several subconductance states, and an example was given of one at approximately 60% of the main conductance. As 147 pS is 64% of the main 228 pS, this relationship supports the possibility that the 147 pS "channel type" is in fact a subconductance level. However, much clearer records allowing a more thorough analysis would be needed to distinguish between full and subconductance levels.

VI.B.2. Significance of Cultured Preparation

In this study, viable cultured human RPE cells could be maintained until the seventh passage which retained their pigment and possessed microvilli on their top surface. These observations suggest that the cultured cells were similar to those found in vivo. However, it is important to show more than just a morphological resemblance. The crucial issues in this study are 1) whether polarity is maintained and channels found on the top surface of the cultured cells would be found on the apical membrane in vivo, 2) whether the channels are present at the same density and relative proportions as those in vivo and 3)

whether the specific type of ionic channels found in cultured cells are the same as those found in vivo.

RPE cells in culture are initially undifferentiated and seem to require a precisely defined environment to redifferentiate into cells which resemble those in vivo and display some degree of polarity. Several components of this environment have been elucidated, including cell density, substrate permeability, substrate coating, cell age and donor age. Embryonic chick cells showed more extensive basolateral infolding, a more epithelioid shape, and secreted a thicker basement membrane when grown on semi-permeable filters coated with laminin, than on uncoated filters or coated impermeable plastic. (Rizzolo, 1990). Even under maximal conditions, these cells required 3-4 weeks to form tight junctions. Confluent bovine RPE cells were elongated in shape when initially plated and only assumed the hexagonal epithelioid shape after several weeks in culture (Basu et al., 1983). When these protocols are followed, cells with a polarised morphology have been shown to possess some forms of functional polarity. Cultured embryonic chick cells with a stable transepithelial resistance of 30 $\Omega \cdot cm^2$ could impede the flow of [^{3}H]-inulin (Rizzolo, 1990). In another report, embryonic chick RPE with well developed junctional complexes which could also impede the flow of [^{3}H] inulin showed a polarised secretion of macromolecules, and released more cAMP into the medium bathing the basal membrane when stimulated with VIP (Koh, 1989). However, the binding of [^{3}H]-ouabain was used to show that the Na^+/K^+ pump was shown to be randomly distributed across cells with tight junctions and morphological polarity (Rizzolo, 1990), suggesting that the polarisation of membrane transport proteins has additional requirements.

The cultured RPE cells used in this study were mainly from aged donors. They were used 2-14 days after plating, and recordings were made from subconfluent cells as it was difficult to form gigaseals with confluent cells. Impermeable substrates were used because semi-permeable filters were

opaque, preventing visual inspection of the electrode tip. It is highly improbable, in light of the evidence above, that the ionic channels on these cells were polarised.

It is difficult to determine whether the channels were present at the same density and relative distribution as those in vivo. Using [^{3}H]-ouabain, the density of Na^+/K^+-ATPase molecules on subconfluent human RPE cells has been shown to increase dramatically as the culture density is decreased, although there was considerable variation in the pump density between and within cells (Burke et al., 1991). If the channels are subject to similar modification, this suggests that the channels found on the sub- confluent cells used in this study may be present at a density higher than found in vivo. The three types of potassium channels were detected on a greater proportion of the patches from the cultured preparation than the bovine membrane. However, the current carried by the non-selective channel found in patches from the bovine cell membranes was so large and unsteady that it may have obscured the identification of other channels. Similar arguments make it difficult to determine if the relative proportion of different channel types was the same in culture as in vivo, for it is possible that in some of the records from both types of preparation, the smaller conductance channels were simply not detected. However, it is clear that the large-conductance non- selective channel was lost in the cultured preparation.

When the characteristics of channels found in the cell attached recordings of cultured cell membranes are compared with those expected in vivo, certain basic differences can be predicted. They arise because the cell membrane potential is less hyperpolarized than that it is in vivo and the internal ionic gradients are not expected to be as well maintained. It is impossible to determine if the intrinsic, biophysical properties of the channels in culture are the same as those in vivo because it is not possible to patch clamp in vivo. The Ussing chamber system is the closest electrophysiological preparation to the in

vivo state, and was used to show that the apical and basal membranes of bovine (Joseph and Miller, 1991) and foetal human (Quinn and Miller, 1992) RPE were primarily permeable to potassium. This agrees with the conclusions of this thesis at a gross level. However, it does not provide any evidence that the channels found on cultured cells are the same as those in vivo.

A recent whole cell study of human RPE cells showed that an A-type K^+ current was found in all foetal and in 20 % of cultured cells, but never in fresh adult RPE (Wen et al., 1993). This indicates that channels not present in vivo are induced by culture. It is thus possible that some of the channels identified in cultured cells in this study are not present in vivo.

VI.B.3. Significance of Bovine Preparation.

The characteristics of channels found on the basal membrane of fresh bovine RPE cells were similar to those found on the top, "apical", surface of cultured human RPE cells. The discussion in section VI.B.2 makes it clear that the channels on the cultured cells are unlikely to be polarised. It is important to predict whether channel distribution is polarised in the preparation of fresh bovine cells.

Gigaseal formation required that the bovine cells were enzymatically cleaned. This process transformed a sheet of tissue with tight junctions inbetween the cells into a preparation of single cells. However, tight junctions are thought to restrict the flow of proteins through an otherwise fluid membrane and thus maintain polarity (Handler, 1989). The speed with which polarity is lost was shown by Pisam and Ripoche (1976), who used ^{125}I to label proteins on the apical membrane of intact frog urinary bladder. Autoradiographs taken at intervals showed the labelled proteins had moved beyond the apical membrane only 20 minutes after the tight junctions had been disrupted and were randomly distributed all over the cell surface within 120 minutes. Recordings from bovine RPE cells in this study were made between 30 minutes

and 4 hours after dissociation. One can thus conclude that polarity was not maintained in the fresh bovine RPE cells.

It is possible, however, that the collagenase dissociation caused a temporary change in channel activity. Suspending HeLa cells in 0.1% trypsin, 0.1% pronase and 2mM EDTA caused the K^+ and Na^+ gradients to temporarily dissipate, presumably by creating a leaky hole large enough to allow 2-deoxy-glucose through (Lamb and Ogden, 1985). As my experiments were performed in the cell attached mode, it is possible that patches formed within 30 minutes of the dissociation reflected this changed gradient.

VI.C. Identity of Channels

It was important to determine how the channels found in this study compared with those in the literature. The results from experiments on cultured cells are used for this comparison because they are so much more abundant than results from bovine cell experiments.

VI.C.1. Maxi-K

The largest potassium-selective channel found in both cultured and fresh cells probably belongs to the group of channel types termed "maxi-K", or BK. According to a widely quoted criteria, the maxi-K channels have a conductance of 130-230 pS when excised in symmetrical 150 mM K^+, are highly selective for K^+ over Na^+ , are activated by both membrane depolarization and by internal Ca^{2+} and are blocked by Ba^{2+} (Latorre and Miller, 1983, Latorre et al., 1989). The evidence presented here is sufficient to show that several of these criteria are met; the channel had a conductance of 145 ± 41 pS when the cell-attached recordings were performed with high potassium solution in the electrode (Table V.2), (a configuration which approximates symmetrical 150 mM K+ solutions), activity was clearly increased by depolarisation (Figure. V.14), and activity was decreased by a process assumed to decrease the internal [Ca^{2+}] (Figure V.18).

Further support can be found by comparing these results with other

reports of maxi-K channels. A maxi-K channel on *Necturus* renal proximal tubule shows an almost identical relationship between activity and membrane potential as the one in this study; when cell attached, the channel is usually closed at potentials more negative than -60 mV, but P_o rises steeply to 0.1 when the patch is depolarized by 50 mV (Filipovic and Sackin, 1991). When cell attached, the conductance of this channel is 92 pS and 106 pS when the electrode contains a control and a 70mM K^+ solution , respectively. In cultured medullary thick ascending limb (MTAL) cells, a channel with a conductance of 151 pS (140 mM KCl in the electrode) had a P_o of 0.001 at the membrane potential when cell attached (Taniguchi and Guggino, 1989). Activity increased with depolarization at a rate which closely mirrored the channel seen in RPE cells, and when the patched were excised, activity was shown to be dependant upon internal Ca^{2+}. In N*ecturus* choroid plexus, the only other epithelial tissue which has the Na^+/K^+-ATPase located on the apical membrane, a channel was described which was activated by depolarization and internal Ca^{2+}, has a conductance of 110 pS with 150 mM NaCl in the patch electrode and 150-220 pS with 150mM KCl in the patch electrode (Brown et al., 1988).

These reports confirm that the low levels of channel activity usually seen in this study are common for a maxi-K channel found in cell attached recordings when the internal Ca^{2+} and the external K^+ are low. They also show that 96 pS is within the range of conductances expected for a maxi-K channel when the external K^+ is low, although this channel does fall in the lower range of maxi-K conductances. The dependence of conductance upon external levels of potassium occurs because millimolar amounts of internal Na^+ block maxi-K channels (Yellen, 1984*a*) and this block is relieved by millimolar concentrations of external potassium (Yellen, 1984*b*). This Na^+ block is most apparent at depolarized potentials and can occur with the concentration of Na^+ normally present in cells. This block would explain why nearly all of the large-conductance cells studied with control electrode solution showed a decrease in

conductance as the patches were depolarised. Sodium block would also explain why in some records, such as the one shown in Figure V.6, the conductance was negative when the patch was depolarized 90 mV past the membrane potential. This resembles a maxi-K channel in chick lens epithelium when excised patches were bathed physiological solutions; the maximum conductance of 100 pS reversed at +40 mV (Rae et al., 1990). Na^+ block was not seen with high K^+ in the electrode presumable because it was relieved by the external potassium.

The steady state kinetics of maxi-K channels are well documented and resemble the activity of the 96 pS channel in this study. However, the time-dependent kinetics of maxi-K channels are also similar to those seen in this study . When cultured rat muscle cells are excised and the cytoplasmic face of the membrane is bathed in $6x10^{-7}$ M Ca^{2+}, depolarizing steps cause an increase in channel activity which activates with τ = 20-30 msec and inactivates with τ = 400 - 800 msec (Pallotta, 1985). As the holding potential is made more depolarised, these channels activate less at a given test potential, evidence of steady state inactivation. The time constants for activation and inactivation of this current are roughly the same as those fit to the 96 pS channel in this study, and although steady state inactivation was not tested for, the open probabilities of most of the large conductance channels were similar to the levels seen after inactivation.

The large-conductance potassium channel found in this study can be assigned to the maxi-K group of channels on several grounds; conductance, selectivity, an increase in open time with depolarization, time- and voltage-dependant activation and inactivation, sodium block, and the dependence of open time upon internal calcium levels. Although some of these attributes were only characterised to a limited degree in this study, together they strongly support the identification of this channel type as maxi-K.

VI.C.2. Medium Conductance Potassium Channel

There are a number of different channel types with a conductance similar to that of the medium conductance potassium channel and it is not possible to distinguish between them on the basis of the results presented here. However, it is likely that this is some form of outwardly rectifying channel. The open probability increases with depolarization; when superimposed upon an ohmic conductance this would lead to outward rectification at the whole-cell level. There is preliminary evidence to show that depolarizing steps cause an increase in channel activity which inactivates with time. Due to time constraints, a rigorous investigation of this phenomenon was not carried out, however, and in the absence of any information about the activation time constant it is impossible to perform a stringent comparison of detailed kinetic attributes.

In many respects, this channel resembles an outward rectifier potassium channel found in excised patches of hamster oocytes (Yoshida et al., 1990). The mean outward conductance of this channel was 64 pS and the inward conductance was only 30 pS. This channel was also more active at depolarized potentials, and sensitive to the internal calcium concentration. Although the calcium sensitivity of the medium-conductance channel found in RPE cells has not been tested, other characteristics are very similar to the oocyte channel.

The medium and the high conductance potassium channels seen in this study have similar kinetic characteristics, and it is thus important to remember that they were usually seen without the other, and that the application of the binomial theorem supports their separate identities.

The presence of two potassium channels with similar voltage dependence of activation is not unusual. For example, both a voltage-gated potassium current and a calcium- and voltage-sensitive potassium current have been found in the pigmented ciliary epithelium (Jacob, 1991). Fibroblasts have been shown to contain at least seven different potassium channels, ranging in conductance from 21 pS to 235 pS (French and Stockbridge, 1988).

VI.C.3. Inwardly Rectifying Channel

The small conductance channel has many characteristics in common with inwardly rectifying channels in the literature. When the electrode contained a high potassium solutions, no outward current was detected and the conductance line curved slightly as the zero-current line was approached. This lack of outward current is a defining feature of the inward rectifying channel and has been reported in, among others, guinea-pig ventricular cells (Sakmann and Trube, 1984), rat ventricular cells (Josephson and Brown, 1986), murine macrophages (McKinney and Gallin, 1988) and murine myoblasts (Matsuda and Stanfield, 1989). The decline in open probability as the patch is hyperpolarized beyond Ek seen in this study has also been reported for inward rectifiers in reports mentioned above, and the large proportion of the time the channel spent open near the membrane potential (0.82) is similar to the steady state values in these reports.

One of the most conserved characteristics of the inward rectifier is the dependence of the conductance on external $[K^+]$; the conductance is commonly reported to increase in proportion to the square root of external $[K^+]$ (Sakmann and Trube, 1984; McKinney and Gallin, 1988; Josephson and Brown, 1986). If one assumes that the smallest conductance group seen with control electrode solution was the inward rectifier, then this relationship held for this preparation. The conductance when the pipette contained 100 mM K^+ was 108 pS, and when it contained 5 mM, the conductance was 24 pS.

$$g = a*\sqrt{[K^+]_o} \quad : \quad g/\sqrt{[K^+]_o} = a$$

Where g = conductance; a = constant; K_o= pipette potassium

for high K^+ PFS (108 pS/$\sqrt{}$100mM) = 10.8

for control PFS (24 pS/$\sqrt{}$5mM) = 10.7

The near-identical proportionality constant reinforces the assignments of the channel types seen with each type of electrode solution to each other and to the group of inward rectifiers.

The main difference between the inward rectifiers described in the literature and those descried in this study is in the absolute conductance. Typical values quoted for the inward rectifier are 27 pS with high $[K^+]_o$ and 4 pS with physiological $[K^+]_o$ (Sakmann and Trube, 1984; McKinney and Gallin, 1988). This compares with 108 pS and 26 pS, respectively, in this study (Table V.2). The difference may reflect a characteristic of the RPE inward rectifier.

There seems little doubt that the channels seen when the electrode contained high K^+ and classified as inward rectifies were some type of inward rectifier. However, it is possible that the medium conductance group found when the electrode contained high potassium solution was actually composed of two channel types, a medium and a low conductance group. When divided this way, the channels from cultured cells consist of three outwardly rectifying channels plus an inward rectifier. Grouping the channels this way would clarify certain discrepancies. For example, when the electrode contained control solution only 2 out of 12 records from the small conductance group showed and inward current when hyperpolarized. By definition, an inward rectifier is expected to pass more current when hyperpolarized by a given amount past the potassium equilibrium than when depolarized by the same amount. Sometimes, the activity of this channel increased as the patch was depolarized. This increase in activity would not be expected from an inwardly rectifying channel. In addition, this would mean the "medium" conductance group, observed when the electrode contained high potassium solution, actually consisted of a small and medium channel types. The large standard deviation of this group is consistent with this idea. If channels are classified into only three groups, the conductance of the medium channel decreases when the external potassium was raised. This phenomena is highly unusual and unlikely.

The above arguments suggest that the channels need to be slightly regrouped; medium channel type seen when the electrode contained high potassium solution actually contained small and medium channel types, and the small conductance channel classified with control solution in the electrode probably consisted of both an outwardly rectifying channel, and an inwardly rectifying channel. The major difficulty with this reassignment is that the number of records are too few and there is no objective way to divide the groups. Although logic dictates that the present boundaries need to be redrawn, this logic does not suggest how. The lack of any clearly dividing characteristics was also the reason that the channels were originally placed into these groups.

Because there is no objective method to further divide these groups, the analysis in Chapter V has not been redone. Any regrouping would have only minor implications for most of the conclusions reached. It is unlikely that regrouping would clarify the selectivity analysis. There were only 9 records placed in the "medium conductance" group when the electrode contained high potassium solution, and there was great variation in the reversal potentials. However, as Figure V.12 shows, there was no clear relationship between conductance and reversal potentials. Separating the records on the basis of conductance would not be expected to produce any great change in the calculated selectivity of the channel.

The reclassification doesn't alter the attributes of the inward rectifier, it just makes its less frequently encountered with control electrode solution. If one assumes that none of the small conductance channels are inwardly rectifying, there is no way to verify the relationship between external potassium concentration and conductance. Further speculation is pointless without more concrete data, however.

In conclusion, it is likely that the most of the small conductance channels seen when the electrode contained control solution were outward rectifiers, and that the group of nine channels termed medium conductance

when the electrode contained high potassium solution actually consisted of two types of outward rectifier. The original misclassification was caused by the method of grouping channels, but given the small number of records and the great variation in conductance and reversal potential measurements, there was no other objective way to group the channels. This shift is not expected to alter the conclusions reached in Chapter V substantially. However, it does point out that elaborate analysis, such as the calculation of channel permeability constants described in section V.C.3.b, should only be undertaken when there is a sufficiently large data base, with sufficiently low standard deviation, to provide the accurate figures needed.

VI.C.4. Large Conductance Bovine Channel

The general identity of the large-conductance channel seen in bovine cells is unclear. In their study of cultured human RPE cells, however, Fox et al.(1988) found a 300 pS channel. Inside out experiments in which the patch was bathed with asymmetric NaCl and KCl solutions showed that the channel did not distinguish between the two cations. The report also mentions one attempt at a dilution experiment and claims that the results indicate the channel does not select between anions or cations. Information about the 228pS channel in the present study came from channels with an enormous range of conductances; from 162 pS to 290 pS. In addition, several channels existed with conductances up to 360 pS. These were not included on the basis of the distribution histogram, but with a larger, better controlled sample it is possible that the mean conductance of the group will move up. Although no conclusive information was obtained about the selectivity of the 228pS channel found in this study, the data from cell attached experiments when the electrode contained control solution are consistent with a non-selective channel.

Non-selective channels have been reported in a variety of ocular epithelia including corneal endothelium (Rae et al., 1988), lens epithelium (Rae

et al., 1988) and pigmented ciliary epithelium (PCE) (C. Mitchell, unpublished observations). The occurrence in the PCE is particularly relevant, as this tissue is the anterior continuation of the RPE. In these reports, the conductances of this channel range from 240 to 320 pS.

VI.C.5. Summary of Classification

The channels identified in this study share certain characteristics with channels observed in other epithelia, and it is tempting to try and match up the channel types. This exercise has both advantages and disadvantages. The analysis of the channels in this study is somewhat incomplete, and it is hoped that by identifying the RPE channels with other channels which are more thoroughly described characterised channels, it may be possible to extrapolate the characteristics onto the RPE. This has been possible for the 96 pS channel. However, there is a large variety of potassium channels, and the information available from this work may be insufficient to distinguish between different varieties. Thus no clear "identity" has been found for the other channel types, but the most relevant possibilities have been discussed.

It has become clear, while trying to identify channel types from the literature, that the classification of channels into discrete groups should proceed with caution. For example, the maxi-K channel type is one of the most widely reported, yet conductances range from 90-300 pS. This implies that the maxi-K^+ family of channels consists of many different types of channel which have some characteristics in common. The need to find common patterns in channel activity should not obscure the possibility that a channel from a particular species or cell type is unique, or *vice versa*. A more accurate taxonomy should soon emerge with the use of molecular biological techniques.

VI.D. Comparisons with Other Patch Clamp Studies on the RPE

The only other previous study on the single channels of RPE cells also

used cultured human cells (Fox et al., 1988). When conductance and selectivity information are considered, there are many similarities between this study and theirs. The potassium selective channel types had conductances of 99 ± 19 pS, 45 ± 1 pS and 27 ± 3 pS. The groups identified under similar conditions in this study had conductances of 96 ± 10 pS, 59 ± 10 pS and 24 ± 9 pS (Table V.2). The different channels were observed by Fox et al. (1988) with a relative frequency similar to that found in this study. Fox et al. (1988) were able to excise patches successfully and found that under biionic conditions, all three channels types were primarily permeable to potassium. Their finding supports the estimates performed in this study based upon cell-attached measurements of the reversal potential (Table V.4).

The concurrence of conductance and selectivity values suggests the channel types identified in this study were the same as those described in the study of Fox et al. (1988). Groups of channels belonging to the same channel type, and thus with a similar mean conductance were obtained independently from both bovine and cultured experiments in the study presented here (Figure III.5; V.1). The fact that they agree so closely with the groupings described by Fox et al. (1988) provides very persuasive support for these assignments.

Fox et al. (1988) also reported a very large conductance channel which could not discriminate between Na^+, K^+ and possibly Cl^- ions. This channel is similar to the channel seen in fresh bovine but not cultured human recordings in this study (Figure III.3). It is not known why the channel was seen in their cultured preparation; it is tempting to speculate that the channel disappears with passage and time in culture, but as they gave no information regarding passage number, this hypothesis cannot be verified.

The main difference between this study and that of Fox et al. (1988) is that they did not detect any voltage -dependence of channel activity and in the present study, all three potassium channels were more active at depolarised potentials (Figure V.14). This discrepancy may have been caused by the

choice of electrode solution. In this study, the voltage dependence of channel activity was only obvious when the channel contained control solution. When the electrode contained high K^+ solution, there was no clear relationship between P_o and V_m (Appendix III, Table 3 and Table 5). In the study by Fox et al. (1988), the number of records obtained when the electrode contained control solution was low: only 5, 3 and 3 cell-attached recordings were made of the 99 pS, 45 pS and 27 pS channels, respectively. They showed a plot of P_o against potential for each channel type, but they pooled the data from experiments with both control and high K^+ electrode solution. A few of their records did show an increase in P_o with depolarisation while most of them did not, leading to their conclusion that activity was not voltage dependent for any of the potassium selective channels. However, the data as presented is also consistent with the theory that channel activity is voltage dependent when the electrode contains control solution.

It is also possible that Fox et al. (1988) did not detect an increase in channel open probability because of their voltage protocol. In my study, sudden depolarization of the patch caused a time-dependant increase in the probability of finding the channel open. Care was taken to assure that this effect did not influence the measurement of steady state open probability; the voltage was usually changed by only 10 or 20 mV at a time and in most cases the open probability was calculated from a section of data several hundred times longer than the time constant of inactivation. If Fox et al. (1988) did not pay attention, some of their open probability measurements could have been made before this time dependant increase had inactivated. The resulting values of P_o would be spuriously high, and would obscure any relationship between P_o and potential. Fox et al. (1988) did not provide a description of the voltage protocol they followed during their experiments. They also made no mention of any time and voltage-dependant increase in channel activation. It is thus possible that they disregarded any time and voltage-dependant increase in channel activity.

Fox et al. (1988) also reported that neither the 100 pS K+-selective channel or the 300 pS non- selective cation channel they found on cultured human RPE was effected by bathing the cytoplasmic side of an inside-out patch with 10^{-8} M Ca^{2+}. The reasons for the discrepancy between my results (Table V.8) and theirs on this matter are not clear.

Some of the recordings used for kinetic analysis by Fox et al.(1988) were performed in the inside-out mode with 0.95 mM or 1.1 mM Ca^{2+} bathing the cytoplasmic face of the patch. The voltage-dependence of maxi-K channel activity has been reported to disappear when the internal calcium concentration is high (Rae et al., 1990). It is possible, therefore, that high internal calcium contributed to the inability of Fox et al. (1988) to detect the voltage dependence of channel activation, at least in the largest potassium channel.

It is extremely unlikely that the voltage-dependant activity seen in this study is an artefact, for voltage-gated potassium currents have been shown from the RPE of frog (Hughes and Steinberg, 1990; Hughes and Segawa, 1993) turtle (Fox and Steinberg, 1992), monkey and both fresh and cultured human tissue (Wen et al., 1993). An inwardly rectifying current was observed in all preparations except turtle, and it has some qualities in common with the currents seen at the single channel level. For example, when frog cells were bathed in high K^+ solution, the conductance increased when the cells were hyperpolarized beyond -60 mV (Hughes and Steinberg, 1990). This shift in the IV curve near -60 mV to -70 mV was also seen in three single channel records when the electrode contained high potassium solution (see Appendix III.2). However, in frog cells, there was a substantial outward current when the cell was bathed in control solution; at any particular voltage, the chord conductance was actually increased with a decrease in external potassium concentration. This implies that, at the single channel level, the current would be expected to have a relatively large conductance, and supports the idea that some of the small conductance record with control electrode solution were from

inward rectifier channels. The inward rectifier was seen in all fresh human RPE cells examined at the whole cell level and did not inactivate; while it was found in only 20% of cultured human RPE cells and inactivated when the cells were hyperpolarized past -120 mV (Wen et al., 1993). This inactivation was described in experiments where the cells were bathed in control solution, but it is unclear whether inactivation also occurred when the cell was bathed in a high potassium solution. This would indicate if the low conductance channels seen with control electrode solution (Figure V.3) were inward rectifiers.

The outward currents from these whole cell experiments were activated when the cells were clamped at potentials more depolarized than -30 mV (-43 mV in turtle (Fox and Steinberg, 1992). This figure agrees closely with the single channel data, which shows that channel activity was usually detected when the patch was depolarized 40-60 mV (Fig.V.14). The outward potassium currents identified so far in the various preparations differ mainly in the extent of their inactivation; in turtle (Fox and Steinberg, 1992)., foetal human and some of the cultured human cells (Wen et al, 1993), steady state current was less than half of the peak current after a depolarizing pulse; in frog (Hughes and Steinberg, 1990), the current inactivated by one third; in fresh human and most of the cultured human cells, the outward current showed little, if any, inactivation (Wen et al, 1993). Generally, the greater the inactivation, the shorter the activation time constant, but these values changed in a continuum with the preparation and did not seem to fall into distinct groups. As far as one can extrapolate from single channel to whole-cell, the activation and inactivation seen at the single channel level here (Fig.V.17). would most likely account for the inactivating outward currents seen at whole cell level. In addition the outward currents of turtle (Fox and Steinberg, 1992) and frog (Hughes and Steinberg, 1990), were shown to be subject to a steady-state inactivation; as the holding potential was made more depolarised, the peak outward current decreased.

seen in fresh human cells, and only 33% of the currents seen in cultured RPE cells inactivated. This may reflect a shift in the relative proportion of small, medium and maxi-K^+ channel types. Although no such shift was detected in this study, a gradual shift would not have been detected with the relatively low number of recordings made. This theory would also depend upon the presence of a non-inactivating channel type; by a process of elimination, the results here tentatively suggest this would have to be the small conductance, as the other two inactivate.

Another possible explanation for the development of inactivating currents in culture involves the type, or sub-type, of channel shown in Figure V.15. Four of the maxi-K^+ channels seen with control solution in the electrode, or 22%, had open probabilities substantially higher than expected. It is unlikely that this increase is caused by a spontaneous increase in the membrane potential because this would alter the conductance and reversal potential; instead the values remained close to the group mean. The closeness of these measurements to the group means also helps eliminate the possibility that these records are from different channel types. It is possible that this increase in activity is caused by a spontaneous elevation in internal calcium. It is more likely that the steady-state inactivation present in maxi-K^+ channels is lower in these four recordings than it is in the remaining records. If this assumption is allowed, then a pattern begins to emerge because the cultured cells used in the whole cell study are from passages 1-4, while those used in my single channel study are from passage 4-8. Thus, an inactivating outward current was seen in none of the fresh adult RPE cells, 33% of the cultured adult cells from passages 1-4, 78% of the cultured adult cells from passages 4-8, and all of the fresh foetal cells (Wen et al, 1993; Figure V.15). This agrees with the idea that cultured RPE cells develop characteristics of embryonic tissue (Neill and Barnstable, 1990). The theory also predicts that channels responsible for the outward currents in adult, cultured and foetal human RPE cells are the same

except that foetal and cultured cells posses a component responsible for inactivation. As discussed above, Wen et al. (1993) also report that the inwardly rectifying current inactivates in cultured cells but not in fresh adult cells, suggesting that the outward and inward currents might undergo the same type of changes as they develop.

The relationship between the internal calcium level and outward current in frog, turtle, and adult human RPE cells was not investigated. However, the inactivating current seen in foetal cells was claimed not to be calcium dependent (Wen et al., 1993). This is based upon the observation that the current was present with an internal calcium concentration of 10^{-8} M and when external calcium was removed. Details of this experiment were not provided, and thus the reasons for this discrepancy remain unclear. However, it could be that under these conditions of very low calcium, the major outward current is carried by either the medium conductance, the small conductance, or both, types of potassium channel. The effect of raising the internal calcium on any of the preparations used for whole-cell recordings is not known.

Recently, a chloride current has been identified by whole cell recordings in frog and toad RPE (Hughes and Segawa, 1993). This current was only seen when cAMP was applied to the cell. It is thus unlikely that such chloride currents were present in the single channel records presented here.

Throughout this analysis, it has been assumed that all three channel types were impermeable to Cl^-. Although the Cl^- conductance of the apical membrane of the RPE is very low in both frog (Miller and Steinberg, 1977*a*) and bovine RPE (Joseph and Miller, 1991), channels in the cultured cells could have migrated from the basolateral membrane, which contains a considerable Cl^- conductance. Under general physiological conditions, Cl^- flows into the cell while K^+ flows out, but because of the difference in charge, both currents are positive. The most straight forward way to distinguish between current carried by either ion is to impose a large concentration gradient across the membrane

with an excised patch. Both ions will flow in the same direction and the currents can be separated. Unfortunately, attempts to record from excised patched in this study were unsuccessful, and the possibility of a small chloride conductance cannot be eliminated. However, the concentration of Cl^- in the two different electrode solutions is very similar and thus Cl^- cannot be responsible for the shift in reversal potential seen with the different electrode solutions.

In conclusion, the currents seen in RPE cells at the whole cell level support the results of this study. The report that inward rectifier currents are present in only 20 % of cultured human cells and inactivate under physiological conditions agrees with the tentative conclusions reached here about inward rectifier channel. It indirectly supports the observation that the majority of currents seen were outwardly rectifying.

VI.E. Relevance to RPE Physiology
VI.E.1. Polarity

This study has shown that cultured human RPE cells contain various types of potassium channels; an inward rectifier, a maxi-K, and probably two different types of outward rectifier. In a polarised epithelium, the role of the channel types is dictated by their location. Although the techniques used in this study give no indication of the placement of the individual channel populations, possible polarity can be suggested by other studies. In fresh adult and foetal human cells placed in an Ussing chamber, 1mM Ba^{2+} has been shown to block 78% of the voltage change induced by an increase in the concentration of potassium bathing the apical membrane (Quinn and Miller, 1992). In frog, the inwardly rectifying current seen in whole cell recording is blocked by 5 mM Ba^{2+} and Cs^+ , and that the same concentration of these drugs blocked the apical membrane response to a ten-fold increase in potassium much more than they blocked the basal membrane response (Hughes and Steinberg, 1990). This was taken to suggest that the inward rectifier channels are mainly present

on the apical membrane. However, 0.1 - 5mM Ba^{2+} also blocks maxi K^+ channels when applied to the extracellular face of lens epithelial cells and a variety of other tissues (Rae et al., 1990, Latorre et al., 1989). This would tentatively suggest that an inwardly rectifying potassium channel, a maxi-K^+ channel and the smaller conductance outwardly rectifying channels exist on the apical membrane of RPE cells. It also makes it clear that the polarity of Ba^{++} block this is not a particularly effective way to determine the polarity of a mixture of potassium channel types.

VI.E.2. Possible Mechanisms of Channel Activation

None of the channels in this study had a particularly high probability of being open at the resting membrane potential under experimental conditions which mimicked the physiological state. It is possible that the cultured conditions affected channel activity by either modifying the membrane potential, internal ion concentration. Alternatively, a vital cofactor may be present in lower concentration that in vivo, leading to a decrease in channel activity. Without more detailed information, however, it must be assumed that these channels also have a low probability of being open at the resting membrane potential in vivo.

The presence of voltage gated channels is perplexing, for the RPE are not electrically excitable. In foetal human cells a decrease in potassium concentration from 5 to 2 mM, (similar to the decrease induced by light), hyperpolarized foetal human tissue by 20 mV. Increasing the concentration of potassium in sub-retinal space of frogs from 2 to 5 mM (similar to the rise accompanying the onset of darkness) depolarized the apical membrane of frog RPE by 12 mV (Oakley and Steinberg, 1982). However, as the outwardly rectifying and maxi-K^+ channels activated at depolarizations past 40-60 mV, the dark-induced change in membrane potential would not be sufficient to activate the channels. There needs to be a fundamental shift in the activation range of the outwardly rectifying channels if they are to contribute to RPE physiology.

The obvious mechanism for this shift is to increase the internal calcium concentration. In this way, the maxi-K^+ channel provides a mechanism by which pharmacological signals can modify transport across the RPE.

Receptor-coupled activation of the maxi-K channel has been well documented in other epithelial cell types including lacrimal and pancreatic acinar cells (Petersen, 1992). The most common mechanism involves the inositol phosphate pathway. Basically, the receptor-mediated activation of phospholipase C leads to the hydrolysis of phosphatidylinositol 4,5-bis-phosphate into inositol triphosphate (InsP3) and diacylglycerol (DAG) (Berridge and Irvine, 1989). InsP3 causes a release of calcium from the endoplasmic reticulum stores and thus an elevation in the intracellular calcium levels.

Maxi-K channels are often located on the same side of the membrane as the $Na^+/K^+/Cl^-$ cotransporter and the two mechanisms may act together to recycle potassium. Thus a greater intracellular concentration of intracellular calcium increases the potassium conductance of the membrane, more K exits. This provides an increase in the supply of K in extracellular space to act a substrate for the cotransporter. This is supported by the observation that the rate of the cotransporter increases with increased intracellular calcium (Smith and Smith, 1987). Measurements of the uptake of ^{86}Rb in smooth muscle cells suggest that an increase in intracellular calcium increases the rate at which chloride enters the cell; as this movement of chloride goes against its electrochemical gradient it must be actively transported and the most likely candidate for this is the cotransporter. In this way, receptor activation can lead to an increase in chloride transport across the cell.

It is possible that a similar mechanism operates in the RPE, for with the discovery of the maxi-K channels, all the necessary components are present. The $Na^+/K^+/Cl^-$ cotransporter has been tentatively assigned to the apical membrane of mammalian cells (Miller and Edelman, 1990, Kennedy, 1990). Although it is not possible to determine the polarity of the maxi-K channel in the

present study, indirect evidence places it on the apical membrane.

Several substances have been shown to increase the intracellular concentration of calcium, $Ca^{2+}_{i,}$ of the RPE. Bombesin, neuromedin B and neuromedin C all induced a transient increase in Ca^{2+}_{i} in cultured human RPE cells, as measured with the fluorescent Ca^{2+} -binding dye fura-2 (Kuriyama et al., 1992). The production of $InsP_3$ was also increased after stimulation with these agents, supporting the involvement of the inositol pathway. Using similar techniques, carbachol, vassopressin and thrombin were also shown to increase the production of $InsP_3$ in cultured human RPE cells (Crook et al., 1992). Several growth-factors have been shown to cause Ca^{2+} transients and an increase in $InsP_3$: the largest effect was produced by foetal bovine serum which contains a mix of various individual growth factors and by platelet-derived growth factor (PDGF) (Kuriyama et al., 1991). As the RPE lies adjacent to the choroid, it is possible that one or more of these substances could diffuse across the endothelial membrane and activate the RPE, although there is no direct evidence for this as yet.

The evidence above suggest several possible ways in which the level of internal Ca^{2+} could be increased and the activity of a maxi-K channel could theoretically be increased. However, when dealing with a cell type like the RPE with its numerous interacting membrane mechanisms, it is difficult to predict the effect of altering intracellular calcium. Recently the effect of epinephrine on various characteristics of RPE membrane physiology has been studied. As the predominant initial effect of epinephrine is to raise intracellular calcium, this serves as a useful test to suggest how the activity of maxi-K and other potassium channels is organised to give a coodinated cellular response.

Fura-2 imaging has shown that stimulating bovine cells with epinephrine leads to an increase in Ca^{2+}_{i} (Lin and Miller, 1991a).. However, intracellular microelectrode and current clamp techniques have indicated that the main effect of epinephrine is an increase the conductance of the basolateral

membrane followed by a decrease in the conductance of the apical membrane (Joseph and Miller, 1992). The basolateral membrane depolarized and this depolarization is thought to be caused by the exit of Cl^- for three reasons; the response was blocked by lowering cell Cl^-, by current clamping the basolateral membrane to the Cl^- equilibrium potential and by the anion channel blocker DIDS. The epinephrine-induced increase in TEP and fluid transport was blocked by the alpha-1 adrenergic antagonist prazosin, but was unaffected by the beta-adrenergic antagonist propranolol (Edelman and Miller, 1991). This supports the epinephrine-induced increase in Ca^{2+}_i as stimulation of alpha-1 receptors activates the inositol pathway and lead to an increase in Ca^{2+}_i (Minneman, 1988). Epinephrine has a similar effect on the voltage components of foetal human RPE cells (Quinn and Miller, 1992)

The epinephrine-induced decrease in the apical membrane conductance was shown be due to a 50% drop in K^+ permeability by measuring the voltage response to changes in extracellular K^+ (Joseph and Miller, 1992) . Initially it is difficult to see how a maxi-K channel might fit into the model of adrenergic stimulation outlined above. The increase in Ca^{2+}_i caused by epinephrine would be expected to increase the conductance of a maxi-K channel, not reduce it as suggested above. However closer examination provides several possibilities. It is not clear that a maxi-K channel would be effected by the magnitude of Ca^{2+}_i increase produced in the above experiments. On average, activity of the maxi-K^+ channel is maximally activated by 1-10 μ M Ca^{2+}_i while the activity of the Ca^{2+}-sensitive Cl^- channel in airway epithelia increases when calcium rises from approximately 20 to 180 nM (Hille, 1992) and the Cl^- channels in the colonic tumour cell line T84 are activated when the Ca^{2+} is raised above 50nM (Frizzell et al., 1986). However, application of epinephrine to bovine RPE cells causes transient elevations in Ca^{2+}_i of only 200 - 400 nM from a baseline of 165 nM (Lin and Miller, 1991a).

Although this suggests that the epinephrine-induced increase in Ca^{2+}_i

may not be sufficient to activate a maxi-K channel, it does not explain why the conductance should decrease. In addition to the alpha-1 adrenoreceptors, beta-adrenergic receptors, linked to an increase in cAMP have been shown in chick (Koh and Chader, 1984) and human (Frambach et al, 1990) RPE. It is possible that epinephrine activated both receptors and that the rise in cAMP was responsible for the decrease in apical potassium conductance. This is very unlikely, however, because the alpha-1 antagonist prazosin completely abolished the apical membrane response to epinephrine, while the beta-antagonist propranolol had no effect upon the apical response (Joseph and Miller, 1992). In addition, the Ca^{2+} ionophore A23187 produces similar effects on the electrical properties of both membranes to those of epinephrine, suggesting that an elevation of Ca^{2+} alone was sufficient to produce the effects. Evidence from the bovine study suggests that the decrease in apical conductance was caused by the increase in basolateral Cl^- conductance, because both apical and basal responses are blocked by removal of Cl^- from the apical bath, addition of bumetanide to the apical bath and addition of DIDS to the basolateral bath, and because the apical response followed the basal response when high concentrations of epinephrine were used.

The above evidence argues against a primary role for the maxi-K channel in the epinephrine-induced response. It is more likely that the depolarization caused by the exit of Cl^- and shunted to the apical membrane triggers the inactivation of inwardly rectifying potassium. Inactivation upon depolarization is a widely observed characteristic of inward rectifier channels and has been shown to occur at the whole-cell level in the RPE (Segawa and Hughes, 1993). The maxi-K channels would act as a safety valve and prevent the excessive depolarization of the cell. The epinephrine-induced increase in Ca^{2+}_i might shift the activation curve of the maxi-K so that the channel opened when depolarized past a certain potential. This would explain why, according to the rough calculations above, epinephrine produced an increase in Ca^{2+}_i

insufficient to activate the maxi-K at the resting membrane potential; the system is finely tuned by the increase in Ca^{2+}_i so that the channel responds to depolarization. The basolateral depolarization would increase the rate of the Cl^-/HCO^-_3 exchanger, via an increased gradient for Cl^- entry, leading to an increase in intracellular pH (Hughes et al., 1989). As the activity of maxi-K channels increases with increasing pH (Cook et al., 1984), the predicted response of the Cl^-/HCO^-_3 exchanger would be to increase the potassium conductance. The activity of the maxi-K channel would not be detected by in the experiments of Joseph and Miller (1992) because their technique gave only a coarse measure of the total potassium conductance. However, their results do show that both membranes begin to repolarise during a continuous application of 10 μM epinephrine, and the ratio of apical to basolateral membrane resistance decreases while the total resistance decreases. These observations support the hypothesis that an additional potassium conductance was activated shortly after depolarization induced decrease in inward rectifier conductance.

As epinephrine produces its predominant effect on RPE membranes by increasing internal calcium, it can be assumed that a similar sequence of channel events would be produced by any other substances which produces an increase in internal calcium. The feedback role of the maxi-K channel would compensate for any difference in the level of calcium produced; a higher Ca^{2+}_i would lead to an increased rate of Cl^- exit and thus depolarization, but the corresponding increase in the sensitivity of a maxi-K to depolarization.

VI.E.3. Spatial Buffering

As described in Chapter I, the permeability of the apical membrane to potassium depends upon the concentration of potassium in sub-retinal space; following the onset of light, when the concentration is low, the conductance rises. This means that more potassium ions flow from the RPE to the

subretinal space and help restore the subretinal levels. When the concentration is high, the potassium conductance of the apical membrane decreases and excess potassium ions flow out of the basal membrane to the choroid. This spatial buffering of potassium ions across the RPE is thought to help maintain a constant potassium concentration around the photoreceptor outer segments.

The maxi-K^+ channels are unlikely to contribute to this spatial buffering because the theory requires the conductance to increase when the subretinal level of potassium falls. Several characteristics of maxi-K channels predict the opposite. A reduction in subretinal potassium hyperpolarizes the apical membrane (Oakley and Steinberg, 1982) while the probability of the maxi-K channels opening decreases as the membrane is hyperpolarized. The relief of sodium block by small concentration of extracellular potassium also makes the contribution of the maxi-K channels to spatial buffering unlikely (Yellen, 1984*a*, 1984*b*). When the subretinal K^+ levels are reduced, less relief of the block, i.e. a greater channel block, is expected. While the cell is unlikely to be depolarised to the range where sodium block occurs, the conductance of maxi-K channels at the physiological voltage range is always larger when the electrode contained high potassium solution. If one extrapolated this relationship to the levels of potassium present in the dark and light, then the single channel conductance would be higher with the higher potassium concentration, i.e. in the dark.

The only way in which the maxi-K channel might contribute to the spatial buffering of potassium would be if the internal calcium concentration of the RPE was raised by light. The most likely mechanism for this is an indirect one; light causes a substance to be released by the retina which diffuses through to subretinal space, where it binds with a receptor on the apical membrane of the RPE and triggers and elevation in the internal calcium concentration. If the concentration was raised sufficiently, the open probability of the maxi-K

channels would increase and potassium would flow out of the RPE and into subretinal space. Several substances have been shown to lead to an increase in the level of intracellular calcium in the RPE. Epinephrine is thought to be synthesised in the retina of rats, and the total amount is increased after 15 minutes of photic stimulation (Hadjiconstantinou et al., 1983). Although it is not known where the newly-synthesised epinephrine is located, it is possible that it diffuses into subretinal space.

A recent study of fresh human RPE cells using fluorescence microscopy and the pH sensitive dye BCECF has shown that the pH_i decreases 0.06 ± 0.04 units when the concentration of potassium bathing the apical surface drops from 5mM to 2mM (Lin et al., 1992). The activity of the maxi-K channel in pancreatic B cells increases with the pH of the solution bathing the cytoplasmic face of the channel (Cook et al., 1984). However, the potential at which half of the channels were open, P_o50, shifted 61 ± 10 mV more hyperpolarized with an increase in one pH unit. If a similar relationship holds for the maxi-K channels in the RPE, then light would be expected to shift the P_o50 by +3.7 mV. This would mean that for a given $[Ca^{2+}]_i$, the activity of the maxi-K channels would be expected to drop, but the extent of this drop would depend upon the $[Ca^{2+}]_i$; the sigmoidal nature of the relationship between membrane potential and open probability means that when internal calcium was low, this change in pH reduces the open probability only slightly. However, the spatial buffering theory predicts an increase in channel activity after light. Thus, regardless of the magnitude of this pH dependent-decrease in channel activity, it is in the wrong direction to account for spatial buffering.

Recent whole-cell evidence has shown that the outward conductance through the inward rectifier increases as the external potassium concentration decreases (Segawa and Hughes, 1993). The light-evoked decrease in the potassium concentration in subretinal space results in an increased flow of potassium ions out of the RPE and back into subretinal space. In the dark,

when the level of potassium bathing the apical membrane was high, the conductance of the inward rectifier decreases; less potassium leaves through the apical membrane and more is available to pass through the basal membrane. Thus, intrinsic properties of the inward rectifier channel may be responsible for the spatial buffering.

VI.E.4. Non-selective Channel

The function of a non-selective channel would be limited; a large conductance channel which could not distinguish between the major ions of physiological importance would quickly allow gradients to dissipate if it was connected to the outside world. It could only fulfil a positive function if it connected cells together and allowed the exchange of ions across a gap junction.

In the lens, a structure which shows extensive cell to cell coupling, gap junctions are closely associated the major intrinsic proteins (MIP) of the membrane. This MIP has been reconstituted into lipid bilayers and the electrophysiological properties have been studied. The channel has two main conductance states of 160 and 360 pS and three subconductance levels (Ehring et al., 1990). This combination of conductances describes the distribution found in the bovine RPE cells and it is tempting to postulate that the largest channel type found in the bovine RPE records represents an uncoupled gap junction.

The lack of any records of this very large conductance channel in the cultured channel work would support the theory that it was a gap junction. The cells used for culture recording were always subconfluent, and were usually subcultured from a subconfluent population. The cells had little or no cell to cell contact for several passages. It is reasonable to accept that this influenced the expression of gap junctions. Although a 300 pS non-selective channel was reported in cultured human cells by Fox et al. (1988), it was present in only 6% of cell attached records. This compares with over 90% of the fresh bovine cells

in this study. In addition, they gave no information about the culture conditions, under which the cells were kept before experiments were performed and it is thus possible that each passage was allowed to attain confluence before passaging.

Gap junctions present in the RPE of all species examined so far and are the most apically located component of the junctional complex (Hudspeth and Lee, 1973). However, little is known about the electrophysiology of the junction and its contribution to the RPE. Under normal conditions, the tissue would benefit from being connected as a syncytium because any idiosyncratic variations would be buffered out. However, the photoreceptor/RPE interactions may require a localisation of the RPE response and a mechanism able to control the degree of coupling must exist. In the lens, the extent of cell coupling is pH sensitive, with acidification to 6.6 decreasing coupling significantly (Miller et al., 1992)

Although this study presents no direct evidence for the presence of gap junction channels in the membrane of fresh bovine RPE, the circumstantial evidence from many sides points to the conclusion that the large channels seen here are from gap junctions.

VI.F. Future Directions.

The results of this thesis prompt many new questions, and the need to clarify some of the results presented here. While some of these future ideas require new technology, others need new approaches which have become apparent while writing this thesis.

As mentioned in several places in this thesis, the ability to perform inside- out recordings would greatly improve the consistence of these results. By replacing the unknown values of membrane potential and internal ion concentration, the Goldman equation can be utilised to provide a more exact and invariable values of the selectivity of channel types found in this study. This would allow more precise and consistent measurements of both selectivity and

conductance to be made.

The use of excised patches to control the concentration of these ions would allow several theories to be tested. For example, most conductance values quoted in the literature for the maxi-K channel refer to the value found in symmetrical 150 mM KCl. Inside out recordings would allow the conductance of the " maxi-K" channel found in this study to be easily compared with those in the literature. It would also be possible to test theories about sodium block. The reduced conductance seen in the largest channel types when they were substantially depolarised resembled sodium block described in chromaffin cells (Yellen, 1984*a*), and it was assumed that the internal concentration of Na was responsible. This theory would benefit from more rigorous testing.

The ability to record from excised patches could be used to clarify the role of calcium in the activity of the channels observed here. The solution bathing the cytoplasmic face of the patch could be changed from one containing 10^{-6} M Ca to one containing 10^{-8} M Ca and the effect upon the channel open probability could be tested. More specifically, the effect of internal calcium levels upon the voltage dependence of channel activity could be determined. The results of such experiments could strengthen the assignment of maxi-K to the large-conductance channel type found in cultured cells.

Experiments upon excised patches of cultured cells were not performed because the membrane/electrode seal was lost when the electrode was withdrawn. It is unclear why this should have occurred, but the most obvious reason rests upon the fact that the seals were never very tight. The seal resistance was rarely above 1.5 gigaohms, and although this was sufficient to allow the detection of large currents, it probably did not provide sufficient mechanical stability to support patch excision. Tighter seals were occasionally formed on bovine cells, but at the time the bovine experiments were performed, inside-out configuration recordings were not considered.

One of the more interesting findings in this study is the presence of a

noisy, large conductance non-selective channel in bovine cells. The possibility that this channel was one half of a gap junction was suggested, and there are several experiments which might provide more support for this assignment. Double whole cells experiments where pairs of cells are clamped have shown that the conductance of gap junction channels is proportional to internal pH (Spray et al., 1984) and inversely proportional to intracellular concentration of calcium (Lowenstein, 1981). It would be interesting to test if either of these relationships held by changing the solution bathing the cytoplasmic face of the cells in excised patches. In addition, antibodies capable of blocking the gap junction pores are now available (Dr. H.Evans, personal communication). These antibodies depend upon the particular connexin protein making up the gap junction.

The presence of the large conductance non-selective channel in fresh bovine cells but not cultured human cells suggests several experiments. If fresh human tissue was obtainable, it would be possible to rule out species differences as the reason for the channel's absence in cultured human cells. The next series of experiments would involve following the appearance of this channel type as cell passage number increased from primary through the seventh passage, the passage of cells used in this study. This would help identify a temporal/age cause for the channels disappearance. It would also be necessary to record from cells plated at different densities. If the channel is a gap junction channel, the lack of cell to cell contact may lead to underexpression. Once the question of species difference had been resolved, either bovine or human cells could be used for these studies.

VI.G. Conclusion

This thesis has described single channels of bovine and cultured human RPE cells. The data indicate that the activity of these channels is regulated by the membrane potential and by the intracellular level of calcium. The contribution of these channels to RPE physiology can be controlled indirectly by

stimuli which effect these parameters. The single channel information has identified some of the mechanisms which ultimately integrate the dynamic transport of the RPE.

Appendix 1

Table 1. Characteristics of Channels in Bovine RPE Cells

File	Config	Med	PFS	G(pS)	V_{rev}(mV)
B280290a	CA	Mam	Ki	24	1
B221189r	CA	Mam	Ki	35	-46
B080390c	CA	Mam	Low	46	11
B020889j	CA	Mam	Ki	47	-7.9
B280290a	CA	Mam	Ki	52	3
B280290b	IO	Mam	Ki	53	1
B201191m	CA	Mam	Mam	54	10
B210290b	CA	Mam	Ki	55	-2
B200990a	IO	Mam	Ki	55	-35
B201191h	CA	Mam	Mam	58	3
B080390a	CA	Mam	Low	62	34
B080390c	CA	Mam	Low	64	15
B030889b	CA	Mam	Ki	65	-2
B280290b	IO	Mam	Ki	78	11
B140390b	CA	Mam	Low	82	2
B201191d	CA	Mam	Mam	89	5
B201191f	CA	Mam	Mam	97	13
B080290q	CA	Mam	Ki	99	4
B280290a	CA	Mam	Ki	101	0
B221189r	CA	Mam	Ki	103	-14
B080290b	CA	Mam	Ki	109	9
B280290b	IO	Mam	Ki	109	17
B201191h	CA	Mam	Mam	109	2
B210290b	CA	Mam	Ki	110	-6
B020889j	CA	Mam	Ki	111	-4.4
B211191a	CA	Mam	Mam	118	6
B221189a	CA	Mam	Ki	120	-10
B201191m	CA	Mam	Mam	133	2
B221189h	IO	Ki	Ki	142	3
B080390c	CA	Mam	Low	147	
B030889b	CA	Mam	Ki	150	2
B221189i	IO	Ki/Ba	Ki	150	-2
B221189g	IO	Mam	Ki	152	6
B140889e	CA	Mam	Ki	157	-38

Appendix 1

Table 1 (Con't)

File	Config	Med	PFS	G(pS)	V_{rev}(mV)
B280290b	IO	Mam	Ki	176	12
B140390c	IO	Mam	Low	187	-4
B201191h	CA	Mam	Mam	188	5
B210290a	CA	Mam	Ki	198	-1
B210290b	CA	Mam	Ki	207	-1
B201191f	CA	Mam	Mam	209	21
B070290e	CA	Mam	Ki	213	13
B080290b	CA	Mam	Ki	216	2
B211191a	CA	Mam	Mam	229	7
B201191m	CA	Mam	Mam	232	1
B201191d	CA	Mam	Mam	233	2
B280290a	CA	Mam	Ki	236	0
B221189r	CA	Mam	Ki	237	-9
B070290e	CA	Mam	Ki	249	3
B201191b	CA	Mam	Mam	264	35
B080290q	CA	Mam	Ki	264	13
B190990c	CA	Mam	Ki	290	-10
B131191a	CA	Mam	Mam	292	6
B210290b	CA	Mam	Ki	317	-3
B080290b	CA	Mam	Ki	350	1
B070290e	CA	Mam	Ki	362	6
B140390c	IO	Mam	Low	367	14
B140390b	CA	Mam	Low	377	4
B201191b	CA	Mam	Mam	499	38
B080290b	CA	Mam	Ki	618	0
B210290b	CA	Mam	Ki	659	-2
B221189r	CA	Mam	Ki	925	11

Key

CA = Cell attached

IO = Inside out

Med = Bath solution

PFS = Pipette filling solution

G = Conductance

Vrev = Reversal potential with respect to membrane potential

See Table II. 1 for composition of solution used in Med and PFS columns

Appendix I.

Table 2. Characteristics of Channels when the Electrode Contained Control Solution

RECORD	RANGE (mV)	G(pS)	Vrev (mV)	Vm50
Large conductance channels				
C230690d2	0..20	110	-19	b
C240990d	60..120	100	0	139
C150491d	0..70	90	-33	110
C190491j	0..50	93	-10	17
C240491l	30..80	91	1	95
C310591a	40..120	111	-18	145
C310591d	60..120	85	-8	176
C060691a	40..60	91	9	a
C250691k	20..60	99	-29	b
C250691s	60..140	112	-13	157
C260891a	60..80	85	-16	b
C120991a	0,10,40	110	-25	-2
C061191b	80..140	94	0	b
C081191i	0..100	90	-31	127
C141191a	30..100	94	-23	171
C181191f	40..90	94	-20	147
C271191b	30..110	82	10	153
C281191a	50..120	96	-4	139
Medium conductance channels				
C120690a	-80,20..100	59	-40	130
C210690a	-50..0	46	-31	82
C230690d1	-20..20	59	-40	54
C310890e	-60,-80,60	58	0	a
C010990x	20..140	57	-14	130
C030990b1	40..100	57	-34	b
C010691c1	50..90	67	20	a
C010691c2	-10..40	67	-47	a
C010691m	-60..80	78	-21	a
C260691a	-60..120	51	15	140
C210891a	0..40	43	-59	92
C081191q1	0..20	45	-89	66
C091191a	0..80	67	-34	103
C271191e	90..130	71	3	b

Appendix I

Table 2 (Con't)

RECORD	RANGE (mV)	G(pS)	Vrev (mV)	Vm50
Small Conductance Channels				
C010990g	-80..-10	30	21	32
C030990a1	40..100	33	-13	b
C030990a2	60..120	8	-27	b
C030990b2	60..100	8	-23	b
C161190a	10..20	25	-14	b
C140491c1	0..80	22	-38	a
C140491c2	0..80	30	-76	a
C150491a	-60..140	28	76	164
C150491b1	50..70	30	-22	b
C190491f	20..80	33	13	a
C050691a	0..60	20	-61	69
C060691b	-40, 20..80	20	2	a
Ungrouped Channels				
C130491a	30..110	10	-980	159
C270691a	30..120	20	-200	b
C200891a	60..120	60	-100	
C250891a	50..120	51	-105	148
C221191d	70..110	36	-157	144
C271191g	120..150	15	-320	155

Vrev = Reversal potential with respect to membrane potential
Vm50
a = too much scatter
b = >200

Appendix 1

Table 3. Characteristics of Channels when the Electrode Contained High Potassium Solution

Record	Range(mV)	G(pS)	Vrev	PoVm
Large Conductance Channels				
C240490g1	30..100	138	23	a
C240490g2	60..100	200	13	a
C280490b	-30..100	106	9	a
C100590a	-40..100	145	27	157
C100590i	40..60	195	24	77
C140590a	-80..100	111	10	a
C1405902	60..100	85	-12	a
C150590a	60..80	90	-16	a
C060790c	60..80	200	34	-12
C240790g	80..100	149	-3	a
C260790j	60..100	160	24	165
C260790t	-40..40	165	11	a
Medium Conductance Channels				
C210490a	50..80	45	-40	a
C210490d	-80..80	50	27	a
C100590c	-60..100	42	-1	a
C140590c1	-60..100	48	-16	a
C060790a	-60..30	67	43	-23
C240790b1	-100..0	42	31	-12
C100890b1	60..100	18	-83	a
C100890b2	60..100	30	-78	b
C140990b	50..100	83	25	200
Inward Rectifying Channels				
C150590c	-20..40	114	37	a
C240790b2	-80..30	141	34	a
C260790v	-30..20	70	61	-104

Vrev= Reversal potential with respect to membrane potential

Vm50
a = too much scatter
b = >200

Appendix II.

Table 1. Age, Passage and Donor of Cultured Cells Used in Exteriments

	Age(days)	Passage	Donor
C210490a	1	4	2023
C210490d	1	4	2023
C240490g	4	4	2023
C240490g	4	4	2023
C280490b	8	4	2023
C100590a	2	5	2023
C100590c	2	5	2023
C100590i	2	5	2023
C140590a	6	5	2023
C140590c	6	5	2023
C150590a	7	5	2023
C150590c	7	5	2023
C060790a	22	6	2023
C060790c	22	6	2023
C240790b	1	7	2023
C240790g	1	7	2023
C260790d	3	7	2023
C260790h	3	7	2023
C260790j	3	7	2023
C260790t	3	7	2023
C260790v	3	7	2023
C090890a	1	8	2023
C100890b	2	8	2023
C140990b	7	4	2017
C091190b	16	5	2017
C120690a	35	5	2023
C210690a	7	6	2023
C230690d	9	6	2023
C310890e	3	4	2017
C010990g	2	4	2017
C010990r	2	4	2017
C010990x	2	4	2017
C030990a	1	4	2017
C030990b	1	4	2017
C240990d	5	4	2017
C161190a	23	5	2017
C130491a	1	5	2017
C140491c	2	5	2017
C140491i	2	5	2017
C50491a	3	5	2017
C150491b	3	5	2017
C150491d	3	5	2017

Appendix II.

Table 1.(Con't)

	Age(Days)	Passage	Donor
C170491d	1	3	2021
C190491b	3	3	2021
C190491f	3	3	2021
C190491j	3	3	2021
C240491l	7	3	2021
C260491a	3	3	2021
C310591a	4	5	2017
C310591c	4	5	2017
C310591d	4	5	2017
C010691c	5	5	2017
C010691m	5	5	2017
C050691a	9	5	2017
C050691c	9	5	2017
C060691a	10	5	2017
C060691b	10	5	2017
C250691k	1	5	2021
C250691r	1	5	2021
C250691s	1	5	2021
C260691a	2	5	2021
C270691a	14	5	2021
C200891a	1	6	2017
C210891a	2	6	2017
C250891a	2	6	2017
C260891d	3	6	2017
C260891f	3	6	2017
C120991a	1	7	2017
C061191b	2	6	2021
C081191a	2	6	2021
C081191f	2	6	2021
C081191i	2	6	2021
C081191o	2	6	2021
C081191q	2	6	2021
C091191a	3	6	2021
C141191a	7	6	2021
C181191f	11	6	2021
C221191d	4	7	2021
C271191a	7	7	2021
C271191b	7	7	2021
C271191e	7	7	2021
C271191g	7	7	2021
C281191a	8	7	2021

Age = Time since plating

Appendix III. Table 1. Amount of Current Passing Through Channels- Control Electrode Solution

Current Size (pA)

Large Conductance Channels

-Vp(mV)	150	140	130	120	110	100	90	80	70	60	50	40	30	20	10	0	-10	-20	-30	-40	-50	-60	-70	-80	-90	-100
C230690d2														4.2	3.3	2										
C240990d				10		10.9		6		3.4																
C150491d									9.1	8.5	7.8	6.4		5	3.7											
C190491j											6	4.4	3.7	2.6	1.8	1.2										
C240491l								7.1		5.6	4.3		2.66													
C310591a				9		9		8		3.8		2.5														
C310591d				9.8		10.6		7.8		5.1																
C060691a										5.6	2.1	1.4														
C250691k										9.2	7.3	7.1	5.8	5												
C250691s				10.2		11.4	11.7	10.5	9.2	8.4																
C120991a												7.2			3.6	2.9										
C061191b		9.6		9		5.1	4.9	4.8																		
C081191i						5.8	5.9	6.2	6.2	6.1	6.4	5.8	4.6	3.8	3.2	3.5										
C141191a						8.6	9.1	8.5	8.7	8.1	6	6.8	4.7	4												
C181191f		8.5		9.5		9.6	11.3	9.9	9.4	8.2	5.3	5.4														
C271191b					8.9	6.9	6.7	5.6	4.5	3.9	3.1	2.6	2													
C281191a				12.2	10.3	9.8	9.8	7.6	7.3	7	6.1	2.9	3.1													

Ungrouped Channels

C130491c				8.4		9.7		9.6		9.5		9.1														
C170491d																-2.5										
C270691a				6.5		7.1	5.6	5.9						4.9	4.9											
C271191g	7.7	6.5	6.6	6.2									6	5.7												
C221191d					9.7	9	9.1	8.6	8.1	4.6	6	4.1	4.3													
C271191a					7.1	8.4	8.4	8.8	7.1	8.4	8.4	8.8														
C260891d								7	7.7	7																
C250891a				10.9		10.9	10.1	10.3	9.1		7.3															
C310591c												1.4														

Appendix III. Table 1. (con't)

Current Size (pA)

Medium Conductance Channels

-Vp(mV)	150	140	130	120	110	100	90	80	70	60	50	40	30	20	10	0	-10	-20	-30	-40	-50	-60	-70	-80	-90	-100
C120690a						5.6		5.7		5.2	3.7															
C210690a																1.2	1	0.8			-1					
C230690d1														2.2	1.4	1.1		-1.6								
C310890e										4.7												-2.2		-2.4		
C010990x				7.2		7.4		6.1		4.3		2.3		2.6												
C030990b1						7.8		6.5		7		4.5														
C010691c1							5	3.6	3.2	2.7	2.1															
C010691c2												5.8		4.9	4	2.6	2.8									
C010691m								6.7	7.3	6.6	5.3	5.3	3.6	3.5	3.1	2.8		-2.1		-2		-2.4				
C260691a				5.6		4.6		2.9		1.9										-1.7		-4.7				
C200891a		9.4				12		10.2	11.4	5.8																
C210891a												4.5	3.6	3.3	2.9	2.7										
C081191q1														4.7		3.8										
C091191a									6.7	7.1	5.6	4.8	3.6	3.1	2.8	3										
C271191e	8.3	8	9	8.2	7.1	6																				

Small Conductance Channel

C010990g																				-1.9		-2.3		-3.1		
C030990a1						3.9		2.8		2.5		1.8														
C030990a2				1		1.1		0.8		0.6																
C030990b2						1		0.6		0.7																
C161190a														0.8	0.6											
C140491c1								3.6	1.7	1.4	1.9	1.7			1.3											
C140491c2						5	3.5	4.3	4	3.3	3.1	2.9	2.5													
C150491a		6.1		5.6		4.9		3.5	4.8																	
C150491b1									2.8	2.4	2.2															
C190491f								2.1		1.9	1	4.1		1.8												
C050691a										2.5	1.9	2	1.9	1.6	1.7	0.93										

Appendix III. Table 2. Amount of Current Passing Through Channels - High Potassium Solution in Electrode

-Vp(mV)	100	80	70	60	50	40	30	20	10	0	−10	−20	−30	−40	−50	−60	−80
	Current Size (pA)																
Large Conductance																	
C240490g1	10	8		6			0										
C240490g2	17	14		9													
C280490b	10	7		6	4			1.5			−2		−4.2				
C100590a	10.5	8.1		4.7													
C100590i				7.1		3.2											
C140590a	10	8		5										−4.5	−5.8		−6.7
C140590c	6			3.5											−2.7	−2.7	
C150590a		8.6		6.8													
C060790c		9.3		5.3													
C240790g	14.6	12.9															
C260790j	12.1	9		5.7												−2.8	−3.7
C260790t						4.8		1.4		−1.8		−2		−2			
Small Conductance																	
C210490a		5.6		4.7													
C210490d		4		3								−4		−5			−9
C100590c	4.3									0.9	−1	−1.3	−1.5	−1.7	−2	−1.9	
C140590c	9.9	7.2		6.5													
C060790a							−1	−1.9	−2.1	−2.4	−2.7	−3.6	−4.6	−5.4	−6.1	−6.4	
C240790b1										−2.3	−2.5	−2.3	−3.8	−4	−4.7	−4	−5.6
C100890b1	3.3	2.7		2.6													
C100890b2	5.6	4.2		4.4													
C140990b	3.6	5.5	5.6	4.9	3												
Inward Rectifier																	
C150590c						0		−1.8	−2.7	−3.6		−7					
C240790b2							−1.7	−2.2	−3	−4.3	−4.8	−7.3	−8.4	−10.2	−11.8	−13.9	−16.4
C260790v								−2.9	−3.2	−4.3	−5.4	−5.8	−6				

Appendix III. Table 3. Probability of Channel Opening - Control Solution in Electrode

Open Probability

Large Conductance Channels

-Vp(mV)	150	140	130	120	110	100	90	80	70	60	50	40	30	20	10	0	-10	-20	-40	-60	-80	-100
C230690d2														0.003		0.002						
C240990d				0.075	5	0.006		0.001		0.001												
C150491d									0.062	0.035	0.019	0.008	0.002	0.001	0.001							
C190491j											0.884	0.852	0.750	0.584	0.470	0.052						
C240491l								0.23		0.015	0.068		0.041									
C310591a				0.052		0.006		0.002		0.001		0										
C310591d				0.012		0.003		0.001		0												
C060691a									0.29	0.466	0.586	0.416	0.516	0.229					0.004			
C250691k											1.9	4.5										
C250691s				0.061		0.017	0.005	0.003	0.001	0.001												
C260891d								0.004	0.001	0.001												
C120991a												0.909			0.868	0.575						
C061191b		0.002		0.001		0.001		0.001														
C081191i								0.1	0.048	0.022	0.01	0.004	0.004	0.002	0.001	0.001	0.00	0.000				
C081191q2																						
C141191a								0.026	0.012	0.008	0.006	0.002	0.001	0.001	0.000							
C181191f		0.360				0.113		0.021	0.008	0.005	0.001	0.001	0.000	0.000								
C271191b					0.37	0.36	0.27		0.22	0.27	0.14	0.03	0.01	0.051	0.030							
C281191a				0.118	0.032	0.027	0.01	0.005	0.003	0.028	0.002	0.000	0.000									

Ungrouped Channels

C200891a																						
C250891a				0.089		0.017	0.009	0.004	0.001		0.006											
C130491c		0.11		0.039		0.005		0.001														
C270691a				0.01		0.007	0.005	0.005	0.003	0.002	0.008	0.002										
C221191d								0.1	0.07	0.023	0.013	0.004	0.001	0.000	0.000							
C271191g	0.103	0.001	0.002	0.003							0.683	0.530										

Appendix III. Table 3. (con't)

Open Probability

Medium Conductance Channels

-Vp(mV)	150	140	130	120	110	100	90	80	70	60	50	40	30	20	10	0	-10	-20	-40	-60	-80	-100
C120690a						0.038		0.004		0		0										
C210690a																0.006	0.003	0.001				
C230690d1														0.203		0.102						
C310890e										0.08												
C010990x				0.12		0.003		0.001		0		0		0								
C030990b1						0.001		0.001		0.001		0.001										
C150591b2										0.002	0.001											
C260691a				0.65		0.004		0.006		0.003												
C210891a													0.074	0.035	0.061	0.005						
C081191q1																						
C091191a											0.009	0.002	0.001	0.001	0.001	0.000	0	0				
C271191e	0.003	0.005	0.002	0.001	0.000	0.000																

Small Conductance Channels

C010990g																			0.053	0.03	0.003	0.01
C030990a1						0.003		0.001		0.001		0.001										
C030990a2				0.042		0.053		0.037														
C030990b2						0.048		0.038														
C161190a														0.056	0.022							
C140491c1								0.176	0.045	0.057	0.023	0.1	0.116	0.02	0.02							
C140491c2								0.004														
C150491a		0.071		0.009		0.002																
C150491b1									0.013	0.017	0.01											
C190491f								0.038		0.076	0.007	0.068		0.025		0.2						
C050691a										0.25	0.093	0.039	0.005	0.003	0.003	0.002						
C060691b									0.022	0.071	0.003	0.04	0.086									
C271191a	0.119	0.063	0.034	0.019	0.006	0.006	0.003	0.001														

Appendix III. Table 4. Mean Duration of Channel Opening - Control Solution In Electrode

Mean Open Duration (msec)

Large Conductance Channels

-Vp(mV)	160	150	140	130	120	110	100	90	80	70	60	50	40	30	20	10	0	-10	-20	-40	-60	-80
C230690d2															1.1		1					
C240990d					4		1.3		0.6		1.1											
C150491d										2	1.8	1.5	0.9	0.7	0.4	0.5						
C190491j												27.27	19.51	9.62	5.58	4.12	1.51					
C240491l									2.4		1.48	2.86		1.29								
C310591a					2.1		1.02		0.9		0.49		0.29									
C310591d					1.7		1.2		1		0.2											
C250691k												1.9	1.4									
C250691s					1.74		1.21	0.76	0.77	0.5	0.4											
C260891d									1.1	0.9	0.7											
C120991a													24.4			8	3.6					
C061191b			1		1.3		0.3		0.1													
C081191i							2.2	1.9	1.6	1	0.76	0.6	0.7	0.3	0.6	0.3						
C081191q2															1.5		4.2					
C141191a									1.5	1.2	1	0.8	1.2	0.4	1.3	0.7						
C181191f			2.1				1.9		1.1	0.84	0.66	0.37	0.47	0.38	0.27							
C271191b						10.3	7.1	8	5	4.6	8.9	6	2.6	2.1								
C281191a					2.3	1.3	1.4	1	0.6	0.8	0.5	0.6	0.2	0.2								

Ungrouped Channels

C130491c			1.8		1.6		1.1		1.1		0.5											
C270691a					0.86		1.01	0.65	0.84	0.69	0.55	1.4	0.7			0.868	0.575					
C200891a																						
C250891a					2.1		1.2	1.1	0.8	0.6		0.6										
C221191d									3.7	3.9	3.2	2.9	2.4	1.7	2.5	1.3						
C271191g		5.6	0.9	1.2	1.5																	

Appendix III. Table 4. (con't)

Mean Open Duration (msec)

Medium Conductance Channels

-Vp(mV)	160	150	140	130	120	110	100	90	80	70	60	50	40	30	20	10	0	-10	-20	-40	-60	-80
C120690a							2		1.1		1	0.7										
C210690a																	0.6	0.5	0.4			
C230690d1															2.3		1.8					
C310890e																						
C010990x					5		1		0.6		0.3		0.4		0.7							
C030990b1							1.3		1.4		1.4		0.7									
C150591b2											0.8	1.4										
C260691a					4.5		0.9		1.7		1.3											
C210891a														1.4	0.9	1.3	0.6					
C081191q1															2.2		4.5					
C091191a										1.5	0.6	0.5	0.5	0.5	0.3							
C271191e	4.4	2.2	1.9	0.6	1.8	0.7	0.4															

Small Conductance Channels

C010990g																				28.8	12.6	4.9
C030990a1							5		1.9		1.2		0.9									
C030990a2					9.2		11.6		12													
C030990b2							4.3		4.5													
C161190a															4.2	1.5						
C140491c1									2.6	1.4	0.4	1.1	0.8	2.7	0.9	0.5						
C140491c2									2	2.2	1.2	2.9	1.9	1.6	1.6	1.7						
C150491a			2		1.8		0.9															
C150491b1										2.5	2.6	2										
C190491f									1.6		2	0.6	1.1		1.2		0.2					
C050691a											2.2	1.6	2	0.7	0.6	0.5	0.3					
C060691b										12.8	17	6.3	15.4	14.7	8.07							
C271191a		3.9	3.6	2	3	2.8	2.4	1.5	1.2													

Appendix III. Table 5. Probability of Channel Opening - High Potassium Solution in Electrode

-Vp(mV)	100	80	70	60	50	40	30	20	10	0	-10	-20	-30	-40	-50	-60	-80	-100
							Open Probability											
Large Conductance Channels																		
C100590a	0.0086	0.0016		0.0004														
C100590l				0.0299		0.0005												
C060790c		0.1941		0.0057														
C260790j	0.0069	0.0013		0.0008														
C260790n	0.0008															0.0265		
Small Conductance Channels																		
C100590c	0.0016									0.1918	0.2573	0.4222	0.0566	0.1331	0.2063	0.0488		
C140590c	0.0003	0.0004		0.002											0.0295	0.0815		0.0154
C060790a										0.6992	0.5503		0.2123	0.122				
C240790b1											0.5815	0.391	0.3012	0.2002	0.1023	0.1141	0.0227	
C100890b1		0.0027		0.0024														
C100890b2		0.0111		0.011														
C140990b		0.0658	0.0314	0.0601	0.0236													
Inwardly Rectifying Channels																		
C240790b2							0.662	0.8894	0.906		0.841	0.697	0.79	0.7817	0.7045	0.7138	0.4	
C260790v								0.89	0.521	0.82	0.8	0.68	0.66					

Appendix III. Table 6. Mean Duration of Channel Opening - High Potassium Solution in Electrode

Potential(mV)	100	80	70	60	50	40	30	20	10	0	-10	-20	-30	-40	-50	-60	-80	-100
	Mean Open Duration (msec)																	
Large Conductance Channels																		
C100590a	1	0.6		0.5														
C100590i				2.6		0.5												
C060790c		3.7		2.4														
C260790j	2.5	1.6		2.9														
C260790n	1.6															4.9		
Small Conductance Channel																		
C100590c	0.8									11.9	65.3	68.1	21.8	95	13.7	4.6		
C140590c	1	1.7		1.7											2.9	1.7		2.2
C060790a										5.9	3.9		2.5	1.9				
C240790b1											2.2	2.2	3	1.3	1.3	1.1	0.6	
C100890b1		1		0.9														
C100890b2		3.7		3														
C140990b		2.3	2	8.7	0.65													
Inwardly Rectifying Channel																		
C240790b2							20.6	50.7	28.7		13.9	14.6	14	7.9	6	2.1	2.5	
C260790v								19.6	9.7	6.1	7.7	4	4					

Appendix III

Table V.7. Mean Current Through Channels - Control Electrode Solution

96 pS Channel Type

Potential(mV)	140	130	120	110	100	90	80	70	60	50	40	30	20	10	0	-10	-20	-40	-50	-60	-80
Current (pA)	9.1		10.0	9.6	8.8	8.5	7.4	7.8	6.4	5.4	4.8	3.8	4.1	3.1	2.4						
St. Deviation	0.5		1.0	0.7	2.1	2.5	1.6	1.6	1.9	1.7	2.0	1.2	0.8	0.7	0.9						
Number	2	0	7	2	10	7	12	8	14	10	11	7	6	5	4						

59 pS Channel Type

Potential(mV)	140	130	120	110	100	90	80	70	60	50	40	30	20	10	0	-10	-20	-40	-50	-60	-80
Current (pA)	8.7	9.0	7.0	7.1	7.2	5.0	6.0	7.2	5.0	4.2	4.5	3.6	3.5	2.8	2.5	1.9	-1.0	-1.9	-1.0	-3.1	-2.4
St. Deviation	0.7		1.1		2.4		2.2	2.9	1.7	1.4	1.1	1.0	0.9	0.8	0.9	0.9	1.3	0.1		1.1	
Number	2	1	3	1	6	1	7	4	9	4	6	3	7	5	7	2	3	2	1	3	1

24 pS Channel Type

Potential(mV)	140	130	120	110	100	90	80	70	60	50	40	30	20	10	0	-10	-20	-40	-50	-60	-80
Current (pA)	6.1		3.3		3.2	3.5	2.4	3.0	1.8	1.9	2.2	1.6	1.2	1.2	0.9			-1.9		-1.5	-3.1
St. Deviation			2.3		1.8		1.3	1.3	0.9	0.7	1.1	0.9	0.6	0.5						0.8	
Number	1.0		2		5	1	8	5	9	6	6	3	4	3	1			1		2	1

Appendix III

Table 8. Mean Current Through Channels - High Potassium Electrode Solution

147 pS Channel Type

Potential(mV)	100	90	80	70	60	50	40	30	20	10	0	-10	-20	-30	-40	-50	-60	-70	-80
Current (pA)	11.7		9.2		6.2	4	4		1.4		-1.8	-2	-2	-4.2	-3.3	-5.8	-2.8		-5.2
St.Deviation	2.5		2.2		1.2		0.8		0.1										1.5
Number	8		10		10	1	2	1	2		1	1	1	1	2	1	1		2

47 pS Channel Type

Potential(mV)	100	90	80	70	60	50	40	30	20	10	0	-10	-20	-30	-40	-50	-60	-70	-80
Current (pA)	4.6		4.4	5.6	3.9	3		-1	-1.9	-2.1	-1.3	-2.1	-2.8	-3.3	-4.0	-3.9	-3.7		-7.3
St.Deviation	1.1		1.1		0.9						1.5	0.8	1.1	1.3	1.4	1.6	1.7		1.7
Number	5		5	1	6	1		1	1	1	3	3	4	3	4	4	4		2

Inward Rectifying Channel Type

Potential(mV)	100	90	80	70	60	50	40	30	20	10	0	-10	-20	-30	-40	-50	-60	-70	-80
Current (pA)								-1.7	-2.3	-3.0	-4.1	-5.1	-6.7	-7.2	-10.2	-11.8	-13.9		-16.4
St.Deviation									0.4	0.2	0.3	0.3	0.6	1.2					
Number								1	3	3	3	2	3	2	1	1	1		1

Appendix III.

Table V.9. Time Constants Fit to the Open and Close Time Distributions.

-Vp(mV)	State	τ1(ms)	τ2(ms)	R	τT(ms)
		96 pS Channel Type			
-120	O	1.3	3.9	2.2	2.1
-120	C	7.3	22.1	0.3	18.7
-120	O	0.6	18.0	0.6	11.4
-120	C	9.8	19.3	0.4	16.3
		59 pS Channel Type			
-120	O	3.5	12.1	4.4	5.1
-120	C	34.0			34.0
-80	O	0.6	1.5	2.1	0.9
-80	C	0.3	27.0	0.1	25.0
-60	O	1.0			1.0
-60	C	28.4			28.4
-50	O	0.9	1.8	0.8	1.4
-50	C	1.1	10.0	0.5	7.0
-40	O	2.0			2.0
-40	C	10.0	26.5	3.8	13.4
-30	O	2.5	12.7	80.0	2.6
-30	C	3.4	12.3	0.3	10.3
-20	O	3.3	12.3	1.5	6.9
-20	C	1.5	10.3	2.1	4.3
-10	O	2.8	6.8	3.1	3.8
-10	C	1.4	6.6	2.2	3.0
0	O	6.6	15.7	2.5	9.2
0	C	1.4	6.0	2.9	2.6
10	O	2.8	13.8	0.5	10.4
10	C	0.4	2.0	9.2	0.6
40	O	1.1	7.1	10.2	1.6
40	C	1.6	23.1	0.2	19.7

KEY:
O = Channel open duration
C = Channel closed duration
R = Ratio of τ : To estimate the overall time constant of the distribution, the relative weight given to each time constant was taken into account with the following equation;

$$\tau_T = \{(R*\tau_1)+\tau_2\}/(R+1)\,.$$

Appendix III.

Table V.10. Characteristics of the Time and Voltage Dependant Inactivation of Channel Activity.

P_{o50}	Rest(mV)	Test(mV)	τ(sec)	P_o:start	P_o:steady
		96 pS Channel Type			
165	60	100	12.2	0.021	0.002
176	60	100	2.5	0.40	0.004
>200	0	80	3.9	0.027	0.001
	0	100	2.5	0.1	0.006
	0	120	2.0	0.12	0.006
		59 pS Channel Type			
>200	-80	60	*	0.16	0.002
140	0	100	2.1	0.27	0.008
>200	-60	160	*	0.016	0.006
>200	0	80	5.9	0.02	0.001
	0	100	2.4	0.17	0.004
	0	120	3.1	0.28	0.01

The patch potential was suddenly depolarised from the rest potential to the test potential. In records where the patch was held at the test potential long enough for the P_o to reach a steady level, the time constant of the decay , τ, was calculated. In other experiments, marked with a *, the P_o of the channel during the first second after depolarisation was compared to the value predicted by the steady state P_o/ potential plot.

Abbreviations

ADC - analogue-to-digital converter
ATP - adenosine tri-phosphate
BCECF- 2',7'-bis(carboxyethyl)-5(6)-carboxyfluorescein
cAMP - cyclic adenosine monophosphate
cGMP - cyclic guanosine monophosphate
CMF - calcium- and magnesium-free
DAC - digital-to-analogue converter
DAG - diacylglycerol
DBH - delayed basal hyperpolarization
DIDS - 4,4'-diisothiocyanostilbene-2,2'-disulfonate
DMSO - dimethyl sulfoxide
EDTA - ethelenediaminetetraacetic acid
EGTA - ethelene glycol bis(β-aminoethyl ether)N,N,N',N'-tetraacetic acid
ERG - electroretinogram
FCS - foetal calf serum
FOT - fast oscillation trough
GDP - guanosine diphosphate
GTP - guanosine triphosphate
HEPES - N-2-hydroxyethylpiperazine-N'-2-ethanesulfonic acid
IBMX - isobutyl methylxanthine
Ins3 - inositol triphosphate
pA - picoamp
PBS - phosphate-buffered saline
PDE - phosphodiesterase
PFS - pipette filling solution
pS - picosiemens
RPE - retinal pigment epithelium
SEM - scanning electron microscopy
SCC - short circuit current
SITS - 4-acetamido-4'-isothiocyanostilbene
TEA - tetraethylammonium
TEP - transepithelial potential
VIP - vasoactive intestinal peptide

References

Adorante, J.S. and Miller, S.S. 1990. Potassium-dependent volume regulation in retinal pigment epithelium is mediated by Na,K,Cl cotransport. *J. Gen. Physio.* **96**: 1153-1176.

Armstrong, C.M. and Bezanilla, , F, 1974. Charge movement associated with the opening and closing of the activation gates of the Na channels. *J. Gen. Physiol.* **63:** 533-552.

Attwell, D., Wilson, M. and Wu, S.M. 1984. A quantitative analysis of interactions between photoreceptors in the salamander *(Ambystoma)* retina. *J Physiol.* **352:** 703-737.

Barros, F., Lopez-Briones, L.G., Coca-Pradoss, M., and Belmonte, C. 1991. Detection and characterization of Ca^{++} -activated K^{+} channels in transformed cells of human non-pigmented ciliary epithelium cells. *Curr. Eye Res.* **10:** 731-738.

Basu, P.K., Sarkar, P.,Menon, I., Carré, F., and Persad, S. 1983. Bovine retinal pigment epithelial cells cultured in vitro: growth characteristics, morphology, chromosomes, phagocytosis ability, tyrosinase activity and effect of freezing. *Exp. Eye Res. 36*: 671-683.

Beauge, L. 1984. Sodium pump in squid axons. In "The Squid Axon". P.F. Baker, ed. Current Topics of Membr. Trans. Academic Press, New York.

Berridge, M.J. and Irvine, R.F. !989. Inositol phosphates and cell signaling. *Nature.* **34**: 197-205.

Bernstein, J. 1902. Untersuchungen zur Thermodynamik der bioeletrischen Ströme. Erster Theil. *Pflügers Arch.* **92:** 521-562.

Bok, D. 1980. Autoradiogtaphic studies on the polarity of plasma membrane receptors in the retinal pigment epithelium cells. In "IV International Symposium on the Structure of the Eye". ed. J Hollyfield. Elsevier-North Holland.

Bok, D. 1985. Retinal photoreceptor-pigment epithelium interactions: Friedenwald Lecture. *Invest. Ophthalmol. Vis. Sci.* **26**: 1659- 1694.

Boulton, M. and Marshall, J. 1986. Effects of increasing numbers of phagocytic inclusions on human retinal pigment epithelial cells in culture: a model for aging. *British J. Ophthalmol.* **70**: 808-815.

Boyle, P.J. and E.J. Conway. 1941. Potassium accumulation in muscle and associated changes. *J. Physiol.* **100:** 1-63.

Brown, P.D., Loo, D.D., and Wright, E.M. 1988. Ca^{2+}-activated K^{+}channels in the apical membrane of necturus choroid plexus. *J. Membr. Biol.* **105:** 207-219.

Brücke, E. 1843. Beiträge zur Lehre von der Diffusion tropfbarflüssiger Körper durch poröse Scheidenwände. *Ann. Phys. Chem.* **58:** 77-94.

Bunt-Milam, A.H., Saari, J.C., Klock, I.B. and Garwin, G.G. 1985. Zonulae adherentes pore size in the external limiting membrane of the retina. *Invest. Ophthalmol. Vis. Sci.* **26**: 1377-1380.

Burke, J.M., Jaffe, J.J. and Brzeski, C.M. 1991. The effect of culture density and proliferation rate on the expression of ouabain-sensitive Na^{+}/K^{+}-ATPase pumps in cultured human retinal pigment epithelium. *Exp. Cell Res.* **194**: 190-194.

Caldwell, P.C. 1970. In "Calcium and Cellular Function". ed. A.W. Cuthbert. Macmillan. London.

Cervetto, L., Lagnado, L., Perry, R.J., Robinson, D.W. and McNaughton, P.A. 1989. Extrusion of calcium from rod outer segments is driven by both sodium and potassium gradients. *Nature.* **337**: 740-743.

Chaitin, M.H. and Hall, M.O. 1983. Defective ingestion of ROS by cultured distrophic rat pigment epithelial cells. *Invest. Ophthalmol. Vis. Sci.* **24**: 812.

Cilluffo, M.C., Fain, M.J. and Fain, G.L., 1993. Tissue culture of rabbit ciliary body epithelial cells on permeable supports. *Exp. Eye Res.* **57**: 513-526.

Clark, V.M. 1986. The cell biology of the retinal pigment epithelium. In "The Retina: A Model for Cell Biology Studies. Part II." R. Adler and D. Farber, eds. Academic Press, Orlando.

Colquhoun, D. and Hawkes, A.G. 1983. In "Single Channel Recording". B. Sakman and E.Neher, eds. Plennum Press. London.

Colquhoun, D. and Sigworth, F.J. 1983. In "Single Channel Recording". B. Sakman and E.Neher, eds. Plennum Press. London.

Cook, D.L., Ikeuchi, M., and Fujimoto, W.Y. 1984. Lowering of pH_i inhibits Ca activated k channels in parcreatic B cells. *Nature.* **311**: 269-271.

Corey, D.P and Stevens, C.F. 1983. In "Single Channel Recording". B. Sakman and E.Neher, eds. Plennum Press. London.

Crook, RB, Song, MK, Tong, LP, Yabu, JM, Polansky, JR, Lui GM. 1992. Stimulation of inositol phosphate formation in cultured human retinal pigment epithelium. *Brain Res.* **583:** 23-30.

Deary, A. and Burnside. B., 1989. Light-induced dopamine release from telost retinas act as a light-adaptive signal to the retinal pigment epithelium. *J. Neurochem.* **53**: 870-878.

Detwiller, P.B. and Hodgkin, A.L. 1979. Electrical coupling between cones in turtle retina. *J. Physiol.* **291**: 75-100.

DiMattio, J. and Zadunaisky, J.A. 1981. Glucose transport into the occular compartments of the rat. *Exp. Eye Res.* **32**: 517-532.

Dimattio, J. and Streitman, J. 1986. Facillitated glucose transport across the retinal pigment epithelium of the bullfrog (*Rana catesbiana*) *Exp. Eye Res.* **43**: 15-28.

DiMattio, J., Degan, K.J. and Zadunaisky, J.A. 1983. A model for transepithelial ion transport across the isolated retinal pignent epithelium of the frog. *Exp. Eye Res.* **37**: 409-420.

Dorey, C.K., Wu, G., Ebenstein, D. Garsd, A. and Weiterr, J.J. 1989. Cell loss through aging of the retina: relationship to lipofuscin accumulation and macular degeneration. *Invest. Ophthalmol. Vis. Sci.* **30:** 1691-1699.

Dowling, J.E. 1987. "The Retina: An Approachable Part of the Brain." Harvard University Press. Cambridge, Mass. and London.

Dowling, J.E. and Boycott, B.B. 1966. Organization of the primate retina: Electron microscopy. *Proc. Roc. Soc. Ser. B.* **166**: 80-111.

Edelman, JL and Miller, S.S. 1991. Epinephrine stimulates fluid absorbsion across bovine retinal pigment epithelium. *Invest. Ophthalmology Vis Sci.* **32**:3033-3040.

Edelman, J.L. and Miller, S.S. 1992. Epinephrine (EP) stimulates KCl and fluid transport across the bovine retinal pigment epithelium (RPE). Invest. Ophthalmol. Vis. Sci. **33(Suppl)**:1111.

Edelman, J.L., Miller, S.S. and Hughes, B.A. 1988. Regualtion of chloride transport by frog RPE. *FASEB Journal.* **2**:A1722. (Abstr.)

Ehring, G.R., Zampighi, G.A., Horwitz, J., Bok, D. and Hall, J.E. 1990. Properties of channels reconstituted from the major intrinsic proteins of lens fibre membranes. *J. Gen Physiol.* **96**: 631-664.

Fesenko, E.E., Kolesnikov, S.S., and Lyubansky, A.L. 1985. Induction by cyclic GMP of cationic conductance in plasma membrane of retinal rod outer segment. *Nature.* **313**: 310-313.

Filipovic D. and Sackin, H. .1991. A calcium-activated stretch-activated cation channel in renal proximal tubule. *Am J. Physiol.* **260**: F119-F129.

Fong, C.N., Bialek, S., Hughes, B.A. and Miller, S.S.. 1988. Modulation of Cl_i in bullfrog RPE. *FASEB Journal.* **2**: A1722. Abstr.

Fox, J.A. and Steinberg, R.H. 1992. Voltage-dependent currents in isolated cells of the turtle retinal pigment epithelium. *Pflugers Archiv.* **402:** 451-460.

Fox, J.A., Pfeffer, B.A. and Fain, G.L. 1988. Single channel recording from cultured human retinal pigment epithelium. *J. Gen. Physiol.* **91**: 193-222.

Frambach, D.A. and Misfeldt, D.S. 1983. Furosemide-sensitive chloride transport in embryonic chicken RPE. *Am. J. Physiol.* **244** 13:F679-F685.

Frambach, D.A., Valentine, J.L., and Weiter, J.J. 1989. Furosemide-sensitive Cl^- transport in bovine retinal pigment epithelium. *Invest. Ophthaomol. Vis. Sci.* **30**: 2271-2274.

Frambach, D.A., Fain, G.L., Farber, D.B. and Bok, D. 1990. Beta adrenergic receptors on cultured human retinal pigment epithelium. *Invest. Ophthalmol. Vis. Sci.* **31**: 1767-1772.

French, A.S. and Stockbridge, L.L. 1988. Potassium channels in human and avian fibroblasts. *Proc. R. Soc. Lon. B.* **232**: 395-412.

Frizzell, R.A., Halm, D.R., Rechkemmer, G. and Shoemaker, R.L. 1986. Chloride channel regulation in secretory epithelia. *Federation Proc.* **45**: 2727-2731.

Fujii, S., Hughes, B.A. and Steinberg, R.H. 1991. Effects of current clamp on chick retinal pigment epithelium. *Invest. Ophthalmol. Vis. Sci.* **32**: 2047-2057.

Fujii, S., Gallemore, R.P., Hughes, B.A. and Steinberg, R.H. 1992. Direct evidence for a basolateral membrane chloride conductance in toad retinal pigment epithelium . *Am. J. Physiol.* **262**: C374-C383.

Fung, B.K-K. and Stryer, L. 1980. Photolyzed rhodopsin catalyses the exchance of GTP to GDP in retinal rod outer segment membranes. *Proc. Natl. Acad. Sci. USA.* **77**: 2500-2504.

Fung, B.K.-.K., Hurley, J.B. and Stryer, L. 1981. Flow of information in the light triggers cyclic nucteotide cascade of vision. *Proc. Natl. Acad. Sci. USA.* **78**: 152-156.

Gao, H. and Hollyfield, JG. 1992. Aging of the human retina: differential loss of neurons and retinal pigment epithelial cells. *Invest. Ophthalmol. Vis. Sci.* **33**: 1-17.

Gallemore, R.P. and Steinberg, R.H. 1989. Effects of DIDS on the chick retinal pigment epithelium. II. Mechanism of the light peak and other responses originating at the basal membrane. *J. Neurosci.* **6**: 1977-1984.

Gold, G.H. and Dowling, J.E. 1979. Photoreceptor coupling in retina of the toad, *Bufo Marinus*. I. Anatomy. *J. Neurophysiol.* **42**: 292-310.

Goldman, D.E. 1943. Potential, impedence and rectification in membranes. *J. Gen. Physiol.* **27**: 37-60.

Griff, E.R. 1990. Response properties of the toad retinal pigment epithelium. *Invest. Ophthalmol. Vis. Sci.* **31**: 2353-2360.

Griff, E.R., and Steinberg, R.H. 1984. Changes in apical [K^+] produce delayed basal membrane responses of the RPE in Gekko. *J. Gen. Physiol.* **83**: 193-211.

Hadjiconstantinou, M., Cohen, J., and Neff., N.H.1983. Epinephrine: A potential neurotransmitter in retina. *J. Neurochem.* **41**: 1440-1444.

Hageman, GS, ans Johnson, LV. 1987. Chrondroitin 6-sulfate glycosamino-glycan is a major constituent of primate cone photoreceptor matrix sheaths. *Curr Eye Res.* **6**: 639-646, 1987.

Hagins, W.A., Penn, R.D. and Yoshikami, S. 1970. Dark current and the photocurrent in retinal rods. *Biophys. J.* **10**: 380.

Hamill, O.P., Marty, A.,Neher, E., Sakmann, B. and Sigworth, F.J. 1981. Improved patchclamp techniques for high-resolution current recording from cells and cell-free membrane patches. *Pflügers Archiv.* **67**: 621-638.

Handler, J.S. 1989. Overview of epithelial polarity. *Annual Review of Physiology.* **51**: 729-740.

Hille, B. 1992. "Ionic Channels of Excitable Membranes". 2nd Edition. Sinuar Associates Inc. Sunderland, MA. USA

Hodgkin, A.L. and Huxley, A.F. 1952. The dual effect of membrane potential on sodium conductance in the giant axon of *Loligo. J. Physiol.* **116**: 497-506.

Hodgkin, A.L. and Nunn, B.J. 1987. The effects of ions on sodium-calcium exchange in salamander rods. *J. Physiol.* **391**: 371-398.

Hodgkin, A.L., McNaughton, P.A. and Nunn, B.J. 1985. The ionic selectivity and calcium dependence of the light-sensitive pathway in toad rods. *J. Physiol.* **358**: 447-468.

Hogan, M.J., Alvarado, J.A., and Weddel, J.E. 1971. " Histology of the Human Eye - An Atlas and Textbook." W.B. Saunders, Philadelphia.

Hogan, M.J., Wood, I. and Steinberg, R.H. 1974. Phagocytosis by pigment epithelium of human retinal cones. *Nature*: **252**: 305-307

Hudspeth, A.J. and Yee, A.G. 1973. The intercellular junctional complexes of retinal pigment epithelia. *Invest. Ophthalmol. Vis. Sci.* **12**: 354-365

Hughes, B.A. and Steinberg, R.H. 1990. Voltage-dependent currents in isolated cells of the frog retinal pigment epithelium. *J. Physiol.* **428**:273-297.

Hughes, B.A. and Segawa, Y. 1993. cAMP-activated chloride currents in amphibian retinal pigment epithelial cells. *J. Physiol.* **466**: 749-766.

Hughes, B.A., Miller, S.S., and Machen, T.E. 1984. Effects of cyclic AMP on fluid absorbsion and ion transport across frog retinal pigment epithelium: measurments in the open circuit state. *J. Gen. Physiol.* **83**: 875-899.

Hughes, B.A. Miller, S.S. and Farber, D.B. 1987. Adenelate cyclase stimulation alters transport in frog retinal pigment epithelium. *Am. J. Physiol.* **253**: C385-C395..

Hughes, B.A., Miller, S.S., Joseph, D.P. and Edelman, J.L. 1988. cAMP stimulates the Na^+/K^+ pump in frog RPE. *Am. J. Physiol.* **254**: C84-C98.

Hughes, B.A., Adorante, J.S., Miller, S.S. and Lin, H. 1989. Apical $NaHCO_3$ cotransport. A mechanism for HCO_3 absorption across the retinal pigment epithelium. *J. Gen. Physiol.* **94**: 125-150.

Immel, J. and Steinberg, R.H. 1986. Spatial Buffering of K^+ by the retinal pigment epithelium in frog. *J. Neurosci.***6**:3197-3204.

Jacob, T.J.C. 1991. Two outward K^+ currents in bovine pigmented ciliary epithelial cells: $I_{K(Ca)}$ and $I_{K(V)}$. *Am. J. Physiol.* **261**: C1055 - C1062.

Jacob, T.J.C., Bangham, J.A. and Duncan, G. 1985. Characterization of a cation channel on the apical surface of the frog lens epithelium. *Quart. J. Exp. Physiol.* **70**: 403-421.

Joseph, D. and Miller, S.S. 1986. Passive ionic properties of the bovine RPE. *Biophys. J.* **49**: WAME8.

Joseph, D.P. and Miller, S.S. 1991. Apical and basal membrane ion transport mechanisms in bovine retinal pigment epithelium. *J. Physiol.* **435**: 439-463.

Joseph, D.P. and Miller, S.S. 1992. Alpha-1-adrenergic modulation of K and Cl transport in bovine retinal pigment epithelium. *J. Gen. Phys.* **99**: 263-290.

Josephson, I.R. and Brown, A.M. 1986. Inwardly rectifying single- channel and whole-cell K^+ currents in rat ventricular myocytes. *J. Membrane Biol.* **94**: 19-35.

Keller, S.K., Jentsch, T.J., Janicke, I., and Wiederholt, M. 1988. Regulation of intracellular pH in cultured bovine RPE. *Pfluger's Arch.* **411**:47.

Kennedy, B.G. 1990. Na^+-K^+-Cl^- co transport in cultured cells derived from human retinal pigment epithelium. *Am. J. Physiol.* **259**:C29-34.

Koh, S-W. M. and Chader, G.J. 1984. Retinal pigment epithelium in culture demonstrates a distinct ß-adrenergic receptor. *Exp. Eye. Res.* **38**: 7-13.

Kolb, H. 1970. Organization of the outer plexiform layer of the primate retina: electron microscopy of Golgi-impregnated cells. *Philo. Trans. R. Soc. Lon. B.* **258**: 261-283.

Kuffler, S.W., Nichols, J.G. and Martin, A.R. 1984. "From Neuron to Brain". 2nd Edition. Sinauer Associates Inc., Sunderland, Mass. USA.

Kuriyama, S., Ohuchi, T., Yoshimura, N., and Honda, Y. 1991. Growth-factor induced cytosolic calcium transients in cultured human retinal pigmented epithelial cells. *Invest. Ophthalmol. Vis. Sci.* **32**: 2882-2890.

Kuriyama, S., Yoshimura, N., Ohuchi, T., Tanihara, H., Ito, S., and Honda, Y. 1992. Neuropeptide-induced cytosolic Ca^{2+} transients and phosphatidylinositol turnover in cultured human retinal pigment epithelial cells. *Brain Res.* **579**: 227-233.

LaCour, M. 1989. Rheogenic sodium-bicarbonate co-transport across the retinal membrane of the frog retinal pigment epithelium. *J. Physiol.* **419**: 539-553.

LaCour, M., Lund-Anderson, H. and Zeuthen, T. 1986. Potassium transport of the frog retinal pigment epithelium: autoregulation of potassium activity in subretinal space. *J. Physiol.* **375**: 461- 479.

Lake, N., Marshall. J. and Voaden, M.J. 1977. The entry of taurine into the neural retina and pigment epithelium of the frog. *Brain Res.* **128:** 497-503.

Lamb, J.F. and P.Ogden. 1985. Transient leakiness of HeLa cells to Na and K during "rounding up" with trypsin, EDTA and pronase. *J. Physiol.* **358** 70P.

Lasansky, A. and DeFrisch, F.W. 1966. Potential, current, and ionic fluxes across isolated retinal pigment epithelium and choroid. *J. Gen. Physiol.* **49:** 913-924.

Latorre, R., and Miller, C. 1983. Conductance and selectivity in potassium channels. *J. Membr. Biol.* **71**:11-30.

Latorre, R., Oberhauser, A., Labarca, P., and Alvarez, O. 1989. Varieties of calcium-activated potassium channels. *Annu. Rev. Physiol.* **51**: 385-399.

LaVail, M.M. 1979. Dysfunction in mouse and rat models. In "The Retinal Pigment Epithelium." K. Zinn and M.F. Marmour, M.F. eds. Harvard University Press. Cambridge Mass.

LaVail, M.M. 1981. Circadian nature of rod outersegment disc shedding in the rat. *Invest. Ophthalmol. Vis. Sci.* **19**: 407-411.

Light, D.B., Schwiebert, E.M., Fejes-Toth, G., Naray-Fejes-Toth, A., Karlson, K.H., McCann, F.V., and Stanton, B.A. 1990. Chloride channels in the apical membrane of cortical collecting duct cells. *Am. J. Physiol.* **258**: F273-F280.

Lin, H. and Miller, S.S. 1991*a*. pH_i regulation in frog retinal pigment epithelium: two apical membrane mechanisms. *Am. J. Physiol.***261**: C132-C142.

Lin, H. and Miller, S.S. 1991*b*. Apical epinephrine modulates $[Ca^{2+}]_i$ in bovine retinal pigment epithelium. *Invest. Ophthalmol. Vis. Sci.* .**32**(Suppl): 671.

Lin, H., Kenyon, E., and Miller, S.S., 1992. Na-dependent pH_i regulatory mechanisms in native human retinal pigment epithelium. *Invest. Ophthalmol. Vis. Sci.* **33**: 3528-3538.

Lolley, R.N. and Racz, E. 1982. Calcium modulation of cyclic GMP synthesis in rat visual cells. *Vision. Res.* **22:** 1481-1486.

Loo, D.D. and Kaunitz, J.D. 1989. Ca^{2+} and cAMP activate K^+ channels in the basolateral membrane of crypt cells isolated from rabbit distal colon. *J Membr. Biol.* **110**:19-28.

Lowenstein, W.R. 1981. Junctional intercellular communication: the cell to cell membrane channel. *Physiol. Rev.* **61**: 829-913.

Marmor, M.F. 1989. Subretinal fluid absorbsion and the pathogenisis of serous retinopathy. In "Retinal Pigment Epithelium" ed. Zingirian, M. amd Cardillo Piccolino, F. Kugler and Ghedini Publications. Amstelveen, The Netherlands.

Marmor, M.F. and Lurie, M. 1979. Light-induced electrical responses of the retinal pigment epithelium. In "The Retinal Pigment Epithelium." K. Zinn and M.F. Marmour, M.F. eds. Harvard University Press. Cambridge Mass. and London.

Maruyama, Y. and Petersen, O.H. 1983. Control of K^+ conductance by cholecystokinin and Ca^{2+} in single pancreatic acinar cells studied by the patch-clamp technique. *J. Membr. Biol.* **79**:293-298.

Matsuda, H. and Stanfield, P.R. 1989. Single inwardly rectifying potassium channels in cultured muscle cells from rat and mouse. *J. Physiol.* **414**: 111-124.

Mayer, E.A., Loo, D.D.F., Snape, W.J. Jr., and Sachs, G. 1990 . The activation of calcium and calcium-activated potassium channels in mammalian colonic smooth muscle by substance P. *J. Physiol.* **420**: 47-71.

McKinney, L.C., and Gallin, E.K. 1988. Inwardly rectifying whole- cell and single-channel K currents in the murine macrophage cell line J774.1. *J. Membrane Biol.* **103**:41-53.

McNaughton, P.A. 1990. Light response of vertebrate photoreceptors. *Physiol. Rev.* **70**: 847-883.

Menini, A. Rispoli, G. and Torre, V. 1988. The ionic selectivity of the light-sensitive current in isolated rods of the tiger salamander. *J. Physiol.* **402:** 279-300.

Miki, H., Bellhorn, M. and Henkind, P. 1975. Specialization of the retinal-choroidal junction. *Invest. Ophthalmol. Vis. Sci.* **14**:701-707.

Miller, A.G., Zampighi, G.A. and Hall, J.E. 1992. Single-membrane and cell-to cell permeability properties of dissociated embryonic chick lens cells. *J. Membr. Biol.* **128:** 91-102.

Miller, S.S. and Steinberg, R.H. 1976. Transport of taurine, L-menthionine and 3-O-methyl-D-glucose across frog retinal pigment epithelium. *Exp Eye Res.* **23**: 177-189.

Miller, S.S. and Steinberg, R.H. 1977*a*. Active transport of ions across the frog retinal pigment epithelium. *Exp. Eye Res.* **25**: 235-248.

Miller, S.S. and Steinberg, R.H. 1977*b*. Passive ionic properties of the frog retinal pigment epithelium. *J. Membr. Biol.* **36**: 337-373.

Miller, S.S. and Steinberg, R.H. 1982. Potassium transport across the frog retinal pigment epithelium. *J. Mem. Biol.* **67**: 199-209.

Miller, S.S. and Farber, D. 1984. Cyclic AMP modulation of ion transport across frog retinal pigment epithelim. Measurments in the short-circuited state. *J. Gen. Physiol.* **83:** 853-874.

Miller, S.S. and Edelman, J.L. 1990. Active transport pathways in the bovine retinal pigment epithelium. *J. Physiol.* **424**: 283-300.

Miller, SS, Steinberg, RH and Oakley,B. II. 1980. The electrogenic sodium pump of the frog retinal pigment epithelium. *J Gen Physiol* **74**: 237-259.

Minneman, K.P., 1988. Alpha-1 adrenergic receptor subtypes, inositol phosphates and sources of cell Ca^{++}. *Pharmacol. Rev.* **40**: 87-119.

Mullins, L.J. 1959. An analysis of conductance changes in sqiud axon. *J. Gen. Physiol.* **42:** 1013-1035.

Nakatani, K. and Yau, K-W. 1988. Calcium and light adaptation in retinal rods. *Nature.* **334** : 69-71.

Negi, A. and Marmour, M.F.1986. Quantitative estimation of metabolic transport of subretinal fluid. *Invest. Ophthalmol. Vis. Sci.* **27**:1564-1568.

Neill, J.M., and Barnstable, C.J. 1990. Expression of the cell surface antigens RET-PE2 and N-CAM by rat retinal pigment epithelial cells during development and in tissue culture. *Exp. Eye. Res.* **51**: 573-583.

Newmann, E.A. 1985. Membrane physiology of retinal glial (Müller) cells. *J. Neurosci.* **5**: 2225-2234.

Nilsson, S.E.G. 1964. Receptor cell outersegment development and ultrastructure of the disk membranes in the retina of the tadpole (*Rane pipiens*). *J. Ultrastructure Res.* **11**: 581-620.

Nilsson, S.E.G. and Skoog, K-O. 1975. Covariation of the simultaneously recorded c-wave and standing potential of the human eye. *Acta. Ophthalmol.* **53:** 721-730.

Oakley, B. II. 1977. Potassium and the photoreceptor dependent pigment epithelial hyperpolarization. *J. Gen. Physiol.* **70**: 405-424.

Oakley, B. II, and Green, D.G. 1976. Correlation of light-induced changes in retinal extracellular potassium concentration with the c-wave of the electroretinogram. *J. Neurophysiol.* **39**:1117-1133.

Oakley, B.II. and Steinberg, R.H. 1982. Effects of intracellular potassium upon $[K^+]_o$ in the sub-retinal space of the frog retina. *Vision Res.* **22:** 767-773.

Oakley, B.II. , Miller, S.S. and Steinberg, R.H. 1978. Effect of intracellular potassium upon the electrogenic pump of frog pigment epithelium. *J. Membr. Biol.* **44:** 281-307.

Oakley, B.II, Flaming, D.G and Brown, K.T. 1979. Effect of rod receptor potential upon extracellular potassium ion concentration. *J. Gen. Physiol.* **74:** 713-728.

Ostwald, T. and Steinberg, R.H. 1980. Localization of frog retinal pigment epithelium (Na-K) - ATPase. *Exp. Eye Res.* **31**: 351-360.

Overton, E. 1899. Ueber die allgemeinen osmotischen Eigenschaften der Zelle, ihve vermutlichen Ursachen und ihre Bedetung für die Physiologie. *Vierteljahrsschr. Naturforsch. Ges. Zurich.* **44:** 88-114.

Pallotta, B.S. 1985. Calcium-activated potassium channels in rat muscle inactivate from a short-duration open state. *J. Physiol.* **363:** 501-516.

Paulter, E.L. and Tengerdy, C. 1986. Transport of acidic amino acids by the bovine pigment epithelium. *Exp. Eye Res.* **43:** 207-214.

Petersen, O.H. 1992. Stimulus-secretion coupling: cytoplasmic calcium signals and the ontrol of ion channels in exocrine acinal cells. *J. Physiol.* **448**: 1-51.

Peterson, M.D., and Mooseker, M.S. 1993. An in vitro model for the analysis of intestinal brush border assembly. I. Ultrastructural analysis of cell contact-induced brush border assembly in Caco-2(BBe) cells. *J. Cell Sci.* **105**: 445-460.

Pfeffer, B.A. 1991. Improved methodology for cell culture of human and monkey retinal pigment epithelium. In "Progress in Retinal Research. V10" . N. Osborne and G. Chadler, eds. Pergamon Press, Oxford.

Pisam, M., and Ripoche, P. 1976. Redistribution of surface macromolecules in dissociated epithelial cells. *J. Cell. Biol.* **71**: 907- 920.

Poo, M.M. and Cone, R.A. 1974. Lateraldiffusion of rhodopsin in the photoreceptor membrane. *Nature.* **247**: 438-441.

Porrello, K. and LaVail, M.M.1986. Immunocyotchemical localization of chrondroitin sulfates in the interphotoreceptor matrix of the normal and dystrophic rat retina: *Curr Eye Res.* **5:** 981-993.

Pugh, E.N. Jr., and Cobbs, W.H. 1986. Visual transduction in vertebrate rods and cones: a tale of two transmitters, calcium and cyclic GMP. *Vision Res.* **26**:1613-1643.

Quinn R.H. and Miller, S.S. 1992. Ion transport mechanisms in native human retinal pigment epithelium. *Invest. Ophthalmol. Vis. Sci.* **33:** 3513-3527.

Rae, J.L.and Levis, R.A. 1984a. Patch voltage clamp of lens epithelial cells: theory and practice. *Molecular Physiol.* **6**:115- 162.

Rae, J.L.and Levis, R.A. 1984b. Patch clamp recordings from the epithelium of the lens obtained using glasses selected for low noise and improved sealing properties. *Biophys. J.* **45**: 144-156.

Rae, J.L., Levis, R.A. and Eisenberg, R.S. 1988. Ionic channels in occular epithelia. In "Ion Channels, 1" ed. Narahashi, T. Plenum Publishing Corp., New York.

Rae, J.L., Dewey, J. Rae, J.S., and Cooper, K. 1990. A maxi calcium-activated potassium channel from chick lens epithelium. *Curr. Eye Res.* **9:**847-861.

Rizzolo, L.J. 1990. The distribution of Na^+,K^+-ATPase in the retinal pigmented epithelium from chicken embryo is polarized in vivo but not in primary cell culture. *Exp. Eye Res.* **51**: 435-446.

Sakmann, B, and Trube, G. 1984. Conductance properties of single inwardly rectifying potassium channels in ventricular cells of guinea-pig heart. *J. Physiol.* **347**: 641-657.

Salceda, R. 1989. ^{45}Ca uptake by retinal pigment epithelial cells. *Invest. Ophthalmol. Vis. Sci.***30**:2114-2117.

Scharschmidt, B.F., Griff, E.R. and Steinberg, R.H. 1988. Effect of taurine on the isolated retinal pigment epithelium of the frog electrophysiological evidence for stimulation of an apical, electrogenti Na^+-K^+ pump. *J. Membr. Biol.* **106**: 71-81.

Schnetkamp, P.P.M. , Basu, D.K. and Szerencsei, R.T. 1989. Na^+-Ca^{2+} exchange in bovine retinal rod outer segments requires and transports K^+. *Am. J. Physiol.* **257**: C153-C157.

Segawa, Y and Hughes, B.A., 1993. Properties of the inwardly-rectifying K^+ conductance in isolated retinal pigment epithelial(RPE) cells of the toad. *Invest. Ophthalmol. Vis. Sci.* **34**(Suppl):873.

Shimazaki, H. and Oakley, B. II. 1984. Reaccumulation of $[K^+]_o$ in the toad retina during maintained illumination. *J. Gen Physiol.* **84**: 475-504.

Sigelman, J. and Ozanics, V. 1982. In "Biomedical Foundations of Ophthalmology. Vol. 1." T.D. Duane and E.A. Jaeger, eds.

Slaughter, M.M. and Miller, R.F. 1983. The role of excitory amino acid transmitters in the mudpuppy retina: an analysis with kainic and N-Methyl aspartate. *J Neuroscience.* **3**: 1701-1711.

Smith, J.B. and Smith, L. 1987. Na+/K+/Cl- cotransport in cultured vascular smooth muscle cells:stimulation by angiotensin II and calcium ionophores, inhibition by cyclic AMP and calmodulin antagonists. *J.Membrane .Biol.* **99**:51-63.

Spector, I. 1983. A primer in cell culture for patchologists. In " Single Channel Recording". ed. B. Sakmann and E. Neher. Plenum Press, London.

Spittznas, M. and Hogan, M.J. 1970. Outersegments of the photoreceptors and the RPE: interrelationship in the human eye. *Arch. Ophthalmol.* **84**: 810-819.

Spray, D.C., White, R.L., Campos Decarvalho, A., Harris, A.L. and Bennett, M.V.L. 1984. Gating in gap junctions. *Biophys. J.* **45**: 219-230.

Steinberg, RH. 1986. Research update: report from a workshop on cell biology of retinal detachment. *Exp Eye Res* **43:** 695-706.

Steinberg, RH and Miller, SS. 1973. Aspects of electrolyte transport in frog pigment epithelium. *Exp Eye Res.* **16**: 365-372.

Steinberg, R.H. and Wood, I. 1974. Pigment-epithelial cell ensheathment of cone outer segments in the retina of the domestic cat. *Proc. Roy. Soc. Lon. (Biol.)* **187**: 461- 478.

Steinberg, R.H. and Wood. I. 1975. Clefts and microtubules of photoreceptor outer segments in the retina of the domestic cat. *J. Ultrastruct. Res.* **51:** 397-412.

Steinberg, R.H., Schmidt, R. and Brown, K.T. 1970. Intracellular responses to light from cat pigment epithelium: origins of the electroretinogram c-wave. *Nature* **227**: 728-730.

Steinberg, R.H., Miller, S.S. and Stern, W.H. 1978. Initial observations of the retinal pigment epithelium-choroid of the cat. *Invest. Ophthalmol. Vis Sci.* **17**: 675-682.

Steinberg, R.H. , Oakley, B.II., and Niemeyer, G. 1980. Light-evoked changes in $[K^+]_o$ in the retina of the intact cat eye. *J. Neurophysiol.* **44:** 897-921.

Taniguchi, J., and Guggino, WB. 1989. Membrane stretch: a physiological stimulator of Ca^{2+} -activated K^+ channels in thick ascending limb. *Am. J. Physiol.* **257**:F347-F352.

Torre, V., Matthews, H.R. and Lamb. T.D. 1986. Role of calcium in regulating the cyclic GMP cascade of phototransduction in retinal rods. *Proc. Natl. Acad. Sci. USA.* **83:** 7109-7113.

Tsuboi, S. 1987. Measurments of the volume outflow and hydraulic conductivity across the isolated dog retinal pigment epithelium. *Invest. Ophthalmol. Vis. Sci.* **28**: 1776-1782.

Tsuboi, S., Manabe, R. and Iisuka, S. 1986. Aspects of electrolyte transport across isolated dog retinal pigment epithelium. *Am. J. Physiol.* **250**:F781- 784.

Warwick, R. 1976. " Eugene Wolff's Anatomy of the Eye and Orbit" 7th ed. W.B. Saunders. Philadelphia.

Wen, R., Lui, G.M, and Steinberg, R.H. 1993. whole-cell K^+ currents in fresh and cultured cells of the human and monkey retinal pigment epithelium. *J. Physiol.* **465**:121-147.

Yau, K.-W. and Baylor, D.A. 1989. Cyclic-GMP activated conductance of retinal photoreceptor cells. Annu. Rev. *Neurosci.* **12:** 289-327.

Yellen, G. 1984*a*. Ionic permeation and blockade in Ca^{2+}- activated K^+ channels of bovine chromaffin cells. *J. Gen. Physiol.* **84**:157- 186.

Yellen, G. 1984*b*. Relief of Na^+ block of Ca^{2+}--activated K^+ channels by external cations. *J. Gen. Physiol.* **84**:187-199.

Yoshida, S., Plant., S., McNiven, A.I, and House, C.R. 1990. Single Ca^{2+}-activated K^+ channels in excised membrane patches of hamster oocytes. *Pflügers Arch.* **415** : 516-518.

Young, R.W. and Bok, D. 1969. Participation of the retinal pigment epithelium in the rod outer segment renewal process. *J.Cell Biol.* **42**:392-403.

Zimmermann, A.L. and Baylor, D.A. 1986. Cyclic GMP-sensitive conductance of the retinal rods consists of aqueous pores. *Nature.* **321**: 70.